Long distance transport of micronutrients in bread wheat (*Triticum aestivum*): exploring the role of phloem composition and sources of variability.

Candidate: Lachlan Palmer

Supervisors: Assoc. Prof. James Stangoulis and Prof. Robin Graham

Flinders University

Faculty of Science and Engineering

School of Biological Sciences

Declaration

I HEREBY DECLARE that the work presented in this thesis has been carried out by myself and does not incorporate any material previously submitted for another degree in any university. To the best of my knowledge and belief, it does not contain any material previously written or published by another person, except where due reference is made in the text. I am willing to make the thesis available for photocopy and loan if it is accepted for the award of the degree.

L. J. Palmer

Acknowledgments

Harvest Plus for helping to fund my scholarship

My supervisors, Associate Professor James Stangoulis and Professor Robin Graham

Mike Rutzke at Cornell University and Jason Young at Flinders Analytical for their help with developing and establishing the ICP-MS method.

Berin Boughton, Daniel Dias and Ute Roessner at Melbourne University for their assistance in developing the metabolite profiling methods

Lyndon Palmer at the Waite Analytical Service for his help in all things ICP

The members of the Stangoulis, Soole and Anderson laboratories, with special thanks to Nick Paltridge, Georgia Guild, My-My Huynh, Matthew Wheal, Emma de Courcy-Ireland, Nick Warnock for all their support, friendship and sound advice over lots and lots of coffee.

Finally, I would like to thank my family, my wife Michelle and sons Austin and Chester along with my parents, brothers, sister and in-laws whose love, support and patience have been invaluable during my candidature.

"Success is not final, failure is not fatal: it is the courage to continue that counts."

Winston Churchill

Summary/Abstract

Aphid stylectomy and mass spectrometric techniques were used as tools for analyzing wheat phloem exudate and to determine what changes are occurring in its composition during the reproductive/grain loading phase. Further to this, the phloem composition of wheat genotypes that differ in grain Zn concentration were investigated along with nutrient changes within the phloem at different times of the day (diurnal variability). Phloem was collected from the peduncle 1cm below the head to gain insight into the phloem flux into the developing head.

Two improved methods for the accurate measurement of nano-litre volumes of phloem exudate were developed and their accuracy and precision quantified. The first method involved the use of paraffin oil to prevent evaporation due to the small sample size and the method consisted of optically measuring the droplet formed after a phloem sample had been collected and expelled into an optimised volume of paraffin oil. A change in oil volume of ±1.75 % from an optimum volume of 285 µl had a statistically significant effect on droplet measurement either under or over-estimating droplet volume due to optical effects caused by a convex or concave oil surface. The second method involved measuring exudate volumes without oil by estimating the flow-rate from photo sequences taken of droplets forming on the severed stylet during the collection period. Phloem volumes measured in air without correction were found to be on average 19.9 nl less (SD 18.87, $p < 0.001$) than those made under oil, with a strong linear relationship between volumes measured in air and those measured in oil ($R^2 = 0.942$). After correction, there was no significant difference between the volume measurement methods with the average difference between the methods being 0.5 nl ± SD 23.3 or less than 0.5 % of the average phloem sample volume.

Methods for analysing the elemental and metabolite profile were refined to enable the measuring of nl sized phloem samples. K, Mg, Zn and Fe were successfully quantified in phloem exudate using inductively coupled plasma mass spectroscopy in volumes as small as 15.5 nl. Semi-quantitative data were able to be produced for 79 metabolites using gas chromatography mass spectroscopy (GC-MS) in volumes as small as 19.5 nl. An amine group derivitization method coupled with liquid chromatography mass spectroscopy (LC-MS) based metabolomics was able to

quantify 26 metabolites and semi-quantitative data were available for a further 2 metabolites. Using the LC-MS method, it was possible to quantify the concentration of the important Fe and Zn binding metabolite nicotianamine, at a mean concentration of 255.4 µmol L^{-1} (SE 96.71, n =3).

Using the methods developed, further exploration of wheat phloem transport was possible. There were significant increases in the concentration of Mg, Zn and Fe within the phloem from the start of anthesis (1-2 days after anthesis) to the period of peak grain loading (8-12 days after anthesis). For K, there was a significant decrease across the grain loading period. Within the metabolite profile produced by GC-MS, 39 metabolites showed significant changes within the profile from the peak of grain loading to the end of grain loading (17-21 days after anthesis). Of these 39 metabolites, 21 were found to increase and 18 decreased within the phloem metabolite profile as the plant matured.

Changes within the phloem sampled at mid-day and mid-afternoon were explored and a significantly higher Fe concentration was observed in samples taken at mid-afternoon, 1-2 and 8-12 days after anthesis. There were also significantly higher concentrations of K in the phloem of samples taken at mid-afternoon only at 1-2 days after anthesis. Within the metabolite profile, 39 metabolites showed significant variability when sampled at different times of the day. Of these, the metabolites 3-hydroxybenzoic acid, glutamine, histidine and an unknown compound (UN16) had significant variability at both maturity times sampled. 22 additional metabolites had significant changes at peak grain loading and another 13 metabolites had significant variability at the end of grain loading. Of the metabolites identified, of particular interest were the metabolites glutamate, citrate and the unknown metabolite UN8. Both glutamate and citrate may play a role in Fe and Zn transport and were found to have significant changes with maturity. UN8 was found to have significant diurnal variability similar to that found for Fe concentration in the phloem and has been tentatively identified as a precursor (Cys-Gly) of the tripeptide glutathione, which is an antioxidant and phytochelatin precursor.

Finally phloem was collected from two wheat genotypes SAMNYT 16 (Zn-dense grain) and Carnamah (low Zn grain). SAMNYT 16 was found to have significantly more Fe and K in the phloem at the start of the peak grain loading period (8-12 days

after anthesis) when compared to Carnamah. There were 19 metabolites that had significant genotypic differences within the metabolite profile. The metabolite 4-aminobutyric acid (GABA) was significantly higher in the metabolite profile of SAMNYT 16 than Carnamah at both maturity times sampled. At the start of peak grain loading, the metabolites proline, ornithine, glutamine, 3-amino-piperidin-2-one, arginine and serine were significantly higher in the phloem of SAMNYT 16. The metabolites fumarate, sucrose and shikimic acid were significantly higher in the phloem of Carnamah at the same maturity time. At the end of peak micronutrient grain loading, the metabolites Glyceric acid-3-phosphate, UN14, UN17, UN21, UN23 andUN24 were significantly higher in the phloem of SAMNYT 16. The metabolites urea, trehalose and orotic acid were significantly higher in the phloem of Carnamah at the same maturity. From a mechanistic perspective, the metabolites of interest were again glutamate and UN8 as these showed significant maturity changes in SAMNYT 16 but not in Carnamah. Also of interest was the difference in the amount of GABA within the phloem of these two genotypes, with SAMNYT 16 having greater than 8 fold more GABA present within the metabolite profile of the phloem. GABA is considered to be involved in C and N cycling and possibly plays a role in signalling within the plant.

The work presented in this thesis provides tools needed for measuring and analysing nano-litre volumes of phloem. The work presented also further expands on the variability present within the phloem that needs to be accounted for to further expand our knowledge of the long-distance Zn and Fe transport pathways within plants.

Contents

Figures

Tables

Abbreviations

AAS	atomic absorption spectrometry
ACDT	Australian central daylight savings time
ANOVA	analysis of variance
Carn	Carnamah
CBRT	cube root transformation
DAA	days after anthesis
DALY	disability adjusted life year
DMA	2'-deoxymugineic acid
EDTA	ethylenediaminetetraacetic acid
GABA	4-Aminobutyric acid
GC-MS	gas chromatography mass spectrometry
GFAAS	graphite furnace atomic absorption spectrometry
h	hour
ICP-MS	inductively coupled plasm mass spectrometry
ID	internal diameter
InvCBRT	inverse cube root transformation
ISTD	internal standard
LC-MS	liquid chromatography mass spectrometry
Ln	natural log transformation
LOD	limit of detection
min	minute
MX	methoxyamine derivative
n	sample number
NA	Nicotianamine
nl	nano litre
p	calculated probability value
rpm	revolutions per minute
S16	SAMNYT 16
SD	Standard Deviation
SE	standard error
SQRT	square root transformation
TIC	*Time for Coffee* gene
TMS	Trimethylsilyl derivative
UN	unknown metabolite (refer to section 4.3.1 for more detail on numbering system used)
WSPO	water-saturated paraffin oil

Chapter 1. Introduction

Human deficiencies of Fe and Zn have been identified as a serious issue of concern for developing countries. In a 2002 World Health Organisation report it was estimated that in 2000, 1.6 million people died in that year as a direct result of Fe and Zn deficiency and during the year a further 60 million disability adjusted life years (DALY) were lost (World Health Organisation, 2002). A DALY is a measure of overall disease burden, expressed as the number of years lost due to ill-health, disability or early death. Approximately 60 % of the DALYs lost due to Fe and Zn deficiency occurred in developing countries within Africa and South-East Asia (World Health Organisation, 2002). In a more recent analysis of WHO data sourced from between 1993 and 2005 it was estimated that anaemia affected 24.8 % or 1.62 billion people worldwide (McLean et al., 2009), with preschool children, pregnant women and non-pregnant women being the most affected (McLean et al., 2009).

Biofortification of staple crops has been identified as a possible way of combating the issue of micronutrient deficiency (Mayer et al., 2008) and attempts to increase the levels of micronutrients and vitamins in the harvested and edible plant parts, using genetic or agronomic techniques is currently underway. An important part of the mineral biofortification process is the transport of these elements from source to sink (i.e. from soil, through to the roots, leaves and then to the seed). Within a plant, the critical part of this transport occurs through the long distance transport pathways of the xylem and phloem (Atwell et al., 1999). In the case of wheat and barley, the phloem is very important as there is a xylem discontinuity at the base of the grain (Zee and O'Brien, 1970). This discontinuity in the xylem indicates that all macro and

micro nutrients must transfer into the phloem before being available for unloading for transport into the grain. With phloem playing such a crucial role in the transport of micronutrients to the grain, an understanding of the composition and variability within the phloem is crucial.

1.1 Phloem

Phloem loading and transport of phytoassimilates has been extensively reviewed (Thompson, 2006; Turgeon, 1996; Van Bel, 1993; Van Bel, 2003; Wolswinkel, 1999). Phloem transport occurs within a symplastic space which is composed of en-nucleated sieve tube cells connected via their associated companion cell which forms the sieve element–companion cell (SE-CC) complex. The sieve tube cells are connected via enlarged plasmodesmata to allow the translocation of the phytoassimilates. The flow of phloem is driven by the loading of solutes and nutrients in “source” tissues and the unloading and use of those nutrients at “sink” tissues. The loading of sugars at the source tissues creates an osmotic gradient which draws water into the cells. This movement of water drives the bulk flow of the phloem to sites of unloading (sinks) (Taiz and Zeiger, 2002). Loading can occur at any point along the phloem pathway but the majority occurs in mature photosynthesizing leaves. Sink tissues include new growth, roots and reproductive organs. The loading of sugars into the phloem can be either symplastic or apoplastic and sometimes even both in the same plant. In Fig 1.1 an example of the phloem physiology found in monocots is presented. From this representation it can be clearly seen that there is close proximity between xylem and phloem and also that the sieve tube cells making up the phloem strand are small in cross section. The physiology of vascular bundles has meant that the sampling of phloem is difficult.

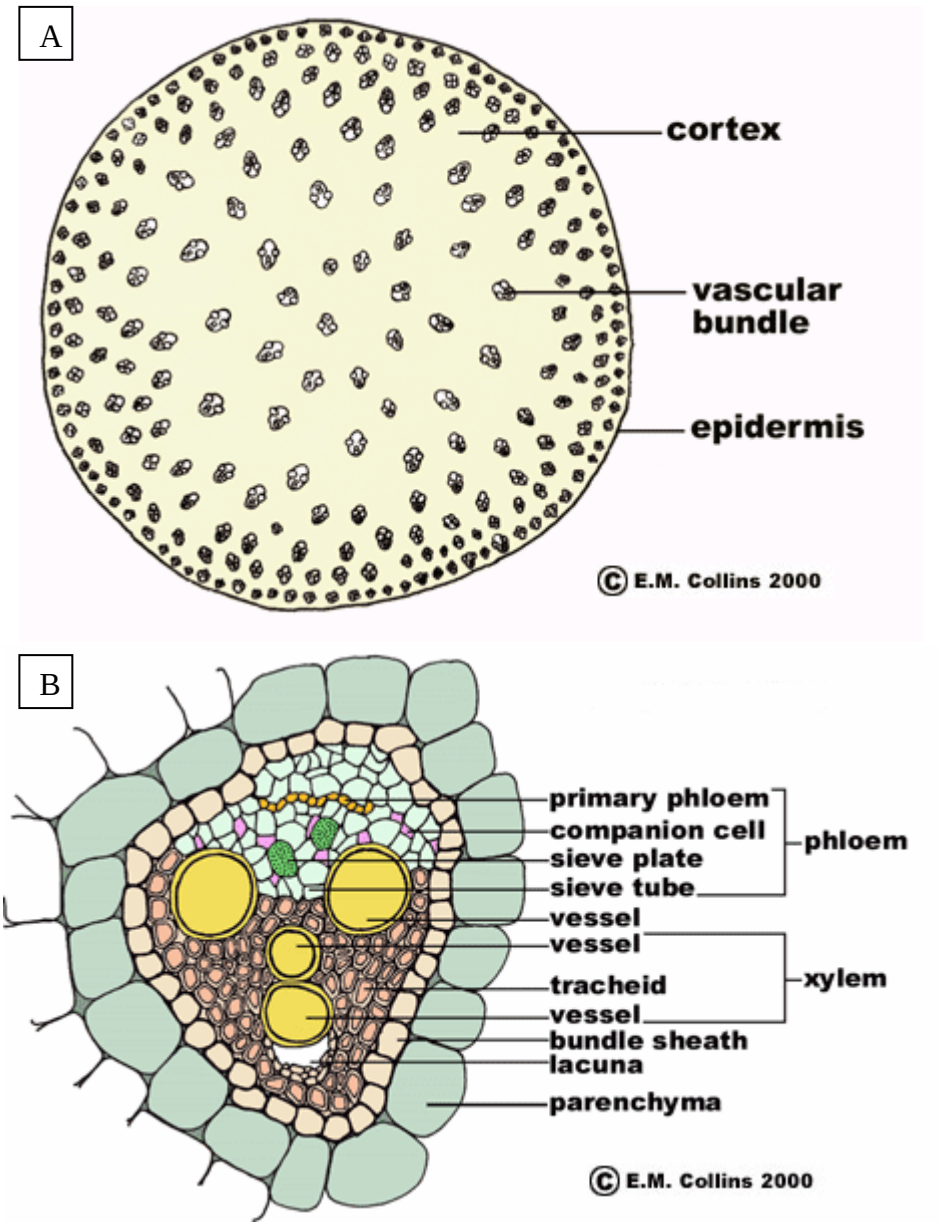

Figure 1.1 : A = cross section of Maize (*Zea mays*) stem.
B = expanded view of a vascular bundle with tissues indicated.

Sourced from:
http://www.uic.edu/classes/bios/bios100/summer2002/monocotstem.htm
November 2014

1.2 Phloem sampling

There are three main methods used for collecting phloem sap: 1. cutting the stem and collecting the liquid that exudes; 2. making use of an EDTA solution to allow a freshly cut plant part to continue to exude; 3. using insect stylectomy to collect phloem exudate (see Dinant & Kehr (2013) for further detail). The first two methods

have limitations when it comes to cereal crops. Cutting the stem for collecting phloem is limited to a small selection of plant species such as castor bean (Hall and Baker, 1972) and cucurbits (Richardson et al., 1982) and is not possible for cereals. There are also concerns with contamination when collecting from cut stems, as exudates collected from the cut tissue of cucurbits were found to be contaminated with solutes from other sources such as xylem and non-conductive tissues (Zhang et al., 2012; Zimmermann et al., 2013). In wheat and other monocots, phloem will not exude from cuts made to the stem or leaf under normal conditions, however phloem will exude from the grain pedicel after the removal of the seed (Fisher and Gifford, 1986). This method of collection is limited to older plants where the grains are firm enough to be grasped for separation from the pedicel. Fisher and Gifford (1986) sampled phloem exudate at 20 to 22 days after anthesis (DAA) which is around the middle of grain loading and they mention that they had trouble collecting from seed that had already turned brown. This description puts an approximate Zadoks stage of 85 or soft dough (Bowden et al., 2008; Zadoks et al., 1974). With peak grain loading for Fe and Zn occurring at 10-14 DAA (Stomph et al., 2011) or Zadoks 71 to 75 (water ripe to early milk) this method is not likely to be a viable option for monitoring micronutrient loading into the grain owing to the softness and size of the grain at this stage.

EDTA facilitated exudation is limited owing to the difficulty in quantifying phloem volume for accurate concentration measurements and also because EDTA facilitated exudation may be contaminated by components from damaged cells other than the phloem and the apoplastic space (Dinant and Kehr, 2013).

Insect stylectomy using aphids (Lohaus et al., 2000) and planthoppers (Hayashi and Chino, 1990) has been used to access the phloem of cereal crops for the analysis of elemental content. Insect stylectomy consists of the severing of the stylet (piercing mouthpart) of a phloem feeding insect and collecting phloem exuding from this severed stylet (Fisher and Frame, 1984). A variety of methods have been used for severing stylets (Fisher and Frame, 1984), but the main techniques used consist of either the use of a laser (Barlow and McCully, 1972) or RF microcauterisation (Downing and Unwin, 1977). The main limitation of stylectomy based collection of phloem is the small volumes involved. With exudation rates ranging from 4.2 to 354 nl h^{-1} (Palmer et al., 2013), volumes collected are in the low microlitre to nanolitre range (Mittler, 1958; Palmer et al., 2013). Owing to these small volumes, accurate measurement of phloem collections has been difficult. In previous work reporting the elemental composition of phloem, exudate volumes were measured using calibrated microcapillaries of different volumes (i.e. 1 µl (Hayashi and Chino, 1986) or 0.5 µl (Lohaus et al., 2000)). At these flow rates, the collections could take five or more hours to complete. Regardless of the limitations, insect stylectomy has been the main technique used for the exploration of phloem composition in cereals.

1.2.1 Insect stylectomy

Since the first report of collecting phloem exudate by insect stylectomy (Kennedy and Mittler, 1953), the technique has been used to gain access to the phloem for the study of a broad variety of its physiological, mechanical and molecular properties (see reviews Peel, 1975; Thompson and van Bel, 2012; Turgeon and Wolf, 2009). Owing to the small exudate volumes flowing from severed stylets, evaporation has been identified as a significant factor in accurate quantification of phloem exudate components. In a review of the work done on the Salix sp.-*Tuberolachnus salignus*

model (Peel, 1975), evaporation of phloem exudate was identified as a significant concern for quantitative analyses. At that time there was no system available for experimentally countering evaporation in this model. With the development and use of laser stylectomy (Barlow and McCully, 1972) and radio frequency microcautery stylectomy (Downing and Unwin, 1977), the number of potential insect-host models was expanded to 46 plant species (Fisher and Frame, 1984). The issue of evaporation was still of concern and has been demonstrated to cause increases in osmotic pressure measurements (Downing, 1978; Pritchard, 1996), with as much as a two-fold increase in osmotic pressure being reported for droplets collected in air when compared to those collected in oil (Pritchard, 1996). Accordingly, various approaches were developed to counter this problem. The main technique involved minimising evaporation through the use of mineral oil, where a droplet of oil is placed directly onto the plant surface, over the severed stylet (Downing and Unwin, 1977). Containers have been deployed to surround stem sections that are then filled with oil after stylectomy (Pritchard, 1996). Another technique of gluing wells, to contain oil, onto the plant surface prior to stylectomy (Gaupels et al., 2008) or after stylectomy (Fisher and Cash-Clark, 2000) is commonly used. Other techniques used for minimising evaporation have included placing a capillary directly over the severed stylets of aphids (Kennedy and Mittler, 1953) or plant hoppers (Fukumorita and Chino, 1982) and collecting from a severed stylet into an oil back-filled capillary and adjusting for evaporation losses (Gattolin et al., 2008).

Accurate and precise measurements of exudate volume are difficult. Phloem volumes ranging from as little as 2.1 nl (Gattolin et al., 2008) to as much as 100 µl (Mittler, 1958)have been reported in individual collections from a single stylet. Volume measurements have been made in a variety of ways, including direct measurement

from bulked collections, averaging across a number of stylets (Gaupels et al., 2008); or combining the length of collection with the time taken for a droplet to reach a certain diameter under oil (Fisher and Cash-Clark, 2000) or in air (Gattolin et al., 2008), the size of the collection droplet suspended in oil (Ponder et al., 2000); or the length of liquid within a micro-capillary of a known diameter (Fukumorita and Chino, 1982). Recently it has been noted that oil can cause interference in the subsequent analysis using capillary electrophoresis with laser-induced fluorescence detection (Gattolin et al., 2008). It has also been the experience of the candidate that paraffin oil can seriously interfere with metabolite profiling of phloem samples by GC-MS, by affecting the baseline resolution and by contaminating the mass spectrum response for low abundance compounds (see chapter 3). It is the author's concern also that for measurements made under oil, the shape of the oil surface may impact significantly on volume measurements made within the oil. The convex surface of the meniscus formed on the surface of an oil droplet or by overfilling a well with oil will have a positive focal length and if the droplet is in a position less than two times the focal length behind the surface, it will be magnified (Hecht, 2002). In the case of a convex meniscus formed by under filling a well, the focal length will be negative and the droplet will appear reduced in size regardless of its position (Hecht, 2002). The accurate measurement of the phloem is an important step in exploring the composition of the phloem especially if quantification of phloem components is desired.

1.3 Phloem composition

1.3.1 Micronutrients

To date, the measurement of cereal phloem for macro and micronutrients has been limited. Elemental composition of the phloem has been reported in wheat (Fisher,

1987; Hayashi and Chino, 1986), maize (Lohaus et al., 2000) and rice (Amiard et al., 2005; Fukumorita et al., 1983; Hayashi and Chino, 1990; Nishiyama et al., 2012; Yoneyama et al., 2010) and in these experiments, the exudate volumes collected were quite high to allow for effective analysis and accurate volume measurement. Table 1.1 shows concentrations of four elements and the analytical methods used (Palmer et al., 2014b). Most reports of elements in the phloem do not report the limitations of the method, with no mention of blanks or detection limits. These limitations are critical for measurement of micronutrients such as Fe and Zn which are in low concentrations in the phloem and results are susceptible to contamination issues (Wheal et al., 2011).

Table 1.1 : Comparison of average Fe, Zn, Mg and K concentrations in the phloem of a variety of plant species.

Plant species	Fe (mg L^{-1})	Zn (mg L^{-1})	Mg (mg L^{-1})	K (mg L^{-1})	Analytical method	Reference
Triticum aestivum	-	-	119	11690	IC	(Hayashi and Chino, 1986)
Triticum aestivum (anthesis/ end of grain loading)	-	-	-	1760/782	K sensitive microelectrode	(Fisher, 1987)
Zea mays	-	-	32 - 51	1950 - 2850	IC	(Lohaus et al., 2000)
Oryza sativa	3.0 – 4.1	0.9 – 1.6	-	-	GFAAS (Fe only) and ICP-MS	(Ando et al., 2013)
Oryza sativa	153	71.9	287	5880	ICP-AES	(Fukumorita et al., 1983)
Oryza sativa	-	-	-	1580 - 5890	IC	(Hayashi and Chino, 1990)
Oryza sativa	3.0	3.5	-	-	GFAAS and ICP-MS	(Nishiyama et al., 2012)
Oryza sativa (14^{th} leaf stage/ early grain fill)	2.8/3.5	2.2/7.5	-	-	GFAAS	(Yoneyama et al., 2010)
Ricinus communis	-	-	109 - 122	2300 - 4400	AAS	(Hall and Baker, 1972)
Nicotiana glauca	9.4	15.9	104	3670	AAS	(Hocking, 1980)
Grevillea leucopteris	4.7	4.3	102	1892.3	AAS	(Hocking, 1983)
Ricinus communis	-	-	90.17	2620	AAS	(Peuke, 2010)
Brassica oleracea	-	7.1-16.0	297 - 316	2330 - 2680	AAS	(Shelp, 1987)
Ricinus communis	2.5	2.5	-	-	AAS	(Schmidke and Stephan, 1995)
Ricinus communis	2.1					(Schmidke et al., 1999)
Ricinus communis	0.4 - 1.8		-	-	Colorimetric	(Maas et al., 1988)

IC = Ion Chromatography, GFAAS = Graphite Furnace Atomic Absorption Spectrometry, ICP-AES = Inductively Coupled Plasma Atomic Emission Spectroscopy, AAS = Atomic Absorption Spectrometry, reproduced from Chapter 3

The only reported value for direct quantification of K concentration in the phloem of wheat was 11690 mg L^{-1} (Hayashi and Chino, 1986) which seems high compared to the other reported values (See Table 1.1). This value was obtained from a single collection so it would be difficult to determine if any contamination or analytical issues may have affected the result due to lack of replication. Another potential source of variability in K concentration may also be due to the growth conditions with the values reported for cereals in Table 1.1 being done under solution culture type conditions, where K may be passively taken up and transported throughout the plant. In work done on the osmotic composition of phloem sap, the K concentrations in the phloem at anthesis (1759 mg L^{-1}) and at the end of grain loading (782 mg L^{-1}) were estimated using a K sensitive microelectrode (Fisher, 1987). These samples were taken from plants grown in a sand matrix with nutrients supplied from Hoagland's solution and this along with greater replication and may be a better representation of K in the phloem of wheat (Fisher, 1987).

A concentration of 119.1 mg L^{-1} has been reported for Mg in wheat phloem (Hayashi and Chino, 1986) and 287 mg L^{-1} was measured in rice (Fukumorita et al., 1983). These Mg concentrations are much higher than those reported in maize of between 31.6 and 51.0 mg L^{-1} (Lohaus et al., 2000).

Concentrations of K and Mg have also been reported in the phloem of the following Eudicots; *Ricinus communis*, *Nicotiana glauca*, *Brassica oleracea* and *Grevillea leucopteris* (Hall and Baker, 1972; Hocking, 1980; Hocking, 1983; Peuke, 2010; Shelp, 1987) shown in Table 1.1. Concentrations of K in the phloem of these Eudicots ranged from 1892.3 mg L^{-1} (Hocking, 1983) to 4400 mg L^{-1} (Hall and

Baker, 1972), while Mg in the phloem ranged from 90.17 mg L^{-1} (Peuke, 2010) to 316 mg L^{-1} (Shelp, 1987) (Table 1.1).

The only work examining micronutrients in the phloem of cereals has been done on rice. The Fe concentration in rice phloem has been reported to be as low as 2.8 mg L^{-1} (Yoneyama et al., 2010) and as high as 153 mg L^{-1} (Fukumorita et al., 1983). Zn concentration in the phloem of rice has been reported as low as 0.9 mg L^{-1} (Ando et al., 2013) and as high as 71.9 mg L^{-1} (Fukumorita et al., 1983). The concentrations reported by Fukumorita et al. (1983) are much higher than other values reported in rice and there is no detail on replication and no error estimates reported for these concentrations which makes it difficult to make comparisons to these values. The other reports for Fe and Zn concentration in the phloem of rice range between 2.8 to 4.1 mg L^{-1} and 0.9 to 7.5 mg L^{-1} respectively (Ando et al., 2013; Nishiyama et al., 2012; Yoneyama et al., 2010). These reports are much more consistent although differences in phloem concentration may be because most collections were made during the vegetative phase. The one report where collections were made during early grain loading accounted for the highest Zn phloem concentration of 7.5 mg L^{-1} and in this study the highest Fe concentration of 3.5 mg L^{-1} was also found during grain loading (Yoneyama et al., 2010). Fe and Zn concentrations in phloem have also been reported in the eudicots as shown in Table 1.1. In *Ricinus communis* it has also been found that the nutritional status of the plant can affect the levels of micronutrients in the phloem (Maas et al., 1988). Another point of difference is the collection methods involved. For the eudicot values, phloem was collected by making incisions on the stem and collecting bleeding exudate. This enables the quick collection of relatively large volumes but is not a viable method for cereals as they do not readily “bleed”. For the values reported previously for phloem collected from

cereals, collections were made by using stylectomy and then placing a microcap of a known volume over the stylet and waiting for the capillary to fill. This method requires long collection times with maize phloem flow rates of between 100 to 250 nl h^{-1} (Lohaus et al., 2000) and 200 nl h^{-1} in rice (Kawabe et al., 1980). This means that for a 500 nl microcap it would take between 2 and 5 h to complete a collection (Lohaus et al., 2000). Collections made over long time periods would reduce throughput and make it difficult to study diurnal variability or compare genotypes or treatments. For the transport of Fe and Zn, these elements must be complexed whilst within the phloem due their reactive nature (Blindauer and Schmid, 2010), so exploration of the metabolite profile of the phloem is critical for understanding the limitations in the transport of these crucial elements.

1.3.2 Metabolites

Phloem is a complex matrix which consists of water, sugars, amino acids, organic acids, secondary metabolites, peptides and hormones along with ions and a number of macromolecules, including proteins, small RNAs and mRNAs (Dinant et al., 2010; Turgeon and Wolf, 2009). A variety of metabolites have been theorised to complex Fe, Zn and other essential minerals within the phloem (Harris et al., 2012). Of these, nictoianamine and cystine are proposed to play a major role in the modelled transport of Fe and Zn (Harris et al., 2012), and in rice, nicotianamine (NA) has been found to complex Zn in the phloem (Nishiyama et al., 2012). In recent reviews the importance of phloem composition in long distance transport and signalling throughout the plant has been highlighted (Dinant et al., 2010; Turgeon and Wolf, 2009). The analysis of the metabolite profile of phloem has been restricted in the past due to limitations in the amount collected and the availability and sensitivity of analytical techniques. Recent work has made advances in volume measurement:

work examining the diurnal effect on the concentration of amino acids in the phloem made use of a correction factor for air based droplet volume measurements (Gattolin et al., 2008). This technique used measurements made under oil, which reduces the effect of evaporation, as a comparison for collections measured in air and enabled a correction factor to be derived. It has been established that sucrose is the dominant sugar involved in sugar transport (Liu et al., 2012) and it is assumed that hexoses (glucose and fructose) are not normally present, and when they are, they are mostly seen when using EDTA facilitated exudation (Liu et al., 2012). Glucose and fructose have been shown to exist (5.5 % and 1.5 % respectivly) in the phloem of perennial ryegrass (*Lolium perenne* L.) collected from aphid stylectomy (Amiard et al., 2004). A change in sugar composition was found when plants were defoliated with a decrease of more than 80 % for sucrose concentration and decreases of 42 % and 47 % in glucose and fructose concentrations, respectively (Amiard et al., 2004). This may indicate a source other than leaf for hexoses within the phloem.

In a theoretical model of metabolite and micronutrient speciation in the phloem it was found that 54.4 % of Zn was likely to be bound to NA and the remaining Zn complexed with amino acid complexes of cysteine and cysteine with histidine (41.2 % and 2.8 % respectively) (Harris et al., 2012). In the case of Fe, 99 % of the ferrous ions would be complexed by NA and only 19.3 % of ferric ions would be complexed by NA while the remaining ferric ions would be complexed with glutamate and citrate (70 % and 9.2 % respectively) (Harris et al., 2012). A potential fault with this model is that it does not incorporate 2'-deoxymugineic acid (DMA) as a potential candidate for complex formation. In work performed on the phloem of rice, the concentration of DMA was found to be between 152 µmol L^{-1} (Kato et al., 2010) and 150 µmol L^{-1} (Nishiyama et al., 2012). This was much higher than the NA values

reported of 66 µmol L^{-1} (Kato et al., 2010) and 76 µmol L^{-1} (Nishiyama et al., 2012). In rice it has been found that the main Zn complex ligand was NA whilst for Fe, DMA was the main metabolite responsible for complexing this metal (Nishiyama et al., 2012). Glutathione has been found to play a role in Cd transportation as part of the detoxification process (Mendoza-Cózatl et al., 2008). Glutathione was tested as a chelating agent in the speciation model but was found to complex less than 2 % of Zn, although it was mentioned that if Cd was included this may affect the model dynamics (Harris et al., 2012). The concentration of NA has also been reported in the phloem of castor bean (Schmidke and Stephan, 1995).The concentration of NA in the phloem of castor bean 4 and 8 days after imbibition was 206 µmol L^{-1} (Schmidke and Stephan, 1995).

The ability to obtain a profile of a broad range of metabolites is a powerful tool not only for understanding the transport of essential micronutrients to the grain and other vegetative tissues, but also for examining responses to toxic or deficient conditions. An example of this is where it was possible to identify a metabolite complex responsible for boron mobility in the phloem (Stangoulis et al., 2010) that could lead to efficiency in boron utilization (Stangoulis et al., 2001). Metabolite profiling has also been used widely on plant tissues to examine tissue level dynamics such as changes involved in tolerance to nutrient deficient conditions such as Fe deficiency in pea (Kabir et al., 2013), and also metabolite variation during the ripening process in capsicum (Aizat et al., 2014).

1.4 Sources of phloem variability

1.4.1 Maturity

Due to the nature of sample sizes, little has been done directly to explore changes in phloem composition with changes in maturity. As previously mentioned, for work done on the osmotic composition of phloem sap, Fisher et al. (1987) found differences in the estimated K concentrations in the phloem from anthesis (1759 mg L^{-1}) and to the end of grain loading (782 mg L^{-1}) . In rice, the concentrations of Zn and Fe were found to be higher in the phloem during grain loading; 7.5 mg L^{-1} and 3.5 mg L^{-1} respectively when compared to concentrations in the phloem during vegetative growth 2.8 mg L^{-1} and 2.2 mg L^{-1} respectively (Yoneyama et al., 2010). In this case the phloem samples were taken from different tissues with the vegetative samples collected from the leaf sheath whilst the grain loading samples were from the uppermost internode of the stem (Yoneyama et al., 2010).

To my knowledge, there are no reports of maturity variability in metabolite composition of the phloem.

As previously mentioned, the role of the phloem is crucial during grain development in wheat due to the presence of a xylem discontinuity at the base of the developing grain (Zee and O'Brien, 1970). Understanding changes within the phloem as the plant matures is central to better understand the dynamics of micronutrient loading.

1.4.2 Diurnal variability

Circadian clocks play an important role in the regulation of metabolic pathways across all forms of life (Wijnen and Young, 2006). In the model plant *Arabidopsis thaliana*, it has been found that up to 89 % of the transcriptome show a cyclic behaviour due to variability in light or temperature and up to 53 % of the

transcriptome show fluctuations with diurnal changes (Michael et al., 2008). There is an extensive body of work already reported that examines the interactions between circadian rhythm and solute transport in Arabidopsis (Haydon et al., 2011) and from a nutritional perspective, the relationship between the circadian clock and micronutrient transport is of great interest. In Arabidopsis, the homeostasis of Cu (Andrés-Colás et al., 2010) and Fe (Duc et al., 2009) have been linked to circadian clock genes and in the case of Fe it's been shown that there is a link between the expression of *Arabidopsis Ferritin 1* (*AtFer1*) and *Time for Coffee* (TIC) (Duc et al., 2009). *AtFer1* codes for a 28 kDa ferritin protein which in *Arabidopsis* has the highest expression under Fe excess (Ravet et al., 2009), whilst *TIC* encodes a nuclear located regulator of the circadian clock responsible for maintaining amplitude and timing of the *Arabidopsis* circadian clock (Ding et al., 2007; Hall et al., 2003). Ferritin production was found to be repressed by the expression of *TIC* under low Fe supply and in the presence of light and diurnal cycles (Duc et al., 2009). Furthermore, links have been made between Fe and the regulation of circadian rhythms, with the Fe supply affecting the length of the circadian period (Tissot et al., 2014). Interactions between ferritin genes and light have also been observed in rice, with the presence of light stimulating the expression and production of ferritin in rice seedlings (Stein et al., 2009). Ferritin is an important Fe storage protein with an important role in protecting against oxidative stress (Ravet et al., 2009). For most cereals, phytosiderophores which include NA and DMA, play an important role in the uptake of Fe and Zn from the soil (Rengel and Römheld, 2000) and phytosiderophore secretion has also been shown to have diurnal regulation in wheat (Reichman and Parker, 2007; Zhang et al., 1991), rice (Nozoye et al., 2014) and barley (Negishi et al., 2002). The interconnection between diurnal and circadian

rhythm, nutrient flux and long distance transport is crucial when exploring the mechanisms of micronutrient unloading into the grain. These relationships are also important to ensure that variability caused by diurnal and circadian rhythms are taken into account when sampling from the phloem.

1.4.3 Genotypic

An important part of the mineral biofortification process is the efficient transport of target micronutrients (i.e. Fe and Zn) from source to the sink (i.e. from soil, through to the roots, stems and leaves, and then to the seed) and therefore, the long-distance vascular pathways play a significant role in delivering nutrients to seeds (Borg et al., 2012). Genotypic differences in Zn turnover rates into the grain during grain loading have demonstrated in two wheat varieties, SAMNYT 16 and Carnamah (Stomph et al., 2011). SAMNYT 16 had a significantly higher turnover rate into the grain during peak grain loading under high Zn supply (Stomph et al., 2011). Previous research on genotypic variability of the phloem has been limited. To the candidate's knowledge there is only one report on genotypic differences in the element profile; significant differences in the concentration of Cd have been reported in the phloem of four rice genotypes (Kato et al., 2010). There have been more reports of genotypic differences in metabolites within the phloem, though for the most part, these reports have covered differences in amino acids and sugars (Lohaus et al., 1998; Lohaus et al., 1994; Lohaus and Moellers, 2000; Sandström and Pettersson, 1994; Winzer et al., 1996). The genotypic differences for amino acids and sugars have been demonstrated in five genotypes of sugar beet (Lohaus et al., 1994; Winzer et al., 1996), two maize genotypes (Lohaus et al., 1998) and two genotypes of rapeseed (*Brassica napus*) (Lohaus and Moellers, 2000). Genotypic differences have been reported for amino acids only in the phloem of five genotypes of pea (*Pisum sativum*) (Sandström and

Pettersson, 1994). In more recent work, genotypic differences in the concentrations of glutathione and phytochelatin were reported within four genotypes of rice (Kato et al., 2010).

In all the cases listed above, significant genotypic variability was observed for phloem composition showing that there is the potential for exploring the role of long distance transport in genotypes that differ in a particular phenotype (i.e. differences in grain micronutrient content).

1.5 Summary

Investigations into the composition of the phloem have started to reveal the complex nature of this critical plant transport pathway. Limitations in sampling and volume measurement have hampered the expansion of our understanding of the phloem. Regardless of the limitations, maturity, diurnal and genotypic changes have been observed to occur within the phloem.

There is a need to build greater knowledge on the mechanisms of Zn and Fe transport in cereal crops. More knowledge of the remobilization, xylem and phloem interaction, complex formation dynamics and long distance molecular or signalling controls is needed. This information will allow a better understanding of micronutrient transport in cereal crops and the identification of areas of interest for breeding or genetic manipulation to increase the nutritional value of cereal crops.

The aims of this work are to explore sources of variability, both experimental and biological that may interfere in the exploration of phloem composition and then to use this knowledge in an attempt to examine genotypic variability. Sampling and volume measurement will be explored and attempts made to demonstrate the potential to reduce error in the measurement of sub-micro litre volumes of phloem

sample. Exploration of advances in mass spectroscopy based analysis will be attempted to demonstrate the potential for analysis of much smaller volumes than are the norm. With the establishment of robust sampling and analysis methods variability based on what maturity and time of day the samples are taken will be examined.

Chapter 2. Improved techniques for measurement of nanolitre volumes of phloem exudate from aphid stylectomy

Lachlan James Palmer[1*], Lyndon Thomas Palmer[2], Jeremy Pritchard[3], Robin David Graham[1] and James Constantine Roy Stangoulis[1]

[1] School of Biological Science, Flinders University, Bedford Park, South Australia 5042, Australia, [2] School of Agriculture Food and Wine, University of Adelaide, Waite Campus, South Australia 5064, Australia, [3] School of Biosciences, University of Birmingham, Edgbaston, Birmingham, B15 2TT, UK

*To whom correspondence should be addressed. E-mail: Lachlan.palmer@flinders.edu.au

Full reference for chapter publication; refer to section 2.7 for author contributions:

Palmer LJ, Palmer LT, Pritchard J, Graham RD, Stangoulis JCR (2013) Improved techniques for measurement of nanolitre volumes of phloem exudate from aphid stylectomy. Plant Methods **9**: 18

2.1 Abstract

2.1.1 Background

When conducting aphid stylectomy, measuring accurate rates of phloem exudation is difficult because the volumes collected are in the nanolitre (nl) range. In a new method, exudate volume was calculated from optical measurement of droplet diameter as it forms on the tip of a severed aphid stylet. Evaporation was shown to decrease the accuracy of the measurement but was countered with the addition of water-saturated mineral oil. Volume measurements by optical estimation of the volume of a sphere suspended in oil was affected by the curvature of the oil surface. In contrast, measuring the exudate volume from optical measurement of droplet-diameter as formed on the tip of a severed aphid stylet, removes any inaccuracies due to oil surface curvature. A modified technique is proposed for measuring exudate volumes without oil by estimating the flow rate from photo-sequences of the collection period; a correction for evaporation is applied later.

2.1.2 Results

A change in oil volume of ±1.75 % from an optimum volume of 285 µl had a statistically significant effect on droplet measurement, under or over-estimating droplet volume due to optical effects caused by the oil surface. Using microscope image capture and measurement software, a modified method for measuring phloem volume in air was developed, by reducing air exposure during measurement to approximately 5 s for each measurement. Phloem volumes were measured using both techniques with measurements in air being on average 19.9 nl less (SD 18.87, $p < 0.001$) than those made in oil, and there was a strong linear relationship ($R^2 = 0.942$) between the techniques. This linear relationship enabled the development of a

correction equation with no significant difference at the 5 % level between corrected volumes and actual volumes measured under oil.

2.1.3 Conclusions

This study showed that oil has a significant role in countering evaporation but oil volume must be carefully optimised for optical measurement of droplets to ensure measurement accuracy. A linear correction factor was generated to correct the volumes measured in air for loss due to evaporation and the method provides for a much simpler alternative to earlier approaches for measuring exudation rates and volumes from a cut aphid stylet.

2.1.4 Keywords

Aphid stylectomy, Exudate, Phloem, Volume measurement

2.2 Background

Since the first report on collecting phloem exudate after insect stylectomy (Kennedy and Mittler, 1953), the technique has been used to gain access to the phloem for the study of a broad variety of its physiological, mechanical and molecular properties (see reviews Peel, 1975; Thompson and van Bel, 2012; Turgeon and Wolf, 2009). Owing to the small exudate volumes flowing from severed stylets, evaporation has been identified as a significant factor in accurate quantification of phloem exudate components. In a review of the work done on the *Salix* sp.-*Tuberolachnus salignus* model (Peel, 1975), evaporation of phloem exudate was identified as a significant concern for quantitative analyses. At that time there was no system available for experimentally countering evaporation in this model. With the development and use of laser stylectomy (Barlow and McCully, 1972) and radio frequency microcautery stylectomy (Downing and Unwin, 1977), the number of potential insect-host models was expanded to 46 plant species (Fisher and Frame, 1984). The issue of evaporation was still of concern and has been demonstrated to cause increases in osmotic pressure measurements (Downing, 1978; Pritchard, 1996), with as much as a two-fold increase in osmotic pressure being reported for droplets collected in air when compared to those collected in oil (Pritchard, 1996). Accordingly, various approaches were developed to counter this problem. The main technique involved minimising evaporation through the use of mineral oil, where a droplet of oil is placed directly onto the plant surface, over the severed stylet (Downing and Unwin, 1977). Containers have been deployed to surround stem sections that are then filled with oil after stylectomy (Pritchard, 1996); another technique of gluing wells, to contain oil, onto the plant surface prior to stylectomy (Gaupels et al., 2008) or after stylectomy (Fisher and Cash-Clark, 2000) is commonly used. Other techniques used for minimising evaporation have included placing a capillary directly over the

severed stylets of aphids (Kennedy and Mittler, 1953) or plant hoppers (Fukumorita and Chino, 1982) and collecting from a severed stylet into an oil back-filled capillary and adjusting for evaporation losses (Gattolin et al., 2008).

Accurate and precise measurements of exudate volume are difficult. Phloem volumes ranging from as little as 2.1 nl (Gattolin et al., 2008) to as much as 100 µl (Mittler, 1958) have been reported in individual collections from a single stylet. Volume measurements have been made in a variety of ways, including direct measurement from bulked collections; averaging across a number of stylets (Gaupels et al., 2008); or combining the length of collection with the time taken for a droplet to reach a certain diameter under oil (Fisher and Cash-Clark, 2000) or in air (Gattolin et al., 2008); the size of the collection droplet suspended in oil (Ponder et al., 2000); or the length of liquid within a micro-capillary of a known diameter (Fukumorita and Chino, 1982). Recently it has been noted that oil can cause interference in the analysis using capillary electrophoresis with laser-induced fluorescence detection (Gattolin et al., 2008). It has also been the experience of the authors that paraffin oil can seriously interfere with metabolite profiling of phloem samples by GC-MS, by affecting the baseline resolution and by contaminating the mass spectrum response for low abundance compounds (unpublished data). It is the author's concern also that for measurements made under oil, the shape of the oil surface may impact significantly on volume measurements made within the oil. The convex surface of the meniscus formed on the surface of an oil droplet or by overfilling a well with oil will have a positive focal length and if the droplet is in a position less than two times the focal length behind the surface, it will be magnified (Hecht, 2002). In the case of a convex meniscus formed by under filling a well, the focal length will be negative and the droplet will appear reduced in size regardless of its position (Hecht, 2002).

The aim of this work was to explore the effect that oil surface shape, due to oil volume, has on optical measurements of droplets contained within the oil. It also details a refinement to measuring droplets in air by making use of image capture and measurement software to shorten exposure times to air and to allow a measurement using a single time length for all measurements in air.

2.3 Results

2.3.1 Establishing optimum oil volume

The cap from a 1.5 ml micro-centrifuge tube was selected to contain the oil for volume measurement owing to its hydrophobic surface which enabled droplets of aqueous solutions to remain spherical. Nine oil volumes were tested using 10 µl droplets of MilliQ water. Figure 2.1 shows the difference between the average microscope measurement and weight measurement for the droplets at each total volume (oil + water). Clearly the shape of the liquid surface is having an impact on droplet measurement using microscope measurement. There was no significant difference in droplet weights across all total volumes ($p = 0.123$), but the total volume had a significant effect on the microscope measured volume ($p < 0.001$). For a total volume of 285 µl there was no significant difference between the volume measured by weight and that measured using the microscope technique ($p = 0.954$). For all other total volumes there were statistically significant differences (see Table 1 for a summary of the mean differences). From these results it can also be seen that a total volume change of 1.75 % or 5 µl is enough to produce a statistically significant difference in the microscope measurement of the droplet. Based on these results a volume of 285 µl oil was selected for measuring nl droplets. Inductively Coupled Plasma Mass Spectroscopy (ICP-MS) analysis of nl droplets of a 1000 mg kg^{-1} cobalt (Co) stock solution was used to confirm 285 µl of oil as a suitable volume for the

measurement of nl volumes. Co was selected as it is a single mass element with high sensitivity and reduced risk of contamination owing to its very low abundance in plant tissues. Attempts were made to repeat the oil volume trial with nl droplets of Co stock solution, but results were much more variable. This is most likely due to differences in liquid surface curvature when oil volumes are sub-optimal. Small droplet size could also contribute to the variability as the larger volume of a 10 µl Milli-Q droplet showed less variability but nl volume of droplets of Co solution still indicated that 285 µl was closest to the ideal volume.

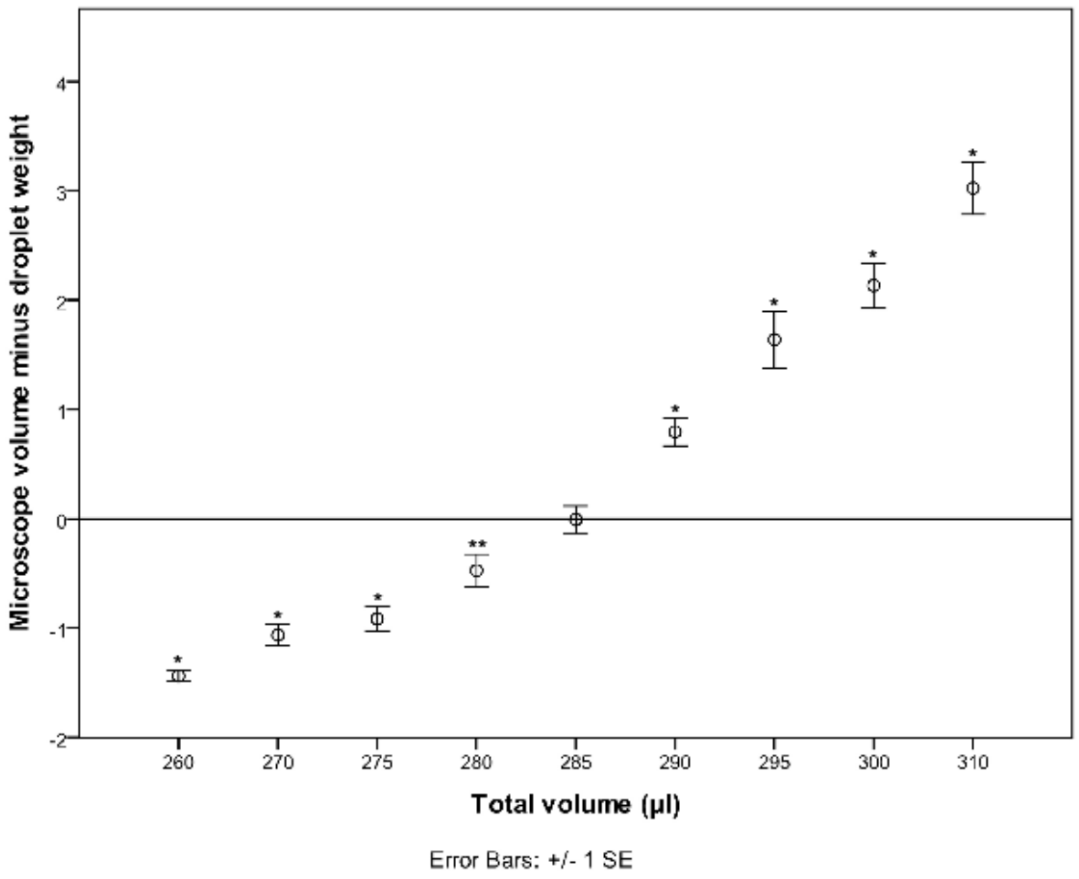

Figure 2.1 : Plot of the difference between the mean droplet volumes measured optically (µl) and by weights (mg) for each total liquid volume (oil + MilliQ water) with significant differences indicated.
(*= p > 0.001, ** = p > 0.01).

2.3.2 Standard Addition

Owing to the analysis of Co by ICP-MS it was necessary to test if the presence of oil would have an effect on the nebulizer or plasma performance (matrix effect). This was tested using a standard addition trial. For the results used in the standard addition test there was a significant difference between the results with and without an internal standard (ISTD) correction. The un-corrected (no ISTD) data were on

average 0.18 ± 0.05 µg L^{-1} (n = 19, p = 0.001) higher than the ISTD corrected measurements. This is equivalent to an average reduction of 1.5 % ± 0.039 (n = 19) in sample concentrations when results are corrected using the ISTD. Therefore standard additions were calculated using both data sets.

There was no significant difference between the values estimated from the standard addition samples measured with and without ISTD correction (n = 3, p = 0.096). For the standard addition results calculated using values without ISTD correction there was no significant difference between the estimated values and the original sample measurements made with and without ISTD correction (n = 3, p = 0.144 and 0.979 respectively). For the standard addition results calculated with ISTD corrected values the estimated values were significantly different from the original results for samples measured with and without ISTD correction. The standard addition estimate using ISTD corrected values was 0.37 ± 0.05 µg L^{-1} (p = 0.018) higher than the ISTD corrected values and 0.25 ± 0.03 µg L^{-1} (p = 0.018) higher than the values without ISTD correction.

This result indicates that there is no matrix effect caused by the oil in the analysis by ICP-MS. It also indicates that the use of the internal standard is not required and that the use of the ISTD may actually be producing an artificial matrix effect. Therefore for the remaining work, results from ICP-MS analysis were calculated without ISTD correction.

2.3.3 Method for measuring nl volumes

Droplets (n = 28) of 1000 mg L^{-1} Co stock solution were measured in 285 µl of oil using the microscope and by ICP-MS. Microscope-measured volumes ranged from 86 nl to 194 nl (mean 111.8 nl, SD 23.0). There was no significant difference

between the microscope measurement and ICP-MS volume measurement ($p = 0.799$). On average, the microscope measurement underestimated the volume by 0.15 nl, SD 3.02.

2.3.4 Oil vs Air

To test the oil measurement technique on real phloem exudate collections and to determine the accuracy of volumes measured based on an estimated flow rate made from droplets measured in air, samples were collected from 71 successfully severed stylets. Each collection was measured using both methods and the estimated volumes compared.

The average collection time was 45.6 min, SD 7.21. Flow rates measured in air averaged 1.8 nl min^{-1}, SD 1.3 with a range of between 0.07 nl min^{-1} to 5.9 nl min^{-1}. The average estimated collection volume in air was 83.4 nl, SD 56.6 with a range between 2.0 nl and 269.2 nl. The average oil measured volume collected was 103.3 nl, SD 63.8 with a range of between 2.89 nl and 283.5 nl. There was a significant difference in volume measured using the two techniques, with the volume measured under oil being on average 19.9 nl larger (SD 18.9, $p < 0.001$) than that of the volume measured in air. The volumes of the 71 phloem collections measured using both techniques were transformed by taking the square root to ensure data was normally distributed. From the 71 measured samples, a random subsample of 51 collections (Calibration (Cal) set) was selected and used to produce a linear regression and correction equation. The remaining 20 samples were used for validation of the method (Validation (Val)set). For the Cal set subsample, there is a significant regression between the two techniques ($R^2 = 0.942$, $p > 0.001$) (Fig 2.2).

From the regression analysis, the following equation can be calculated for correcting measurements made in air:

Corrected volume = $(\sqrt{Air}vol \times 1.014 + 0.942)^2$

This equation was applied to volumes measured under air from the Val set to calculate the corrected volume for these samples. There was no significant difference between the corrected volume and the volume measured in oil for the Val set (p =0.932). For the samples in the Val set, on average the corrected air measurement was 0.5nl SD 23.3 larger than the direct measurement in air.

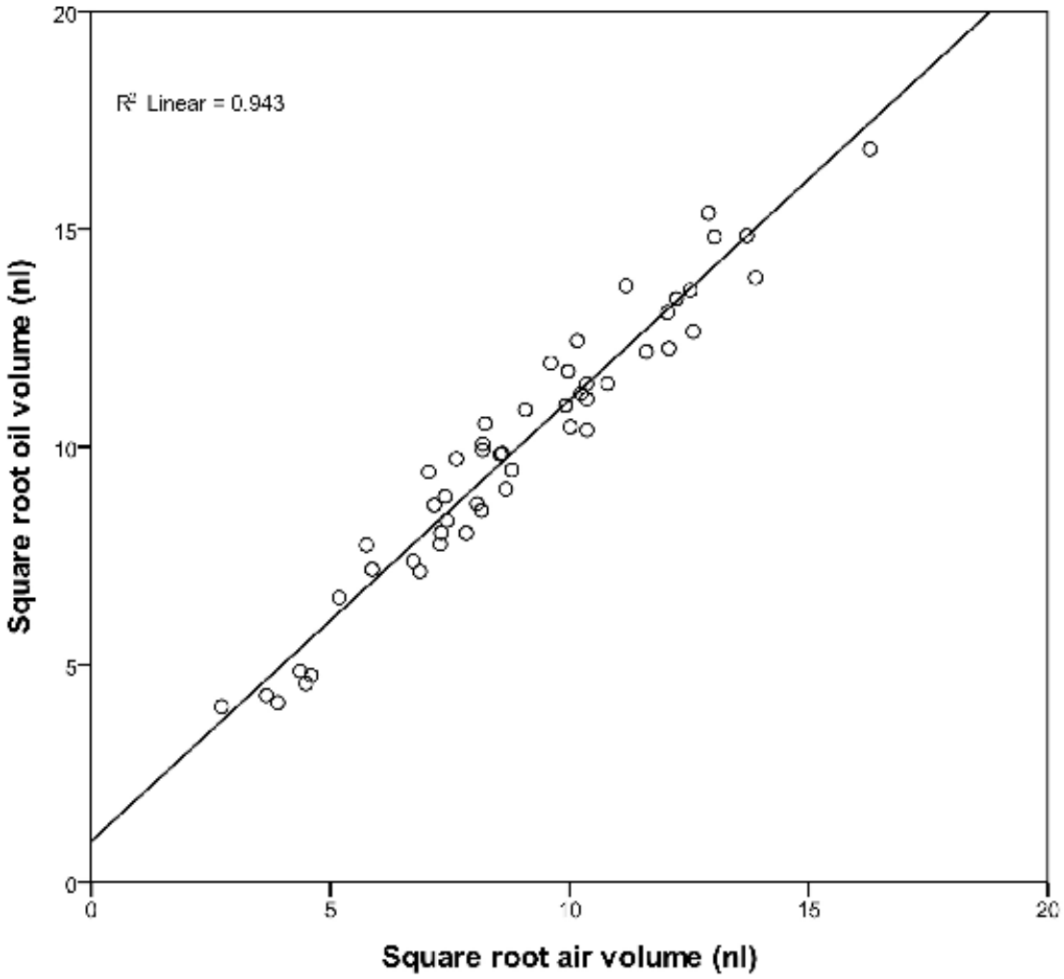

Figure 2.2 : Linear regression of 51 Cal set samples with square root transformed phloem collection volumes measured in 285 µl of oil versus square root transformed volumes estimated using flow rates measured in air and collection length

2.4 Discussion

The use of oil in the collection of phloem exudate had been used primarily to reduce errors caused by evaporation. Evaporation during collection in air has been shown to cause a significant increase in magnitude and variance of measurements of osmotic pressure in phloem exudate when compared to collections made under oil (Downing, 1978; Pritchard, 1996). The use of oil to minimise evaporation during the collection of phloem exudate by insect stylectomy is the accepted method for reducing

evaporation effects (Dinant and Kehr, 2013). Moreover the results from this work have demonstrated that the shape of the oil surface plays a significant role in accurate measurement when using optical volumetric measurement techniques. Methods making use of a droplet of oil either on the plant surface (Downing and Unwin, 1977) or for measurement of complete collection (Ponder et al., 2000) may lead to an overestimation due to the convex surface of a droplet. In this study, at the largest oil volume there was an average error of 31.2 % when compared to droplet weights (see Table 2.1), so droplets measured in droplets of oil on a flat surface may potentially over-estimate by as much as 30 %; a significant potential source of variability for quantitative analysis. For techniques using wells located on the plant surface (Fisher and Cash-Clark, 2000) or surrounding the plant (Pritchard, 1996) it may be possible to standardise the volume of oil used to ensure correct measurements. In these published methods there is no mention of the well/container size so it is difficult to know what volumes are involved but any inconsistency in the size of the well or oil container may affect oil volume and thus create errors in volume measurements. In Table 2.1 it can be seen that a variation in oil volume of less than 2 % has a significant effect on the accuracy of volume measurements under oil. So it can clearly be seen that small variations in oil volume will significantly affect volume measurement.

Table 2.1 : Droplet measurement error (%) due to different total liquid volumes (oil + MilliQ volume) and difference of the total liquid volume from optimum (%).

Total liquid volume (µl)	n	% error	% difference in oil volume from optimum volume
260	10	-14.4	8.77
270	10	-10.8	5.26
275	10	-9.2	3.51
280	14	-4.9	1.75
285	15	-0.1	0
290	15	8.1	1.75
295	13	17.0	3.51
300	15	21.6	5.26
310	10	31.1	8.77

% error = (mean optical volume – mean droplet weight) * 100/ mean droplet weight

For analytical techniques where oil may cause interferences, collection and measurement in air has been used with a correction factor (Gattolin et al., 2008). The correction factor developed by Gattolin et al. was a power function owing to the method used where the time taken for the droplet to reach a specific size is used to calculate flow rate. Slower-flowing stylets require longer measurement times and so are exposed to greater evaporation bringing about the power function relationship. This work has demonstrated that image capture and software can be used to reduce the time that droplets are exposed to air and when combined with the improved accuracy of the oil measurement, a linear correction equation can be calculated. Both techniques could be used in future work exploring the elemental, metabolite and protein composition of phloem exudate collected from single stylets. This will help expand on the current body of work in phloem proteomics (Aki et al., 2008; Gaupels et al., 2008), micronutrient transport (Stangoulis et al., 2010) and phloem metabolomics (Mendoza-Cózatl et al., 2008).

2.5 Conclusion

Oil is commonly used to counter evaporation during the collection of phloem by aphid stylectomy. This work demonstrates that oil volume has a significant effect on the accuracy of optically measured volume. When oil volume is optimised, optical measurement of nl volumes in oil is extremely accurate. Oil also has the potential to interfere with analysis of phloem exudate and this work demonstrates an improved technique for measuring phloem volume in air. An equation to correct for evaporation was able to be calculated to ensure the accuracy of volume measurement was maintained.

2.6 Methods

2.6.1 Solutions

Oil (Paraffin oil, LABCHEM™, Ajax Finechem) was produced by mixing two parts oil with one part Milli-Q™ water and shaking for 2 hours on a rotary shaker, then allowed to separate after which excess water was removed. All nitric acid solutions used in this research were prepared using Instrument Quality acid (Seastar) diluted v/v in Millipore Milli-Q™ water (>18.2 MΩ cm^{-1}) using acid washed volumetric glassware. All ICP-MS standards used in this research were prepared using a Gilson dual syringe auto-dilutor from certified single element stock solutions (1000 µg ml^{-1} High-Purity Standards). All final solutions contain 2 µg L^{-1} Indium (In) as an ISTD to aid spectrometric analysis.

2.6.2 Volume measurement under oil

Using a positive displacement pipette, volumes of oil were measured onto the lid removed from a 1.5 ml centrifuge tube. For µl volume droplets, droplets were deposited onto the oil surface using an air displacement pipette and weighed to the nearest 0.1 mg. For nl volume droplets, a glass microcapillary was used to deposit

the droplet immediately beneath the oil surface. All droplets were photographed in oil using a Leica microscope (M165C or MZ16) with an attached camera (DFC295 or DFC280). The radius (µm) of the droplet was measured using the Leica Application Suite (v 3.6.0) with the additional Interactive Measurements Module and the volume of the droplet estimated.

2.6.3 Using ICP-MS to measure nl volumes

After samples were photographed, a 1.5 ml centrifuge tube was placed over the cap containing the oil and droplet and centrifuged briefly at 13,000 rpm. 1 ml of diluting solution (2 % nitric acid, 2 µg L^{-1} In) was added, vortexed briefly, inverted 10 times and poured into a 15 ml Greiner tube. This was repeated with four 1 ml rinses of the dilution solution. For the final rinse, a pipette was used to remove the rinse solution. A final 5 ml of diluting solution was added to the 15 ml Greiner tube to make to 10 ml + oil. 3 ml aliquots were loaded into 6 ml polypropylene vials (G3160-65303, Agilent) and analysed by ICP-MS (Agilent 7500cx with integrated autosampler). A 0.1 ml min^{-1} MicroMist nebulizer (Glass Expansion) was used with 0.89 mm ID peristaltic tubing (0.89-ORG, Glass Expansion). The reaction cell was run in Helium mode with a gas flow rate of 4.5 ml min^{-1} and the equipment was tuned using the autotune function. Mass spectrum data acquisition was repeated three times per sample. For each replication three points were used for integration, for Cobalt (Co), mass 59 was integrated for 3 seconds per point and for In, masses 115 and 118 were integrated for 1 second per point. Fe masses 56 and 57 and Zn mass 66 were also acquired at 1 second per point, to check for contamination (data not shown). This gave a total acquisition time of 76.38 seconds per sample. Using the ICP-MS result, in combination with the concentration of the Co standard solution, the volume of the droplet could be estimated.

2.6.4 Standard addition

From the nl samples, three Co and one blank sample were selected. After the samples had been diluted, four 1.5 ml aliquots were taken. To each aliquot from each sample, 1.5 ml of a calibration standard (0, 5, 10 and 20 µg L^{-1}) were added, mixed well and the 3 ml volume run as detailed above.

2.6.5 Plant Material

Wheat (*Triticum aestivum* L. genotype 'SAMNYT 16') seedlings were grown in 70x100 mm pots in Debco™ Green Wizard potting mix within a growth room. Growth room conditions were 13/11 h light/dark at 20°C/10°C with a minimum of 400 µmol m^{-2} s^{-1} light at the leaf surface. Plants were transferred to a glasshouse immediately prior to addition of aphids. Plants were grown until full emergence of the inflorescence and used for up to approximately 20 days after anthesis.

2.6.6 Aphid Stylectomy

Aphid stylectomy procedures were adapted from Downing and Unwin (1977). Aphids were secured to wheat plants using specially prepared cages; a minimum of 12 h prior to stylectomy. Aphids were taken from an anholocyclic *Sitobion miscanthi* (Indian grain aphid) culture maintained at Flinders University on wheat plants kept under glasshouse conditions. Only apterous aphids were used in the experiments. Plants were watered to saturation at time of the addition of aphids. On the day of collection, plants were taken from the glass house between 2 and 3pm (Australian central daylight savings time, ACDT) and stylets cut up until 5pm ACDT. Stylectomy was performed using high-frequency micro-cauterisation under a Leica microscope (M165 C or MZ16) using an electrolytically-sharpened tungsten needle in combination with a micromanipulator. Exudate samples were collected using oil backfilled glass micro-capillaries (30-0017, Harvard Apparatus) pulled using a

capillary puller (Narishige). Collections were made between February and April with the relative humidity during collection ranging from 41 % to 50 %.

2.6.7 Microscope measurement of nl phloem exudate collections

Measurement of exudate collections was modified from previously reported methods (Fisher and Cash-Clark, 2000; Gattolin et al., 2008). The volumes for each collection were measured twice by multiplying an estimated average flow rate by the length of collection and total volume of the finished collection measured in oil contained within a 1.5 ml centrifuge tube cap (as detailed previously). Exudate flow rates were estimated from photo sequences taken using a Leica microscope (M165C or MZ16) with an attached camera (DFC295 or DFC280) and the multi-time module from the Leica Application Suite software (v3.6.0). Photo sequences were taken immediately after obtaining an exuding stylet, approximately every 15 minutes during collection and immediately prior to the end of the collection. Photo sequences consisted of five photos with a one second interval between each photo. The droplet radius for each photo in a sequence was measured using the interactive measurement module within the Leica Application Suite and an estimate of droplet volume calculated. Using the time interval between each photo in a sequence the exudation flow rate was estimated from the change in volume between photos. The average of the estimated flow rate from all sequences in each collection was multiplied by the respective collection length to give an estimate of the collection volume.

2.6.8 Abbreviations

oil: Water saturated mineral oil; ICP-MS: inductively coupled plasma-mass spectrometry; ISTD: Internal Standard; ACDT: Australian central daylight saving time.

2.6.9 Competing interests

The authors declare that they have no competing interests.

2.7 Authors' contributions

LJP helped in conceiving study, collected phloem samples, did ICP-MS analysis, statistical analysis and drafted the manuscript. LTP was involved ICP-MS analysis and study design. JP provided the stylectomy collection methods and assisted in study design. RG helped in the design of the study and was responsible for the idea of using the ICP-MS for measuring droplet volume. JS participated in conception and design of the study and assisted with drafting of manuscript. All authors read and approved the final manuscript.

2.8 Acknowledgements

The authors wish to acknowledge HarvestPlus for helping to fund this work. We would also like to acknowledge Jason Young at Flinders Analytical for his assistance with the use of the ICP-MS

Chapter 3. Nutrient variability in phloem: examining changes in K, Mg, Zn and Fe concentration during grain loading in common wheat (*Triticum aestivum* L.).

Lachlan J. Palmer[1*], Lyndon T. Palmer[2], Michael A. Rutzke[3], Robin D. Graham[1] and James C. R. Stangoulis[1]

[1] School of Biological Sciences, Flinders University, Bedford Park, South Australia 5042, Australia, [2] School of Agriculture Food and Wine, University of Adelaide, Waite Campus, Urrbrae, South Australia 5064, Australia, [3] Agriculture and Health, Cornell University, Ithaca, NY 14853

*Corresponding Author: Lachlan James Palmer

Email: Lachlan.palmer@flinders.edu.au

Full reference for chapter publication; refer to section 3.7 for author contributions:

Palmer, L. J., Palmer, L. T., Rutzke, M. A., Graham, R. D. and Stangoulis, J. C. R. (2014), Nutrient variability in phloem: examining changes in K, Mg, Zn and Fe concentration during grain loading in common wheat (Triticum aestivum). Physiologia Plantarum. doi: 10.1111/ppl.12211

3.1 Abstract

In wheat, nutrients are transported to seeds via the phloem yet access to this vascular tissue for exudate collection and quantitative analysis of elemental composition is difficult. The purest phloem is collected through the use of aphid stylectomy with volumes of exudate collected normally in the range of 20 to 500 nl. In this work a new method using inductively coupled plasma mass spectroscopy (ICP-MS) was developed to measure the concentration of K, Mg, Zn and Fe in volumes of wheat (*Triticum aestivum* L. genotype, SAMNYT 16) phloem as small as 15.5 nl. This improved method was used to observe changes in phloem nutrient concentration during the grain loading period. There were statistically significant increases in phloem Mg and Zn concentration and a significant decrease in K over the period from 1-2 days after anthesis (DAA) to 9-12 DAA. During this period, there was no statistically significant change in phloem Fe concentration.

3.1.1 Key words

ICP-MS, iron, magnesium, phloem, potassium, transport, wheat, zinc

3.1.2 Abbreviations

ICP-MS = Inductively Coupled Plasma Mass Spectroscopy, DAA = Days after anthesis, WSPO = water-saturated paraffin oil

3.2 Introduction

Of the elements in the periodic table, there are a selection that is essential to maintaining health in both plants and humans. These have been divided into macronutrients and micronutrients with the former making up 0.1 % or more of dry weight mass in higher plants (Marschner, 1995) and are required in the range of grams per kilogram in the human diet (O'Dell and Sunde, 1997). In contrast, micronutrients are found in milligrams per kilogram (or less) of plant dry weight and dietary intake (Marschner, 1995; O'Dell and Sunde, 1997). In higher plants, N, P, S, K, Mg and Ca make up the essential macronutrients whilst Fe, Mn, Zn, Cu, B, Mo, Cl and Ni are the main essential micronutrients (Marschner, 1995). From these essential minerals required for plant growth: Ca, Cl, P, K, Mg and N are also essential macronutrients and Fe, Cu, Mn, Mo, Zn are essential micronutrients needed for maintaining human health (O'Dell and Sunde, 1997). This implies that there is a consistency with essentiality between plant and animals for many essential elements. Plants are an important part of direct and indirect nutrient intake in human diets and so nutrient status of crops play an important role in human nutrition.

Human deficiency in Fe and Zn has been identified as a serious issue of concern for developing countries. In a 2002 World Health Organisation report it was estimated that in 2000, 1.6 million people died as a direct result of Fe and Zn deficiency and more than 60 million DALYs were lost (World Health Organisation, 2002). Of those DALYs lost, approximately 60 % occurred in developing countries within Africa and South and South-East Asia (World Health Organisation, 2002). Biofortification of staple crops has been identified as a possible way of combating the issue of micronutrient deficiency (Mayer et al., 2008) and attempts to increase the levels of mineral and vitamin micronutrients in the harvested and edible plant parts using

genetic or agronomic techniques is currently underway. An important part of the mineral biofortification process is the transport of these elements from the source to the sink (i.e. from soil, through to the roots, leaves and then to the seed). Within a plant, the critical part of this transport occurs through the long distance transport pathways of the xylem and phloem (Atwell et al., 1999). In the case of wheat and barley, the phloem is very important as there is a xylem discontinuity at the base of the grain (Zee and O'Brien, 1970) which results in all macro and micro nutrients first moving into the phloem before unloading into the grain. If we are to identify genotypic variation and the mechanisms involved in nutrient transport to seeds, we first need robust methods of collecting and analysing very small volumes of phloem exudate.

There are three main methods used for collecting phloem sap: 1. cutting the stem and collecting the liquid that exudes; 2. making use of an EDTA solution to allow a freshly cut plant part to continue to exude; 3. using insect stylectomy to collect phloem exudate (see Dinant & Kehr (2013) for further detail). The first two methods have limitations when it comes to cereal crops. Cutting the stem for collecting phloem is limited to a small selection of plant species such as castor bean (Hall and Baker, 1972) and cucurbits (Richardson et al., 1982) and is not possible for cereals. There are also concerns with contamination when collecting from cut stems, as exudates collected from the cut tissue of cucurbits were found to be contaminated with solutes from other sources such as xylem and non-conductive tissues (Zhang et al., 2012; Zimmermann et al., 2013). In wheat, phloem will not exude from cuts made to the stem or leaf under normal conditions, however phloem will exude from the grain pedicel after the removal of the seed Fisher and Gifford (1986). This method of collection is limited to older plants where the grains are firm enough to be

grasped for separation from the pedicel. Fisher and Gifford (1986) sampled phloem exudate at 20 to 22 days after anthesis (DAA) which is around the middle of grain loading and they mention that they had trouble collecting from seed that had already turned brown. This description puts an approximate Zadoks stage of 85 or soft dough (Bowden et al., 2008; Zadoks et al., 1974). With peak grain loading for Fe and Zn occurring at 10-14 DAA (Stomph et al., 2011) or Zadoks 71 to 75 (water ripe to early milk) this method is not likely to be a viable option for monitoring micronutrient loading into the grain due to the softness and size of the grain at this stage.

EDTA facilitated exudation is limited due to the difficulty in quantifying phloem volume for accurate concentration measurements and also because EDTA facilitated exudation may be contaminated by components from damaged cells other than the phloem and the apoplastic space (Dinant and Kehr, 2013). Insect stylectomy using aphids (Lohaus et al., 2000) and planthoppers (Hayashi and Chino, 1990) has been used to access the phloem of cereal crops for the analysis of elemental content. The main limitation of stylectomy based collection of phloem is the small volumes involved. With exudation rates ranging from 4.2 to 354 nl h^{-1} (Palmer et al., 2013) volumes collected are in the low microlitre to nanolitre range (Mittler, 1958; Palmer et al., 2013). Due to these small volumes, accurate measurement of phloem collections has been difficult. In previous work reporting the elemental composition of phloem, exudate volumes were measured using calibrated microcapillaries of different volumes, 1 µl (Hayashi and Chino, 1986) or 0.5 µl (Lohaus et al., 2000), at the reported flow rates these collections could take five or more hours to complete. The work reported here will demonstrate the use of a new approach using inductively coupled plasma mass spectroscopy (ICP-MS) which enables the quantification of K, Mg, Zn and Fe concentration in phloem collections of less than one hour and

volumes as small as 15.4 nl. This technique will be applied to examine changes in phloem composition for K, Mg, Zn and Fe over the course of grain development in the period after anthesis.

3.3 Materials and Methods

3.3.1 Solutions

Water-saturated paraffin oil (WSPO, LABCHEM™, Ajax Finechem) was produced by mixing two parts oil with one part MilliQ water and shaking for 2 h on a rotary shaker. The solution was centrifuged briefly at 5000 rpm and excess water was removed. All nitric acid solutions used in this research were prepared using Instrument Quality acid (Seastar) diluted v/v in high purity water (>18.2 MΩ cm^{-1} resistivity) using acid washed volumetric glassware. All inductively coupled plasma-mass spectrometry (ICP-MS) standards used in this research were prepared using a Gilson dual syringe auto-dilutor from certified single element stock solutions (1000 µg ml^{-1} High-Purity Standards). All final calibration and diluting solutions contain 2 µg L^{-1} indium (In) as an internal standard.

3.3.2 Plant Material

Wheat (*T. aestivum* L. cv. 'SAMNYT 16') seedlings were grown in 70x100 mm pots in Debco™ Green Wizard potting mix within a growth room. Growth room conditions were 13/11 h light/dark at 20°C/10°C with a minimum of 400 µmol m^{-2} s^{-1} photosynthetic photon flux density at the leaf surface. Plants were transferred to a greenhouse where aphids were applied and kept there for a maximum of 48 h.

3.3.3 Aphid Stylectomy

Aphid stylectomy procedures were adapted from Downing and Unwin (1977). Aphids were taken from an anholocyclic *Sitobion miscanthi* (Indian grain aphid)

culture maintained at Flinders University on wheat plants kept under greenhouse conditions. Only apterous aphids were used in the experiments. Table 3.1 shows the maturity ranges of plants used and the average days after anthesis (DAA) for phloem collections.

Table 3.1 : Mean, standard deviation and samples size for maturity clusters based on days after anthesis (DAA) used for statistical analysis of phloem element concentration.

Maturity range (DAA)	Mean	SD	n
1-2	1.3	0.48	25
9-12	10.3	0.92	17
13-16	14.3	0.72	15
17-21	18.7	1.00	26

Aphids were secured to wheat plants (immediately below the head on the peduncle), a minimum of 12 h prior to stylectomy, using specially prepared cages. Plants were watered to saturation at time of aphid caging. Stylectomy was performed using high-frequency micro-cauterisation under a Leica microscope (M165 C or MZ16) using an electrolytically-sharpened tungsten needle in combination with a micromanipulator. Exudate samples were collected using glass micro-capillaries (30-0017, Harvard Apparatus) pulled using a capillary puller (Narishige).

3.3.4 Microscope measurement of nanolitre phloem exudate volumes

Measurement of exudate volumes was modified from previously reported methods (Fisher and Cash-Clark, 2000; Gattolin et al., 2008) as previously reported (Palmer et al., 2013). In brief, using a positive displacement pipette, 285 µl of WSPO was measured into a 1.5 ml centrifuge tube cap. The glass microcapillary containing the collection was then used to deposit the droplet immediately beneath the oil surface. Each droplet was immediately photographed within the WSPO using a Leica

microscope (M165C or MZ16) with an attached camera (DFC295 or DFC280). The radius (µm) of the droplet was measured using the Leica Application Suite (LAS 3.6.0) with the additional Interactive Measurements Module and the volume of the droplet estimated.

After samples were photographed, a 1.5 ml centrifuge tube was placed over the cap (containing the oil and the nanolitre droplet) and centrifuged briefly at 13,000 rpm to ensure the droplet was removed from the cap. 1 ml of diluting solution (2 % HNO_3, 2 µg L^{-1} In) was added and the tubes were vortexed briefly, and centrifuged at 13,000 rpm for approximately 30 s. The final aqueous solution was transferred, by pipette, to a new tube to reduce the amount of WSPO present during analysis.

3.3.5 ICP-MS analysis of phloem exudate

Samples were analysed by ICP-MS (Agilent 7500cx). Samples were manually drawn directly from the 1.5 ml centrifuge tubes using a 500 mm length of 0.25 mm internal diameter (ID), sample tubing connected to 0.89 mm ID peristaltic tubing (0.89-ORG, Glass Expansion) with the attached peristaltic pump set at an uptake speed of 6 revolutions per minute. A 0.1 ml min^{-1} MicroMist nebulizer (Glass Expansion) was used for sample introduction. The reaction cell was run in helium mode with a gas flow rate of 4.5 ml min^{-1} and the equipment was tuned using the autotune function. Mass spectrum data acquisition was repeated three times per sample. For each replication, three points were used for integration (see Table 3.2 for masses and integration times per point for each element). This gave a total acquisition time of 59.1 s per sample. Due to the manual handling required for the analysis of each sample, samples and blanks were processed in three batches with each batch analysed on a different day.

Table 3.2 : Element masses and integration times used for analysis by ICP-MS.

Element	Mass	Integration time per point (s)
K	39	0.1
Mg	24	0.5
Zn	66	3.0
Fe	56, 57	1.0
In	115, 118	0.2

3.4 Results

3.4.1 Blanks and Limit of Detection (LOD)

Zn, Fe and K blank values were consistent between batches with a one way ANOVA showing no significant difference (Table 3.3). There was a significant ($p<0.001$) difference in Mg concentration between batches, with batch three being higher than batches one and two (mean difference of 5.9 and 6.1 respectively with a SE of 0.27). Therefore for Mg, two blank values were used for blank subtractions during the calculation process (see Table 3.3).

Table 3.3 : Mean, standard deviation for the concentration of each element in blank samples.

Element	Mean (µg L^{-1})	Standard deviation	n	LOD (µg L^{-1})
K	4.7	2.20	100	6.6
Mg - Batch 1 and 2	3.0	0.94	60	2.8
Mg - Batch 3	8.9	2.29	40	6.9
Zn	1.3	0.33	100	1.0
Fe	0.7	0.24	100	0.7

n = sample size (n), LOD = calculated limit of detection

Prior to adjusting for collection volume, any ICP-MS phloem sample result that was below the LOD or the blank concentration for each element as listed in Table 3.3, were excluded from the analysis. The LOD is the standard deviation of the blank

results for each element multiplied by 3 (listed in Table 3.3). Based on the values presented in Table 3.3, one Fe result was excluded for being below the LOD and one Zn result was excluded due to being less than the mean blank value. For Fe and Zn, there were several extremely high phloem concentrations with a maximum Fe result of 994.7 µg L^{-1} and Zn of 168.8 µg L^{-1}. These high concentrations were most likely due to contamination that occurred during sample collection or preparation. Phloem concentrations with values greater than three times the interquartile range plus the upper quartile for each element were classed as extreme outliers and excluded from the analysis. This lead to the exclusion of three Zn and three Fe results, the results for all elements from a further two samples were excluded. These two phloem samples were of low volume and may indicate possible evaporation or magnification of measurement errors due to the smaller volumes involved. Table 3.4 shows the number of samples used in the statistical analysis presented in Table 3.5 for each maturity period.

Table 3.4 : Sample numbers for each maturity period used for statistical analysis

Element	Maturity range	n
Fe	1-2 DAA	21
	9-12 DAA	17
	13-16 DAA	15
	17-21 DAA	24
Zn	1-2 DAA	24
	9-12 DAA	15
	13-16 DAA	14
	17-21 DAA	24
Mg	1-2 DAA	24
	9-12 DAA	17
	13-16 DAA	15
	17-21 DAA	25
K	1-2 DAA	24
	9-12 DAA	17
	13-16 DAA	15
	17-21 DAA	25

DAA: days after maturity

Table 3.5 : Differences between maturity ranges for each element and the respective p values as calculated using the Tukey multiple comparison test.

Element	Maturity range (DAA)		Mean Difference (mg L^{-1})	SE of difference	p value
	I	J	J - I		
Fe	1-2	9-12	3.0	2.75	0.701
		13-16	1.6	2.85	0.948
		17-21	-2.7	2.52	0.714
	9-12	13-16	-1.4	2.99	0.963
		17-21	-5.7	2.67	0.158
	13-16	17-21	-4.2	2.78	0.430
Zn	1-2	9-12	7.3	2.88	0.061
		13-16	9.3**	2.94	0.012
		17-21	6.2	2.52	0.074
	9-12	13-16	1.9	3.25	0.933
		17-21	-1.1	2.88	0.980
	13-16	17-21	-3.1	2.94	0.728
Mg	1-2	9-12	112.6*	24.97	0.000
		13-16	87.7*	25.93	0.006
		17-21	110.9*	22.51	0.000
	9-12	13-16	-24.9	27.91	0.808
		17-21	-1.7	24.76	1.000
	13-16	17-21	23.2	25.73	0.803
K	1-2	9-12	-212.4	285.09	0.878
		13-16	-1386.7*	296.01	0.000
		17-21	-1824.6*	257.01	0.000
	9-12	13-16	-1174.3*	318.58	0.002
		17-21	-1612.2*	282.72	0.000
	13-16	17-21	-437.9	293.72	0.448

A mean negative difference indicates that the later maturity (J) was less than the earlier maturity (I) and vice versa. DAA: days after anthesis, **>95 % and * >99 % significance

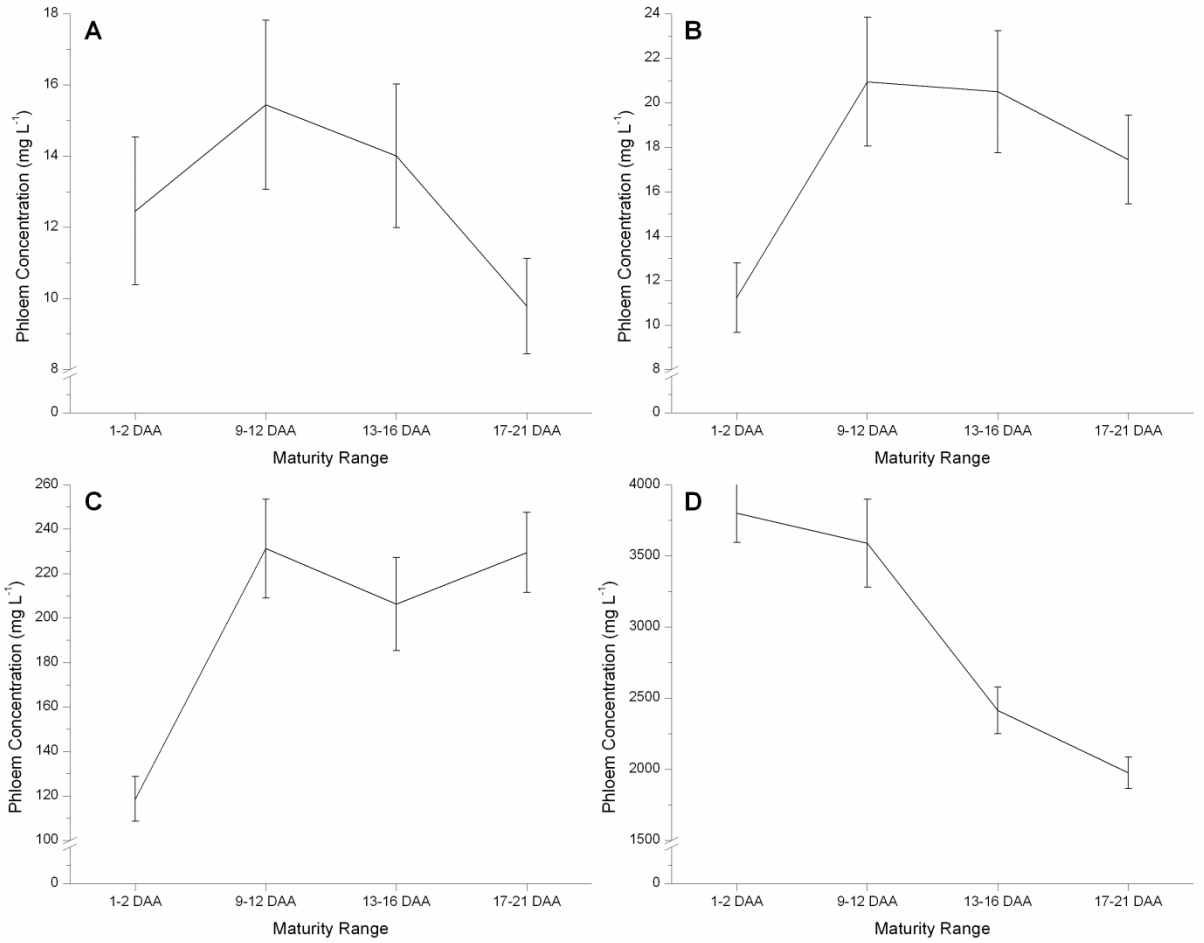

Figure 3.1 : Plot of mean phloem concentrations for Fe, Zn, Mg and K at each maturity range (A = Fe, B = Zn, C = Mg and D = K, DAA = days after anthesis, Bars = ±1 SE).

3.4.2 Potassium

A significant difference between maturities was observed for K concentration in the phloem with a reduction over the full range of sampling time (Fig. 3.1-D and Table 3.5). There was a significant decrease in phloem K concentration of 1174 ± 318.6 µg L^{-1} between 9-12 DAA and 13-16 DAA (Table 3.5). There were also non-significant decreases of K concentration in the phloem from 1-2 DAA to 9-12 DAA of 212 ± 285.1 µg L^{-1} and between 13-16 DAA to 17-21 DAA of 438 ± 293.7 µg L^{-1} (Table 3.5). Over the course of grain loading (1-2 DAA to 17-21 DAA) there was a significant decrease in K phloem concentration of 1825 ± 257.0 µg L^{-1} (Table 3.5). The maximum average K concentration observed in the phloem was 3800 mg L^{-1} (SD 1006.2) at 1-2 DAA and the minimum of 1975 mg L^{-1} (SD 554.4) occurred at 17-21 DAA.

3.4.3 Magnesium

During the exudate collection period, there was a significant increase in Mg phloem concentration (Fig. 3.1-C and Table 3.5) with an increase of 112.6 ± 24.97 µg L^{-1} between 1-2 DAA and 9-12 DAA. The Mg phloem concentration during the maturity ranges of 13-16 and 17-21 DAA were also significantly higher than at 1-2 DAA. From 9-12 DAA there were no further significant changes in Mg phloem concentrations between the other maturity ranges (9-12, 13-16 and 17-21 DAA). The maximum average Mg concentration observed in the phloem was 231.2 mg L^{-1} (SD 91.60) at 9-12 DAA and the minimum of 118.6 mg L^{-1} (SD 49.19) occurred at 1-2 DAA.

3.4.4 Zinc

There was a significant increase in Zn concentration in the phloem associated with changes in maturity (Fig. 3.1-B and Table 3.5), between 1-2 DAA and 13-16 DAA there was a significant increase of 9.3 ± 2.94 µg L^{-1} (Table 3.5). There were also non-significant increases in Zn phloem concentration from 1-2 DAA to 9-12 DAA and from 9-12 to 13-16 DAA and a non-significant decrease in phloem concentration from 13-16 DAA to 17-21 DAA (Table 3.5). The maximum average Zn concentration observed in the phloem was 21.0 mg L^{-1} (SD 11.59) at 9-12 DAA and the minimum of 11.2 mg L^{-1} (SD 7.69) occurred at 1-2 DAA.

3.4.5 Iron

There was no statistically significant change in phloem Fe concentration between any of the maturity ranges (Table 3.5). The plot of mean Fe phloem concentrations (Fig. 3.1-A) shows a trend with an increase in Fe phloem concentration after anthesis and a possible decrease in the Fe phloem concentration towards the end of grain loading. The maximum average Fe concentration observed in the phloem was 15.4 mg L^{-1} (SD 9.78) at 9-12 DAA and with the minimum of 9.8 mg L^{-1} (SD 6.58) occurred at 17-21 DAA.

3.5 Discussion

To date, the measurement of cereal phloem for macro and micronutrients has been limited. Elemental composition of the phloem has been reported in wheat (Fisher, 1987; Hayashi and Chino, 1986), maize (Lohaus et al., 2000) and rice (Ando et al., 2013; Fukumorita et al., 1983; Hayashi and Chino, 1990; Nishiyama et al., 2012; Yoneyama et al., 2010) and in these experiments, the exudate volumes collected were quite high to allow for effective analysis and accurate volume measurement. Elemental analysis of phloem has been done in different ways with sample volume

being a major problem, Table 3.6 shows the analytical methods used in previous work. Most reports of elements in the phloem do not report the limitations of the method, with no mention of blanks or detection limits. These limitations are critical for measurement of micronutrients such as Fe and Zn which are in low concentrations in the phloem and results are susceptible to contamination issues (Wheal et al., 2011).

Table 3.6 : Comparison of average Fe, Zn, Mg and K concentrations in the phloem of a variety of plant species.

Plant species	Fe (mg L^{-1})	Zn (mg L^{-1})	Mg (mg L^{-1})	K (mg L^{-1})	Analytical method	Reference
Wheat	9.8 – 15.4	11.2 – 20.5	119 - 231	1980 - 3800	ICP-MS	This work
Triticum aestivum	-	-	119	11690	IC	(Hayashi and Chino, 1986)
Triticum aestivum (anthesis/ end of grain loading)	-	-	-	1760/782	K sensitive microelectrode	(Fisher, 1987)
Zea mays	-	-	32 - 51	1950 - 2850	IC	(Lohaus et al., 2000)
Oryza sativa	3.0 – 4.1	0.9 – 1.6	-	-	GFAAS (Fe only) and ICP-MS	(Ando et al., 2013)
Oryza sativa	153	71.9	287	5880	ICP-AES	(Fukumorita et al., 1983)
Oryza sativa	-	-	-	1580 - 5890	IC	(Hayashi and Chino, 1990)
Oryza sativa	3.0	3.5	-	-	GFAAS and ICP-MS	(Nishiyama et al., 2012)
Oryza sativa (14^{th} leaf stage/ early grain fill)	2.8/3.5	2.2/7.5	-	-	GFAAS	(Yoneyama et al., 2010)
Ricinus communis	-	-	109 - 122	2300 - 4400	AAS	(Hall and Baker, 1972)
Nicotiana glauca	9.4	15.9	104	3670	AAS	(Hocking, 1980)
Grevillea leucopteris	4.7	4.3	102	1892.3	AAS	(Hocking, 1983)
Ricinus communis	-	-	90.17	2620	AAS	(Peuke, 2010)
Brassica oleracea	-	7.1-16.0	297 - 360	2330 - 2680	AAS	(Shelp, 1987)
Ricinus communis	2.5	2.5	-	-	AAS	(Schmidke and Stephan, 1995)
Ricinus communis	2.1					(Schmidke et al., 1999)
Ricinus communis	0.4 - 1.8		-	-	Colorimetric	(Maas et al., 1988)

IC = Ion Chromatography, GFAAS = Graphite Furnace Atomic Absorption Spectrometry, ICP-AES = Inductively Coupled Plasma Emission Spectroscopy, AAS = Atomic Absorption Spectrometry)

In this work we were able to report concentrations for the macronutrients, K and Mg and the micronutrients Zn and Fe in very low exudate volumes with good sensitivity. The concentrations we have reported for K of between 1975 and 3800 mg L^{-1} compare favourably to those reported in maize and rice as shown in Table 3.6. The only reported value for quantification of K concentration in the phloem of wheat was 11690 mg L^{-1} (Hayashi and Chino, 1986) which seems high compared to the other reported values. This value was obtained from a single collection so contamination or analytical issues may have affected the result, therefore it is hard to draw any conclusions in relation to our work. Another potential source of variability in K concentration may also be due to the growth conditions with the values reported for cereals in Table 3.6 being done under solution culture type conditions, where K may be passively taken up and transported throughout the plant. In work done on the osmotic composition of phloem sap, the K concentrations in the phloem at anthesis (1759 mg L^{-1}) and at the end of grain loading (782 mg L^{-1}) was estimated (Fisher, 1987), and these values are much closer to those we have reported.

The values we have reported for Mg of between 118.6 and 231.2 mg L^{-1} compare well with the value of 119.1 mg L^{-1} reported in wheat (Hayashi and Chino, 1986) and 287 mg L^{-1} reported in rice (Fukumorita et al., 1983), but are much higher than those reported in maize of between 31.6 and 51.0 mg L^{-1} (Lohaus et al., 2000). Levels of K and Mg have also been reported in the phloem of the Eudicots, *Ricinus communis*, *Nicotiana glauca*, *Brassica oleracea* and *Grevillea leucopteris* (Hall and Baker, 1972; Hocking, 1980; Hocking, 1983; Peuke, 2010; Shelp, 1987) shown in Table 3.6. Concentrations of K in the phloem of these Eudicots ranged from 1892.3 mg L^{-1} (Hocking, 1983) to 4400 mg L^{-1} (Hall and Baker, 1972), Mg in the phloem ranged from 90.17 mg L^{-1} (Peuke, 2010) to 316 mg L^{-1} (Shelp, 1987) (Table 3.6).

With the exceptions of the K concentration reported previously in the phloem of wheat (Hayashi and Chino, 1986) the concentration of K in the phloem we have reported is within the range found across cereals and eudicots. This also holds true for concentrations of Mg in phloem with the exception of the concentrations reported in maize (Lohaus et al., 2000).

To our knowledge this is the first report of micronutrients being directly measured in the phloem of wheat. The only work done previously examining micronutrients in the phloem of cereals has been done on rice. The micronutrient values reported in this work, of between 11.2 and 21.0 mg L^{-1} for Zn and between 9.8 and 15.4 mg L^{-1} for Fe, are higher than most values reported in rice (Table 3.6). Fe concentration in the phloem of rice has been reported as low as 2.8 mg L^{-1} (Yoneyama et al., 2010) and as high as 153 mg L^{-1} (Fukumorita et al., 1983). Zn concentration in the phloem of rice has been reported as low as 0.9 mg L^{-1} (Ando et al., 2013) and as high as 71.9 mg L^{-1} (Fukumorita et al., 1983). The values reported by Fukumorita et al. (1983) are much higher than other values reported in rice and there is no detail on replication and no error value reported for these values which makes it difficult to make comparisons to these values. The other reports for Fe and Zn concentration in the phloem of rice range between 2.8 to 4.1 mg L^{-1} and 0.9 to 7.5 mg L^{-1} respectively (Ando et al., 2013; Nishiyama et al., 2012; Yoneyama et al., 2010). These reports are much more consistent though one factor for the difference may be due to most collections having been made during the vegetative phase. The one report where collections were made during early grain loading accounted for the highest Zn phloem concentration of 7.5 mg L^{-1} and in this study the highest Fe concentration of 3.5 mg L^{-1} was also found during grain loading (Yoneyama et al., 2010). Fe and Zn concentrations in phloem have also been reported in the eudicots as shown in Table

3.6. These values for rice, eudicots and our results from wheat indicate that there may be a species related difference for Fe and Zn in the phloem. This combined with the results observed in this work indicating significant changes in wheat during grain loading also points to differences that occur due to plant maturity. In *Ricinus communis* it has also been found that the nutrition status of the plant can affect the levels of micronutrients in the phloem (Maas et al., 1988) which may also help to explain differences between these reports.

Another point of difference is the collection methods involved. For the eudicot values, phloem was collected by making incisions on the stem and collecting bleeding exudate. This enables the quick collection of relatively large volumes but is not a viable method for cereals as they do not readily "bleed". For the values reported previously for phloem collected from cereals, collections were made by using stylectomy and then placing a microcap of a known volume over the stylet and waiting for the capillary to fill. This method requires long collection times with maize phloem flow rates of between 100 to 250 nl h^{-1} (Lohaus et al., 2000) and 200 nl h^{-1} in rice (Kawabe et al., 1980). This means that for a 500 nl microcap it would take between 2 and 5 h to complete a collection (Lohaus et al., 2000). It is our experience that not all stylets flow for these lengths of time. Collections made over long time periods would reduce throughput and make it difficult to study diurnal variability, compare genotypes or treatments. The new method for measurement of phloem collection volume (Palmer et al., 2013) in use for this report demonstrates successful analysis of collections made in under an hour of minimal volume and this increases throughput, with four collections in an afternoon being possible.

The reduction in the concentration of K with maturity has been observed previously in rice and wheat (Fisher, 1987; Hayashi and Chino, 1990). The work in rice observed a decrease of 4172 mg L^{-1} or 72 % in K concentration between the collection times of 7^{th} to 8^{th} leaf stage and one week after anthesis (Hayashi and Chino, 1990). In wheat, an estimated decrease in K concentration of 977 mg L^{-1} or 55 % was observed between anthesis and the end of grain loading (Fisher, 1987) . This compares favourably to the significant decrease in K concentration of 1825 or 48 % observed in this work; between 1-2 DAA and 17-21 DAA. For the work in rice, the much larger change between the two time points may be a combination of the early collection being made prior to head formation and also due to the collections being made at different locations on the plant.

To our knowledge this is the first report of a significant change in Mg and Zn concentrations during the grain loading period in cereals. Work done on Zn turn-over during grain loading has shown that the time of maximum Zn turnover occurs between 10 to 14 DAA (Stomph et al., 2011). This helps explain the significant change in phloem Zn concentration from 1-2 DAA to 9-12 DAA where demand has increased and the level of Zn in the phloem has also increased. Mg may also be following this pattern. The major difference between Zn and Mg is at the 17-21 DAA sampling point where the concentration of Zn decreases and is no longer significantly different to concentrations in the phloem at 1-2 DAA, whilst the concentration of Mg remains constant and significantly higher than 1-2 DAA. The results for Fe concentration in the phloem, though not significant, appear to follow a similar trend to Zn where Fe increases during the peak loading period of 10 to 14 DAA and then falls away after this. This decrease in phloem concentration observed for Zn and Fe after this 10 to 14 DAA period though not significant may be an added

indicator for the importance of the period 10 to 14 DAA for loading of micronutrients into the grain.

In conclusion, the results found in this work give an important insight into what is occurring within the phloem during the critical grain loading period and demonstrates the value of this technique in monitoring the transport of critical elements. It is hoped that in future work, this sensitive technique for elemental analysis may be combined with analysis for metabolites and molecular based analyses to further detail the role of phloem in transport and signalling for element and micronutrient transport.

3.6 Author contributions

LJP helped in conceiving the study, collected phloem samples, did ICP-MS analysis, statistical analysis and drafted the manuscript. LTP was involved in ICP-MS method development, analysis and study design. MAR determined the feasibility of ICP-MS analysis of nl phloem volumes and assisted in study design. RG helped in the design of the study and was responsible for the idea of using the ICP-MS for measuring droplet volume. JS participated in conception and design of the study and assisted with drafting of manuscript. All authors read and approved the final manuscript.

3.7 Acknowledgments

We would like to acknowledge Jason Young at Flinders Analytical for his assistance with the use of the ICP-MS.

Chapter 4. Metabolite profiling of wheat (*Triticum aestivum* L.) phloem exudate

Lachlan James Palmer[1*], Daniel Anthony Dias[2], Berin Boughton[2], Ute Roessner[2], Robin David Graham[1] and James Constantine Roy Stangoulis[1]

[*] Corresponding author Email: Lachlan.palmer@flinders.edu.au

[1] School of Biological Science, Flinders University, Bedford Park, South Australia 5042, Australia

[2] Metabolomics Australia, School of Botany, The University of Melbourne, Parkville, Melbourne 3010, Victoria, Australia

Full reference for chapter publication; refer to section 4.9 for author contributions:

Palmer L, Dias D, Boughton B, Roessner U, Graham R, Stangoulis J (2014) Metabolite profiling of wheat (Triticum aestivum L.) phloem exudate. Plant Methods **10**: 27

4.1 Abstract

4.1.1 Background

Biofortification of staple crops with essential micronutrients relies on the efficient, long distance transport of nutrients to the developing seed. The main route of this transport in common wheat (*Triticum aestivum*) is via the phloem, but due to the reactive nature of some essential micronutrients (specifically Fe and Zn), they need to form ligands with metabolites for transport within the phloem. Current methods available in collecting phloem exudate allows for small volumes (µl or nl) to be collected which limits the breadth of metabolite analysis. We present a technical advance in the measurement of 79 metabolites in as little as 19.5 nl of phloem exudate. This was achieved by using mass spectrometry-based metabolomic techniques.

4.1.2 Results

Using gas chromatography–mass spectrometry (GC-MS), 79 metabolites were detected in wheat phloem. Of these, 53 were identified with respect to their chemistry and 26 were classified as unknowns. Using the ratio of ion area for each metabolite to the total ion area for all metabolites, 39 showed significant changes in metabolite profile with a change in wheat reproductive maturity, from 8–12 to 17–21 days after anthesis. Of these, 21 were shown to increase and 18 decreased as the plant matured. An amine group derivitisation method coupled with liquid chromatography MS (LC-MS) based metabolomics was able to quantify 26 metabolites and semi-quantitative data was available for a further 3 metabolites.

4.1.3 Conclusions

This study demonstrates that it is possible to determine metabolite profiles from extremely small volumes of phloem exudate and that this method can be used to

determine variability within the metabolite profile of phloem that has occurred with changes in maturity. This is also believed to be the first report of the presence of the important metal complexing metabolite, nicotianamine in the phloem of wheat.

4.1.4 Keywords

Aphid stylectomy, Exudate, Grain loading, GC-MS, LC-MS, Metabolomics, Method development, Phloem, Wheat

4.2 Background

Deficiencies of Fe and Zn in humans have been identified as a serious issue of concern for developing countries. In a 2002 World Health Organisation report it was estimated that in 2000, 1.6 million people died as a direct result of Fe and Zn deficiency and a further 60 million DALYs were lost (World Health Organisation, 2002). Approximately 60 % of the DALYs lost occurred in developing countries within Africa and South-East Asia (World Health Organisation, 2002). Biofortification of staple crops has been identified as a possible way of combating the issue of micronutrient deficiency (Mayer et al., 2008) and attempts to increase the levels of mineral and vitamin micronutrients in the harvested and edible plant parts using genetic or agronomic techniques is currently underway (Murgia et al., 2012). An important part of the mineral biofortification process is the transport of these elements from the source to the sink (i.e. from soil, through to the roots, stems and leaves, and then to the seed). Within a plant, the long distance transport pathways of the xylem and phloem are the major routes for nutrient movement to developing seeds (Atwell et al., 1999). In the case of wheat, the phloem is very important as there is a xylem discontinuity at the base of the grain (Zee and O'Brien, 1970) which results in all macro and micro nutrients first transferring to the phloem before unloading into the grain. During the transport of Fe and Zn in the phloem these

minerals must be complexed due to their reactive nature (Blindauer and Schmid, 2010). A variety of metabolites have been theorised to complex Fe, Zn and other essential minerals within the phloem (Harris et al., 2012). Of these, nictoianamine and cystine are proposed to play a major role in the modelled transport of Fe and Zn (Harris et al., 2012), and in rice, nicotianamine (NA) has been found to complex Zn in the phloem (Nishiyama et al., 2012).

Phloem is a complex matrix which consists of water, sugars, amino acids, organic acids, secondary metabolites, peptides and hormones along with ions and a number of macromolecules, including proteins, small RNAs and mRNAs (Dinant et al., 2010; Turgeon and Wolf, 2009). Recent reviews have highlighted the importance of phloem composition in long-distance transport and signalling throughout the plant (Dinant et al., 2010; Turgeon and Wolf, 2009) and these reviews have also examined the difficulty and other issues related to collection of phloem for analysis. There are three main techniques by which phloem can be collected for direct analysis: 1) cutting the stem and collecting the liquid that exudes; 2) making use of an Ethylenediaminetetraacetic acid (EDTA) solution to allow a freshly cut plant part to continue to exude; 3) using insect stylectomy to collect phloem exudate (see 2013) for further details). The first two methods have limitations when applied to cereal crops. Cutting the stem for collecting phloem is limited to a small selection of plant species such as castor bean (Hall and Baker, 1972) and cucurbits (Richardson et al., 1982) and is not possible for cereals. In wheat, phloem will not exude from cuts made to the stem or leaves under field or glasshouse conditions; however phloem will exude from the grain pedicel after the removal of the seed (Fisher and Gifford, 1986). This limits the accessibility to wheat phloem and also involves interference with the developing ear. EDTA facilitated exudation also has its limitations, owing to

the difficulty in quantifying phloem volume for accurate concentration measurements and also because EDTA facilitated exudation may be contaminated by components from damaged cells other than the phloem and the apoplastic space (Dinant and Kehr, 2013). Insect stylectomy using aphids and planthoppers has been used to access the phloem of cereal crops for the analysis of some metabolites within the phloem (Gattolin et al., 2008; Nishiyama et al., 2012). The main limitation of stylectomy based collection is the small volumes involved. With exudation rates ranging from 4.2 to 354 nl h^{-1} (Palmer et al., 2013) volumes collected are in the low µl to nl range (Mittler, 1958; Palmer et al., 2013). Due to these small volumes, accurate measurement of phloem collections has been difficult which has limited the scope of metabolomic profiling of the phloem. In most reports of metabolites in phloem collected by stylectomy, collections were made over several hours to enable sufficient volumes to be collected for analysis as measured using 0.5 µl micro capillaries (Nishiyama et al., 2012; Winter et al., 1992). In more recent work, an alternative technique for measuring phloem volume has been used to measure diurnal variability in amino acid concentrations in volumes as little as 2.1 nl (Gattolin et al., 2008). In this current research, we demonstrate the use of accurate volume measurements for the quantitative analysis of amine-containing metabolites detected by LC-MS and semi-quantitative analysis of the metabolite profile of wheat phloem using GC-MS. We will also present the results of semi-quantitative analysis of changes in the metabolite profile during the grain loading period.

4.3 Results

4.3.1 GC-MS metabolite profiling

GC-MS metabolomic profiling was tested as this has been used previously to profile the metabolites in plant tissues. For example, tissue level changes as a tolerance

response to Fe deficiency in peas (Kabir et al., 2013). Table S1 in Additional file 1 details all 79 metabolites identified by GC-MS and for some metabolites, multiple derivatives are created and these are shown in Table S2 of Additional file 1 as they were included in calculations of the ion ratio. Of the 79 metabolites identified it was found that 40 had non-normal distributions and attempts were made to transform the data prior to statistical analysis. Of the 40 metabolites, 2 were not able to be transformed to produce a normal distribution (Table S3 in Additional file 1) and so were not included in statistical testing.

Of the 79 metabolites detected, there were 26 unknown compounds found and these were not identified using either in-house or commercial libraries nor the GOLM Metabolome Database (Kopka et al., 2005), so they are listed with the following notation. UN1_10.61_158 = Unknown 1 with a retention time of 10.61 minutes with a unique ion at 158 *m/z*. The area of a particular fragment ion was selected and was subsequently adjusted for each sample by dividing it by the volume of phloem collected and then the ratio of this area to the total area for all identified ions in the sample was calculated and used for statistical comparison between different stages during grain loading.

The results from independent student *t*-tests on metabolites showing significant changes between peak grain loading (8-12 DAA) and the end of grain loading (17-21 DAA) are shown in Tables 4.1 and 4.2. The results listed in Table 4.1 show the 18 metabolites had a statistically significant decrease in the phloem as grain loading progressed, from 8-12 DAA to 17-21 DAA. Ornithine had the greatest reduction showing a 4.6 fold decrease, 3-amino-piperidin-2-one, UN08 and Glutamine also declined by 3.5, 3.4 and 2.6 fold respectively (Table 4.1). There were another seven

metabolites that had more than a two-fold decrease as grain loading progressed (Table 4.1).

There were 21 metabolites that had a significant increase in the phloem as grain loading progressed from 8–12 DAA to 17–21 DAA (Table 4.2). Of these, shikimic acid had the greatest increase (2.9 fold), while quinic acid, succinate and glycine also had more than a 2 fold increase (2.5, 2.3 and 2.2 respectively, Table 4.2).

.

Table 4.1 : The fold change in metabolite relative response ratios in the phloem, profiled using GC-MS, that significantly decreased ($p < 0.05$) from 8-12 DAA to 17-21 DAA.

Metabolite	Transformation	Levene's test for equality of variances sig.	*t*-test for equality of means sig. (2-tailed)	Fold change
3-amino-piperidin-2-one 2TMS	SQRT	0.227	0.000	−3.4
Alanine 2TMS	SQRT	0.000^{un}	0.009	−1.9
Arginine 3TMS	Ln	0.286	0.000	−2.3
Glutamate 3TMS	None	0.003^{un}	0.005	−2.3
Glutamine 3TMS	CBRT	0.296	0.001	−2.6
Histidine 3TMS	Ln	0.994	0.032	−1.9
Homoserine 3TMS	None	0.613	0.000	−1.9
Lysine 4TMS	None	0.180	0.006	−1.4
Ornithine 3TMS	None	0.001^{un}	0.007	−4.6
Pyroglutamate 2TMS	None	0.444	0.018	−1.3
Serine 3TMS	None	0.073	0.000	−1.6
Trehalose 8TMS	Ln	0.952	0.000	−3.5
UN01_10.61_158	CBRT	0.360	0.000	−2.3
UN07_17.62_275	Ln	0.177	0.002	−2.0
UN08_17.96_360	CBRT	0.673	0.001	−3.4
UN09_18.15_275	CBRT	0.363	0.003	−2.0
UN11_19.48_299	CBRT	0.003^{un}	0.003	−2.0
UN26_14.48_229	Ln	0.034^{un}	0.001	−1.9

Also shown are the *p* values for Levene's test of equality of variance, where values are less than 0.05 (equal variances not assumed = ^{un}), equal sample variances were not assumed when calculating *t*-test. *x*TMS = Trimethylsilyl derivative where *x* = the number of TMS groups, sample numbers (n) = 8-12 DAA = 15, 17-21 DAA = 16.

Table 4.2 : The fold change in metabolite relative response ratios , profiled using GC-MS, that significantly increased ($p < 0.05$) in the phloem from 8-12 DAA to 17-21 DAA

Metabolite	**Transformation**	**Levene's test for equality of variances sig.**	***t*-test for equality of means sig. (2-tailed)**	**Fold change**
Citric acid 4TMS	None	0.512	0.000	1.8
Fructose_MX1	None	0.002^{un}	0.000	1.8
Fumarate 2TMS	None	0.000^{un}	0.004	1.6
Gluconic acid-1,5-lactone 4TMS	None	0.066	0.002	1.7
Glucose MX1	None	0.008^{un}	0.002	1.7
Glycine 3TMS	None	0.026^{un}	0.000	2.2
Hexadecanoate 1TMS	SQRT	0.004^{un}	0.017	1.9
Methionine 1TMS	None	0.337	0.024	1.3
Octadecanoate 1TMS	SQRT	0.028^{un}	0.021	1.8
Phenylalanine 2TMS	None	0.654	0.018	1.5
Putrescine 4TMS	None	0.697	0.000	1.9
Quinic acid 5TMS	SQRT	0.010^{un}	0.007	2.5
Shikimic acid 4TMS	SQRT	0.060	0.000	2.9
Succinate 2TMS	None	0.000^{un}	0.010	2.3
Tyrosine 3TMS	None	0.180	0.000	1.8
UN04_15.56_185	None	0.000^{un}	0.019	1.8
UN10_19.08_217	None	0.106	0.007	1.4
UN16_25.71_339	None	0.016^{un}	0.015	1.7
UN17_27.24_375	None	0.003^{un}	0.000	1.8
UN18_28.91_437	None	0.011^{un}	0.001	1.6
UN20_32.34_503	InvCBRT	0.020^{un}	0.049	1.8

Also shown are the *p* values for Levene's test of equality of variance, where values are less than 0.05 (equal variances not assumed = ^{un}), equal sample variances were not assumed when calculating *t*-test. *x*TMS = Trimethylsilyl derivative where *x* = the number of TMS groups; MX1 = methoxyamine derivatised product, sample numbers (n) = 8-12 DAA = 15, 17-21 DAA = 16.

4.3.2 LC-MS

Quantification of amine group containing metabolites in the phloem exudates was conducted according to Boughten et al. (2011). The concentrations of the metabolites identified are detailed in Table 4.3. Two metabolites were not able to be quantified due to issues with standard stability affecting the calibration curve and the response relative to the ISTD is presented instead. To the authors knowledge this is the first time that NA has been directly quantified. For metabolites where an authentic standard was not available or could not be generated, the ratio of ion area to internal standard was used to generate a relative response. For the LC-MS analysis, phloem collection volumes used were between 43.4 nl and 180.34 nl, with an mean of 95.7 nl ± 61.43. Due to the exploratory nature of this analysis, only four samples were analysed, two from each maturity, and no significant changes were observed (data not shown). Therefore only the average for all samples is presented in Table 4.3.

Table 4.3 : Amine group containing metabolites identified in the phloem of wheat as measured by LC-MS collected at two maturities (n =4).

Metabolite	**Mean (**mmol L^{-1}***)**	**SE**
Ammonia (ISTD RR)	33.8	1.275
Glutathione (ISTD RR)	0.58	0.0905
Glutamine	170.8	50.895
Valine	75.5	17.52
Histidine	64.7	25.24
Serine	63.1	25.455
Glutamate	36.3	15.32
Arginine	39.8	3.74
Alanine	42.0	6.045
Proline	21.2	8.125
Phenylalanine	58.1	18.365
Threonine	49.7	15.515
Isoleucine	44.3	11.275
Leucine	43.7	16.34
Tryptophan	44.1	8.405
Lysine	48.0	10.315
Glycine	39.9	18.275
Tyrosine	27.7	9.495
Aspartic acid	18.7	7.205
Methionine	18.8	8.31
Asparagine	7.4	2.77
β-Alanine	1.7	0.595
gamma-aminobutyric acid	1.1	0.45
Ornithine	1.2	0.58
Citrulline (μmol L^{-1})	232.3	39.14
Nicotianamine (μmol L^{-1})*	255.4	96.71
Cysteine (μmol L^{-1})	70.9	13.91
4-Hydroxy-proline (μmol L^{-1})	38.5	9.675

*Unless otherwise stated mean and standard error of all quantitated metabolites are reported as mmol L^{-1}. Metabolites that were measured but did not have an external standard are reported as a ratio of response in relation to the internal standard (ISTD RR). * *n* = 3, outlier was removed.

4.4 Discussion

The analysis of the metabolite profile of phloem has been restricted in the past due to limitations in the amount collected and the availability and sensitivity of analytical techniques. With exudate flow rates in wheat ranging from 0.07 to 5.9 nl min^{-1} (Palmer et al., 2013), volumes that are collected per sample are normally less than 1 µl. For previous work examining metabolite profiles in the phloem, volume measurement has been done in a variety of ways (Fukumorita and Chino, 1982; Girousse et al., 1991; Sandström et al., 2000). Phloem volumes or sample amounts are estimated using the length of the liquid within the microcap (Sandström et al., 2000), the weight of sample collected (Girousse et al., 1991) or by collecting to the volume of the microcap (Fukumorita and Chino, 1982). For a series of papers examining metabolites in phloem (Lohaus et al., 1994; Lohaus and Moellers, 2000; Winzer et al., 1996), phloem volumes of between 10 and 60 nl were collected using 0.5 µl microcaps but to our knowledge there is no mention of how volume was estimated in the microcap. Even in the original method, these papers all refer to where volumes of 5 nl were collected using a 0.5 µl microcap (Riens et al., 1991) and there are no details of how the sample volume is derived. The measurement of sample volume is a key part of improving the accuracy of analysis and enables better detection of changes in metabolite profile.

One of the main issues for the accurate measurement of sub-µl volumes is evaporation and work carried out previously has demonstrated an increase in the osmotic potential when phloem samples are collected in air (Downing, 1978; Pritchard, 1996). To counter the effects of evaporation, collection of exudate under oil is the accepted method (Dinant and Kehr, 2013) but in more recent work by our laboratory, we have demonstrated that accurate measurement under oil has technical

difficulties due to the potential for measurement errors arising from the optical nature of the measurement and the surface shape of the oil used in the collection step (Palmer et al., 2013). Recent work has made advances in volume measurement: work examining the diurnal effect on the concentration of amino acids in the phloem, made use of a correction factor for air based droplet volume measurements (Gattolin et al., 2008). This technique used measurements made under oil, which reduces the effect of evaporation, as a comparison for collections measured in air and enable a correction factor to be derived. We have further refined this technique of volume measurement using digital photography and software to further reduce the effect of evaporation and to quantify the accuracy of the volume measurement (Palmer et al., 2013). This method has been used successfully to quantify inorganic components in the phloem of wheat and to detect significant changes with maturity (Palmer et al., 2014b) . Oil has also been identified as a potential contaminant for certain metabolite analyses (Gattolin et al., 2008), and we have also found that for GC-MS profiling, paraffin oil is a significant contaminant suppressing metabolite signal from the phloem causing an increase in the baseline due to the elution of multiple hydrocarbons present in paraffin oil (refer to Additional material 1 for trace images). This observation was consistent with the GC-MS analysis of petroleum based oil as a contaminant (Serra Bonvehi and Orantes Bermejo, 2012).

When using phloem samples that were measured in air we were able to identify, using GC-MS, 79 different metabolites (Table S1 of Additional file 1) and of these, 38 showed significant variability in phloem composition with a change in maturity (Tables 4.1 and 4.2). Of these metabolites with significant changes, 21 increased and 18 decreased in the phloem as the plant aged. For samples analysed using a LC-MS method specific for amine containing compounds, we were able to identify 30

metabolites and of these quantify the concentration of 27 metabolites within the phloem (Table 4.3). For the GC-MS metabolite profiling analysis, full quantification of all metabolites is not feasible. This is due to the large number of metabolites detected by GC-MS, making it unfeasible to establish calibration curves for all metabolites detected and so peak area is used for semi-quantitative analysis. Owing to the use of peak area, metabolites cannot be compared to one another as the peak area is dependent on the derivitisation process, and all metabolites have a different response factor. For specific metabolites, it may be possible to set up calibration curves for quantification of phloem concentrations by GC-MS and so allow further exploration of results of interest identified from metabolite profiling.

One result of interest is the significant changes in sugars other than sucrose within the phloem. For most work on the phloem, only sucrose is reported (Fisher, 1987; Fukumorita and Chino, 1982; Lohaus et al., 2000). It has been established that sucrose is the dominant sugar involved in sugar transport (Liu et al., 2012) and it is assumed that hexoses (glucose and fructose) are not normally present, and when they are, they are mostly seen when using EDTA facilitated exudation (Liu et al., 2012). Glucose and fructose have been shown to exist (5.5 % and 1.5 %) in the phloem of perennial ryegrass (*Lolium perenne* L.) collected from aphid stylectomy (Amiard et al., 2004). A change in sugar composition was found when plants were defoliated with a decrease of more than 80 % for sucrose concentration and decreases of 42 % and 47 % in glucose and fructose concentrations, respectively (Amiard et al., 2004). This may indicate a source other than leaf for hexoses within the phloem. The results from the GC-MS analysis highlighted a significant increase in glucose and fructose levels within the phloem during the grain loading period (Table 4.2).

Of particular interest are the results presented from the LC-MS analysis quantifying NA and demonstrating the presence of glutathione. These two metabolites have been found to play important roles in complexing essential micronutrients during long distance transport in the phloem (Harris et al., 2012; Nishiyama et al., 2012; Schmidke and Stephan, 1995; Stephan and Scholz, 1993). In a theoretical model of metabolite and micronutrient speciation in the phloem it was found that 54.4 % of Zn was likely to be bound to NA and the remaining Zn complexed with amino acid complexes of cysteine and cysteine with histidine (41.2 % and 2.8 % respectively) (Harris et al., 2012). In the case of Fe, 99 % of the ferrous ions would be complexed by NA and only 19.3 % of ferric ions would be complexed by NA while the remaining ferric ions would be complexed with glutamate and citrate (70 % and 9.2 % respectively) (Harris et al., 2012). A potential fault with this model is that it does not incorporate 2'-deoxymugineic acid (DMA) as a potential candidate for complex formation. In work performed on the phloem of rice, the concentration of DMA was found to be between 152 µmol L^{-1} (Kato et al., 2010) and 150 µmol L^{-1} (Nishiyama et al., 2012). This was much higher than the NA values reported of 66 µmol L^{-1} (Kato et al., 2010) and 76 µmol L^{-1} (Nishiyama et al., 2012). In rice it has been found that the main Zn complex ligand was NA whilst for Fe, DMA was the main metabolite responsible for complexing this metal (Nishiyama et al., 2012). Glutathione has been found to play a role in Cd transportation as part of the detoxification process (Mendoza-Cózatl et al., 2008). Glutathione was tested as a chelating agent in the speciation model but was found to complex less than 2 % of Zn though it was mentioned that if Cd was included this may affect the model dynamics (Harris et al., 2012). In this work we have reported for the first time the concentration of NA in the phloem of wheat with an average concentration of

255.4 µmol L^{-1} ± SE 96.71 which is within the range reported in castor bean (Schmidke and Stephan, 1995; Stephan et al., 1994; Stephan and Scholz, 1993) but is much higher than what has been reported in rice (Kato et al., 2010; Nishiyama et al., 2012). Previous work in our laboratory has shown a significant increase in Zn and Mg in the phloem during grain loading (Palmer et al., 2014b) and it is also likely that there is an associated increase in metal complexing metabolites. This relationship has been demonstrated in castor bean where the NA phloem concentrations reported 4 and 8 days after imbibition were 206 µmol L^{-1}, (Schmidke and Stephan, 1995) which is close to what was observed in this work (255.4 µmol L^{-1} ± SE 96.71). Further exploration of NA flux at different maturities may give further insight into the role of NA in essential micronutrient transport.

It is anticipated that further method development would enable the analysis and quantification of DMA and glutathione within the phloem which would assist in the development of a wheat specific speciation model for the long distance transport of essential micronutrients. The amine binding LC-MS method used here gave in-conclusive results for DMA (data not shown) and a different method is required.

The ability to obtain a profile of a broad range of metabolites is a powerful tool not only for understanding the transport of essential micronutrients to the grain and other vegetative tissues, but also for examining responses to toxic or deficient conditions. An example of this is where it was possible to identify a metabolite complex responsible for boron mobilisation in the phloem (Stangoulis et al., 2010) that could lead to efficiency in boron utilization (Stangoulis et al., 2001). Metabolite profiling has also been used widely on plant tissues to examine tissue level dynamics such as changes involved in tolerance to nutrient deficient conditions such as Fe deficiency

in pea (Kabir et al., 2013), and also metabolite variation during the ripening process in capsicum (Aizat et al., 2014). The methods outlined in this study add further capability to researchers interested in metabolite changes both on a whole plant level during maturation and also when plants are under abiotic or nutrient based stresses.

4.5 Conclusion

This study demonstrates the production of a complex metabolite profile from extremely small volumes of phloem exudate using GC-MS. We also demonstrate that this method of metabolite profiling can be used to determine significant maturity based variability within the metabolite profile of the phloem. To our knowledge this is the first report of the presence of and quantification of NA in the phloem of wheat.

4.6 Materials and methods

4.6.1 Plant material

Wheat (*Triticum aestivum* L. genotype 'SAMNYT 16') seedlings were grown in 70x100 mm pots in Debco™ Green Wizard potting mix within a plant growth room. Growth room conditions were 13/11 h light/dark at 20°C/10°C with a minimum of 400 μmol m^{-2} s^{-1} light at the leaf surface. Plants were transferred to a greenhouse where aphids were applied and kept there for a maximum of 48 h prior to stylectomy.

4.6.2 Aphid stylectomy

Aphid stylectomy procedures were adapted from the method established by Downing and Unwin (1977). A short video of the method is presented in Additional material 2 (refer to section 4.11 for access details) and a summary of the method is as follows. Aphids were taken from an anholocyclic *Sitobion miscanthi* (Indian grain aphid) culture maintained at Flinders University on wheat plants kept under greenhouse conditions. Only apterous aphids were used in the experiments.

Aphids were secured to wheat plants (immediately below the head on the peduncle), a minimum of 12 h prior to stylectomy, using specially prepared cages (refer to Appendix 2 for construction specifications). Plants were watered to saturation at the time of aphid caging. Stylectomy was performed using high-frequency micro-cauterisation under a Leica microscope (M165 C or MZ16) using an electrolytically-sharpened tungsten needle in combination with a micromanipulator. Exudate samples were collected using glass micro-capillaries (30-0017, Harvard Apparatus) pulled using a capillary puller (Narishige). The relative humidity during collections ranged from 41 % to 50 %.

4.6.3 Microscope measurement of nanolitre phloem exudate volumes

Exudate volumes were measured using the method published in (Palmer et al., 2013). In brief, exudate flow rates were estimated from photo sequences taken, in air, using a Leica microscope (M165C or MZ16) with an attached camera (DFC295 or DFC280) and the multi-time module from the Leica Application Suite software (v3.6.0). Photo sequences were taken immediately after obtaining an exuding stylet, approximately every 15 minutes during collection and immediately prior to the end of the collection. Photo sequences consisted of five photos with a one second interval between photos. The droplet radius for each photo in a sequence was measured using the interactive measurement module within the Leica Application Suite and an estimate of droplet volume calculated. Using the time interval between each pair of sequential photos in a sequence the exudation flow rate was estimated from the change in volume between photos. The average of the estimated flow rate from all sequences in each collection was multiplied by the respective collection length to give an estimate of the collection volume. A correction factor, as determined

previously, was applied to correct for evaporation (Palmer et al., 2013). Samples were deposited into 200 µl glass vial inserts (Agilent) containing 5 µl of Millipore Milli-Q™ water (>18.2 MΩ cm^{-1}), centrifuged for 20 seconds at 14,000 rpm in a 1.5 ml microcentrifuge tube and insert was transferred to 2 ml auto sampler vials (Agilent) and stored at -80 °C. After samples had been collected samples were lyophilized in a freeze dryer prior to shipment for metabolomics profiling and quantitation at Metabolomics Australia, School of Botany, The University of Melbourne. Table 4.4 shows the average and standard error for the time that sample collection was started, average volume and average maturity (DAA) for the samples allocated to the maturity groupings analysed using LC-MS and GC-MS.

Table 4.4 : Mean, n and SE, for both maturity groups (DAA group), for sample collection start times (hour:minute:second), phloem exudate volumes (nl) and number of days after anthesis (DAA) for samples analysed by GC-MS and LC-MS

Analysis	Variable	DAA Group	n	Mean	SE
GC-MS	collection start	8-12 DAA	16	16:02:33.75	0:06:50.17
		17-21 DAA	20	15:35:45.00	0:11:25.50
	Corrected vol	8-12 DAA	16	90.6	13.26
		17-21 DAA	20	62.3	6.91
	DAA	8-12 DAA	16	9.9	0.22
		17-21 DAA	20	18.5	0.17
LC-MS	collection start	8-12 DAA	2	15:04:30	0:08:30
		17-21 DAA	2	14:58:00	1:24:00
	Corrected vol	8-12 DAA	2	140.6	39.79
		17-21 DAA	2	50.9	7.48
	DAA	8-12 DAA	2	10.0	0.00
		17-21 DAA	2	18.5	0.50

4.6.4 GC-MS analysis of phloem exudate

GC-MS analysis of phloem exudate samples was carried out using a method modified from (Temmerman et al., 2012). The lyophilized phloem samples were re-dissolved in 5 μL of 30 mg mL^{-1} methoxyamine hydrochloride in pyridine and derivatised at 37°C for 120 min with mixing at 500 rpm. The samples were then treated for 30 min with 10 μL *N,O-bis*-(trimethylsilyl)trifluoroacetamide (BSTFA) and 2.0 μL retention time standard mixture [0.029 % (*v*/*v*) *n* dodecane, *n*-pentadecane, *n*-nonadecane, *n*-docosane, *n*-octacosane, *n*-dotriacontane, *n*-hexatriacontane dissolved in pyridine] with mixing at 500 rpm. Each derivatised sample was allowed to rest for 60 min prior to injection.

Samples (1 μL) were injected into a GC-MS system comprised of a Gerstel 2.5.2 autosampler, a 7890A Agilent gas chromatograph and a 5975C Agilent quadrupole MS (Agilent, Santa Clara, USA). The MS was adjusted to 171 according to the manufacturer's recommendations using *tris*-(perfluorobutyl)-amine (CF43). The GC was performed on a 30 m VF-5MS column with 0.2 μm film thickness and a 10 m Integra guard column (Agilent J&W GC Column). The injection temperature was set at 250°C, the MS transfer line at 280°C, the ion source adjusted to 250°C and the quadrupole at 150ºC. Helium was used as the carrier gas at a flow rate of 1.0 mL min^{-1}. For the polar metabolite analysis, the following temperature program was used; start at injection 70°C, a hold for 1 min, followed by a 7°C min^{-1} oven temperature, ramp to 325°C and a final 6 min heating at 325°C. Both chromatograms and mass spectra were evaluated using the Chemstation Data Analysis program (Agilent, Santa Clara, USA). Mass spectra of eluting compounds were identified and validated using the public domain mass spectra library of Max-Planck-Institute for

Plant Physiology, Golm, Germany (http://csbdb.mpimp-golm.mpg.de/csbdb/dbma/msri.html) and the *in-house* Metabolomics Australia mass spectral library. All matching mass spectra were additionally verified by determination of the retention time by analysis of authentic standard substances. Resulting relative response ratios, that is, selected ion area of each metabolite was normalized to phloem volume for each identified metabolite. For metabolites which had multiple TMS derivatives, normalized ion areas were presented.

4.6.5 LC-MS analysis of phloem exudate

Quantification of amine containing metabolites in nl phloem exudate was modified from the method reported in Boughton et al., (2011). To the lyophilized phloem sample 4 µl of Borate buffer (200 mM at pH 8.8 with 1 mM ascorbic acid, 10 mM tris (2-carboxyethyl) phosphine (TCEP) and 25 µM 2-aminobutyric acid (added as an ISTD) was added, then 1 µl of 10 mM 6-Aminoquinolyl-N-hydroxysuccinimidylcarbamate (AQC, dissolved in 100 % acetonitrile). The glass inserts were sealed with parafilm then left to rest at room temperature for 30 minutes. Analysis and quantification by LC-MS was done as previously reported (Boughton et al., 2011).

4.6.6 Statistical analysis

Statistics including Student's *t*-test were calculated using IBM SPSS statistics software (version 22). A normal distribution was determined to have been achieved when the z-scores for the skew and kurtosis were less than 1.96 which is the cut off indicating a significant skew or kurtosis at the 95 % level (Field, 2007). Of the metabolites identified, 40 were found to have significant skew or kurtosis to their distribution. These metabolites were transformed using the following transformations

in increasing power; 16 using square root (SQRT), 8 using cube root (CBRT), 11 using the natural logarithm (Ln) and 3 using the inverse cube root (InvCBRT). A further 2 metabolites were unable to be transformed successfully. For the Student's *t*-test as calculated using SPSS, results are produced with and without the assumption of equal variance between treatments and the Levene's statistic gives an indication if this assumption is met or rejected.

4.7 Abbreviations

GC-MS, Gas chromatography - mass spectrometry; LC-MS, Liquid chromatography - mass spectrometry; EDTA, Ethylenediaminetetraacetic acid; DAA, days after anthesis; ISTD, Internal standard

4.8 Competing interests

The authors declare that they have no competing interests.

4.9 Authors' contributions

LJP helped in conceiving study, collected phloem samples, did ICP-MS analysis, statistical analysis and drafted the manuscript. DAD assisted with GC-MS method development, acquisition and data analysis of phloem samples. BB assisted with LC-MS method development, running of sample and data analysis. UR helped in the design of the study, and GC-MS and LC-MS method development. RG helped in the design of the study and drafting of manuscript. JS participated in conception and design of the study and assisted with drafting of manuscript. All authors read and approved the final manuscript.

4.10 Acknowledgements

The authors wish to acknowledge HarvestPlus for helping to fund this work and Metabolomics Australia (School of Botany, The University of Melbourne), funded through Bioplatforms Australia Pty Ltd., a National Collaborative Research

Infrastructure Strategy (NCRIS) with co-investment from the Victorian State Government and The University of Melbourne.

4.11 Additional files

Additional file 1: Further information on GC-MS analysis, including example of separation traces with and without oil contamination, full list of metabolites detected, replicated derivatives and un-normalisable metabolites as shown in **Appendix 1**.

Additional file 2: Short video outlining the method of aphid stylectomy can be downloaded at:
http://www.plantmethods.com/content/supplementary/1746-4811-10-27-s2.zip

Additional file 3: Specifications and method for constructing aphid cages as shown in **Appendix 2**

Chapter 5. Diurnal variability in the phloem of wheat: changes in the elemental and metabolite profile during grain filling.

Lachlan J. Palmer[1*], Robin D. Graham[1] and James C. R. Stangoulis[1]

[1] School of Biological Sciences, Flinders University, Bedford Park, South Australia 5042, Australia

*Corresponding Author

Phone: +61 8 8201 7997

Fax: +61 8 8201 3015

Email: Lachlan.palmer@flinders.edu.au

Main Conclusion: There was significant diurnal variability in both the elemental and metabolite profile of the phloem and there were changes in this variability over the course of grain loading.

Chapter currently submitted to Planta and under review; refer to section 5.8 for author contributions.

5.1 Abstract

The mechanisms of Fe and Zn transport in staple food crops is of growing interest due to recent work aiming to improve the Fe and Zn density in staple foods through biofortification. To better understand Fe and Zn transport, we made use of the aphid stylectomy technique to collect nano-litre volumes of phloem exudate from wheat (*Triticum aestivum* L. var. SAMNYT 16). Phloem exudate was collected at four maturities during the grain filling, at midday or mid-afternoon. Samples of phloem were analysed for their micronutrient composition or metabolite profile. There were significant changes in the concentration of K, Mg, Fe and Zn during the course of grain loading. There were also significant diurnal differences for Fe and K concentrations in the phloem during the early phases of grain development which correspond to the known peak times for loading micronutrients into the developing seed. Of the 79 metabolites detected within the phloem, 43 had significant maturity differences and 38 had significant diurnal variability. These metabolites include the key metabolites glutamic acid and citric acid which may play a role in the complexing of mineral nutrients for long distance transport. Diurnal and maturity fluctuations of key metabolites and essential elements are critical as these set the limits on the amounts of mineral micronutrients that can be complexed for transport and the amounts of mineral micronutrients present for loading into the seed. The work presented here gives further insight into the complex composition of the phloem and variability that can occur during the day and also with increasing maturity.

Key words: Phloem, Diurnal, Metabolite profile, Wheat, *Triticum aestivum*, Micronutrients,

5.2 Introduction

Circadian clocks play an important role in the regulation of metabolic pathways across all forms of life (Wijnen and Young, 2006). In the model plant *Arabidopsis thaliana*, it has been found that up to 89 % of the transcriptome show a cyclic behaviour due to variability in light or temperature and up to 53 % of the transcriptome show fluctuations with diurnal change (Michael et al., 2008). There is an extensive body of work already reported that examines the interactions between circadian rhythm and solute transport in Arabidopsis (Haydon et al., 2011) and from a nutritional perspective the relationship between the circadian clock and micronutrient transport is of great interest. In Arabidopsis, the homeostasis of Cu (Andrés-Colás et al., 2010) and Fe (Duc et al., 2009) have been linked to circadian clock genes and in the case of Fe it's been shown that there is a link between the expression of *Arabidopsis Ferritin 1* (*AtFer1*) and *Time for Coffee* (TIC) (Duc et al., 2009). *AtFer1* codes for a 28 kDa ferritin protein which in *Arabidopsis* has the highest expression under Fe excess (Ravet et al., 2009), whilst *TIC* encodes a nuclear located regulator of the circadian clock responsible for maintaining amplitude and timing of the *Arabidopsis* circadian clock (Ding et al., 2007; Hall et al., 2003). Ferritin production was found to be repressed by the expression of *TIC* under low Fe supply and in the presence of light and diurnal cycles (Duc et al., 2009). Furthermore, links have been made between Fe and the regulation of circadian rhythms, with the Fe supply affecting the length of the circadian period (Tissot et al., 2014). Interactions between ferritin genes and light have also been observed in rice, with the presence of light stimulating the expression and production of ferritin in rice seedlings (Stein et al., 2009). Ferritin is an important Fe storage protein with an important role in protecting against oxidative stress (Ravet et al., 2009). The role of

the circadian rhythm in homeostasis of essential elements is of great interest. Deficiencies of Fe and Zn in humans have been identified as a serious issue of concern for developing countries. In a 2002 World Health Organisation report it was estimated that in 2000, 1.6 million people died as a direct result of Fe and Zn deficiency and a further 60 million DALYs were lost (World Health Organisation, 2002). Approximately 60 % of the DALYs lost occurred in developing countries within Africa and South-East Asia (World Health Organisation, 2002). In a more recent analysis of WHO data sourced from between 1993 and 2005 it was estimated that anaemia affected 24.8 % or 1.62 billion people worldwide (McLean et al., 2009). With preschool children, pregnant women and non-pregnant women being the most affected (McLean et al., 2009).

Biofortification of staple crops has been identified as one strategy for combating micronutrient deficiency (Mayer et al., 2008) and attempts to increase the levels of micronutrients and vitamins in the harvested and edible plant parts using genetic or agronomic techniques is currently underway (Murgia et al., 2012). An example of this is the over-expression of wheat FER1 (TaFer1) in the endosperm of wheat grain that resulted in a significant increase in the Fe concentration of the endosperm (Borg et al., 2012). An important part of the mineral biofortification process is the efficient transport of target micronutrients (i.e. Fe and Zn) from source to the sink (i.e. from soil, through to the roots, stems and leaves, and then to the seed) and therefore the long-distance vascular pathways play a significant role in delivering nutrients to seeds (Borg et al., 2012).

Within a plant, the long distance transport pathways of the xylem and phloem are the major routes for nutrient movement from vegetative tissues to developing seeds

(Atwell et al., 1999). An example of the importance of nutrient transport has been demonstrated with work done overexpressing ferritin in the endosperm of rice where grain Fe was increased at the expense of leaf tissues (Brinch-Pedersen et al., 2007). In the case of wheat, the phloem is very important as there is a xylem discontinuity at the base of the grain (Zee and O'Brien, 1970) which results in all macro- and micro-nutrients having to transport to the phloem before unloading into the grain. During the transport of Fe and Zn in the phloem these minerals must be complexed owing to their reactive nature (Blindauer and Schmid, 2010). A variety of metabolites have been theorised to complex Fe, Zn and other essential minerals within the phloem (Harris et al., 2012) and of these, nicotianamine (NA) and cystine are proposed to play a major role. In rice, NA has been found to complex Zn in the phloem (Nishiyama et al., 2012). For most cereals phytosiderophores, which include NA and 2'-deoxymugineic acid (DMA), play an important role in uptake of Fe and Zn from the soil (Rengel and Römheld, 2000) and phytosiderophore secretion has also be shown to have diurnal regulation in wheat (Reichman and Parker, 2007; Zhang et al., 1991), rice (Nozoye et al., 2014) and barley (Negishi et al., 2002). The interconnection between diurnal and circadian rhythm, nutrient flux and long distance transport is crucial when exploring the mechanisms of micronutrient unloading into to the grain. These relationships are also important to ensure that variability caused by diurnal and circadian rhythms are taken into account when sampling from the phloem. Recent advances in analytical capabilities have enabled the analysis of phloem composition with a greater sensitivity. The concentrations of four elements (Palmer et al., 2014b) and 79 metabolites (Palmer et al., 2014a) have been shown to change in the phloem of wheat during grain development. A study of the phloem using a similar collection technique explored the diurnal variability of

amino acids in phloem samples as small as 2 nl (Gattolin et al., 2008). Eleven amino acids were found to increase in concentration during the day with three samplings between the times, 12:30 to 17:30 (Gattolin et al., 2008). The work presented here will further explore the diurnal variability within the phloem by examining changes in elemental and metabolite profile. Changes in diurnal variability during the grain loading phase of wheat will also be explored.

5.3 Materials and Methods

5.3.1 Solutions

Water-saturated paraffin oil (WSPO, LABCHEM™, Ajax Finechem) was produced by mixing two parts oil with one part Milli-Q water and shaking for 2 h on a rotary shaker. The solution was centrifuged briefly at 5000 rpm and excess water was removed. All HNO_3 solutions used in this research were prepared using Instrument Quality acid (Seastar) diluted v/v in high purity water (>18.2 MΩ cm^{-1} resistivity) using acid washed volumetric glassware. All inductively-coupled plasma-mass spectrometry (ICP-MS) standards used in this research were prepared using a Gilson dual syringe auto-dilutor from certified single element stock solutions (1000 µg ml^{-1} High-Purity Standards). All final calibration and diluting solutions contain 2 µg L^{-1} Indium (In) as an internal standard.

5.3.2 Plant Material

Wheat (*T. aestivum* L. var. SAMNYT 16) seedlings were grown in a growth room in 70 x 100 mm pots filled with Debco™ Green Wizard potting mix. Growth room conditions were 13/11 h light/dark at 20°C/10°C with a minimum of 400 µmol m^{-2} s^{-1} photosynthetic photon flux density at the leaf surface. Plants were transferred to a greenhouse where aphids were introduced and kept there for a maximum of 48 h.

5.3.3 Aphid Stylectomy

Aphid stylectomy procedures were adapted from Downing and Unwin (1977). Aphids were taken from an anholocyclic *Sitobion miscanthi* (Indian grain aphid) culture maintained at Flinders University on wheat plants kept under greenhouse conditions. Only apterous aphids were used in the experiments.

Aphids were secured to wheat plants (immediately below the wheat head and on the peduncle), a minimum of 12 h prior to stylectomy, using specially prepared cages. Plants were watered to saturation at the time of aphid caging. Stylectomy was performed using high-frequency micro-cauterisation under a Leica microscope (M165 C or MZ16) using an electrolytically-sharpened tungsten needle in combination with a micromanipulator. Exudate samples were collected using glass micro-capillaries (30-0017, Harvard Apparatus), made by a capillary puller (Narishige).

Collections were grouped on the basis of plant maturity and collection start time. Tables 5.1 and 5.2 show the mean maturity in days after anthesis (DAA) and collection start time for samples analyzed for micronutrients (Table 5.1) and metabolites (Table 5.2) for each grouping variable.

Table 5.1 : Sample numbers, average ± standard errors of sample maturities (DAA) and sampling start times (hours:minutes:seconds) for sample groupings used for diurnal variability elemental comparisons.

Factor	Grouping	n	Mean	Std. Error
DAA	1-2 DAA	41	1.2	0.07
	8-12 DAA	87	9.8	0.08
	13-16 DAA	18	14.4	0.16
	17-21 DAA	88	18.9	0.10
start time	before 2pm	84	11:37:12	0:05:10
	after 2pm	150	15:36:10	0:02:57

Table 5.2 : Sample numbers, average ± standard errors of sample maturities (DAA) and sampling start times (hours:minutes:seconds) for sample groupings used for diurnal variability metabolite profile comparisons.

Measurement	Grouping	n	Mean	Std. Error
DAA	8-12 DAA	28	9.7	0.18
	17-21 DAA	26	18.7	0.16
collection start	Before 2pm	18	12:26:23	0:10:22
	After 2pm	36	15:47:40	0:7:18

5.3.4 Microscope measurement of nanolitre phloem exudate volumes

Volumes of phloem samples were measured as reported previously (Palmer et al., 2013). Two methods were used for measuring volumes of phloem collected. Volumes for samples analyzed by ICP-MS were measured under WSPO, with each droplet immediately photographed within the WSPO using a Leica microscope (M165C or MZ16) with an attached camera (DFC295 or DFC280). The radius (µm) of the droplet was measured using the Leica Application Suite (LAS 3.6.0) with the additional Interactive Measurements Module in order to estimate the volume of the droplet.

After samples were photographed, a 1.5 ml centrifuge tube was placed over the cap (containing the oil and the nanolitre droplet) and centrifuged briefly at 13,000 rpm to

ensure the droplet was removed from the cap. 1 ml of diluting solution (2 % $HNO_{3,}$ 2 µg L^{-1} In) was added and the tubes were vortexed briefly, and centrifuged at 13,000 rpm for approximately 30 s. The final aqueous solution was transferred, by pipette, to a new tube to reduce the amount of WSPO present during analysis.

For samples analysed by GC-MS, sample volumes were derived from an estimated flow rate calculated from photo sequences taken during sample collection (start, every 15 minutes and prior to collection end) of the exuding stylet using a Leica microscope (M165C or MZ16) with an attached camera (DFC295 or DFC280) and the multi-time module from the Leica Application Suite software (v3.6.0). The average of the estimated flow rate from all sequences in each collection was multiplied by the respective collection length to give an estimate of the collection volume. A correction factor, as determined previously, was applied to correct for evaporation (Palmer et al., 2013). Samples were deposited into 200 µl glass vial inserts (Agilent) containing 10 µl of Millipore Milli-Q™ water (>18.2 MΩ cm^{-1}), centrifuged for 20 seconds at 14,000 rpm and stored in 2 ml auto sampler vials (Agilent) at -80 °C. After all samples had been collected, samples were lyophilized in a freeze dryer prior to shipment for metabolomics profiling and quantitation at Metabolomics Australia, School of Botany, The University of Melbourne.

5.3.5 ICP-MS analysis of phloem exudate

Samples were analysed by ICP-MS (Agilent 7500cx), with method as previously reported (Palmer et al., 2014b). In brief, samples were manually drawn directly from the 1.5 ml centrifuge tubes using a 500 mm length of 0.25 mm internal diameter (ID) sample tubing connected to 0.89 mm ID peristaltic tubing (0.89-ORG, Glass Expansion) with the attached peristaltic pump set at an uptake speed of 6 revolutions

per minute. A 0.1 ml min^{-1} MicroMist nebulizer (Glass Expansion) was used for sample introduction. The reaction cell was run in He mode with a gas flow rate of 4.5 ml min^{-1} and the equipment was tuned using the autotune function. Mass spectrum data acquisition was repeated three times per sample with a total acquisition time of 59.1 s per sample.

5.3.6 GC-MS analysis of phloem exudate

GC-MS analysis of phloem exudate samples was carried out using a method modified from (Temmerman et al., 2012) as detailed previously (Palmer et al., 2014a). The lyophilized phloem samples were re-dissolved in 5 µL of 30 mg ml^{-1} methoxyamine hydrochloride in pyridine and derivatised at 37°C for 120 min with mixing at 500 rpm. The samples were then treated for 30 min with 10 µL *N,O-bis*-(trimethylsilyl)trifluoroacetamide (BSTFA) and 2.0 µL retention time standard mixture [0.029 % (*v*/*v*) *n* dodecane, *n*-pentadecane, *n*-nonadecane, *n*-docosane, *n*-octacosane, *n*-dotriacontane, *n*-hexatriacontane dissolved in pyridine] with mixing at 500 rpm. Each derivatised sample was allowed to rest for 60 min prior to injection.

Samples (1 µL) were injected into a GC-MS system comprised of a Gerstel 2.5.2 autosampler, a 7890A Agilent gas chromatograph and a 5975C Agilent quadrupole MS (Agilent, Santa Clara, USA). The MS was adjusted to 171 according to the manufacturer's recommendations using *tris*-(perfluorobutyl)-amine (CF43). The GC was performed on a 30 m VF-5MS column with 0.2 µm film thickness and a 10 m Integra guard column (Agilent J&W GC Column). The injection temperature was set at 250°C, the MS transfer line at 280°C, the ion source adjusted to 250°C and the quadrupole at 150ºC. Helium was used as the carrier gas at a flow rate of 1.0 ml min^{-1}. For the polar metabolite analysis, the following temperature program was used;

start at injection 70°C, a hold for 1 min, followed by a 7°C min^{-1} oven temperature, ramp to 325°C and a final 6 min heating at 325°C. Both chromatograms and mass spectra were evaluated using the Chemstation Data Analysis program (Agilent, Santa Clara, USA). Mass spectra of eluting compounds were identified and validated using the public domain mass spectra library of Max-Planck-Institute for Plant Physiology, Golm, Germany (http://csbdb.mpimp-golm.mpg.de/csbdb/dbma/msri.html) and the *in-house* Metabolomics Australia mass spectral library. All matching mass spectra were additionally verified by determination of the retention time by analysis of authentic standard substances. Resulting relative response ratios, that is, selected ion area of each metabolite was normalized to phloem volume for each identified metabolite. For metabolites which had multiple TMS derivatives, normalized ion areas were presented.

5.4 Results

Phloem samples were grouped on the basis of plant maturity and time from when the exudate collection was started. The cut off for the two sample collection start times was 2pm, the mean start times for the "before 2pm" group were 11:37:12 am ± SE 0:5:10 for micronutrient analysis and 12:26:23 pm ± 0:10:22 for metabolite profiling samples. The mean start times for the "after 2pm" group were 3:36:10 pm ± 0:2:57 for micronutrient analysis and 3:47:40 pm ± 0:7:18 for metabolite profiling samples (Tables 5.1 and 5.2).

5.4.1 Diurnal Variability: Elemental

A difference in Fe phloem concentration was observed at the two collection start times with collections starting earlier in the day having a lower concentration than those started later (Fig 5.1). Across the four maturity times sampled, there was a significantly lower level of Fe in the phloem, with on average 5.0 ± 1.06 mg kg^{-1}

more Fe in the phloem in collections made after 2pm when compared to those before 2pm (Table 5.3). For specific maturity times, only the first two maturities (1-2 DAA and 8-12 DAA) showed significant differences (Table 5.3). The greatest difference was just after anthesis at 1-2 DAA where there was on average 7.8 ± 2.25 mg kg^{-1} more Fe in the phloem after 2pm than before 2pm. At 8-12 DAA there was on average 6.2 ± 1.58 mg kg^{-1} more Fe in the phloem after 2pm than before 2pm.

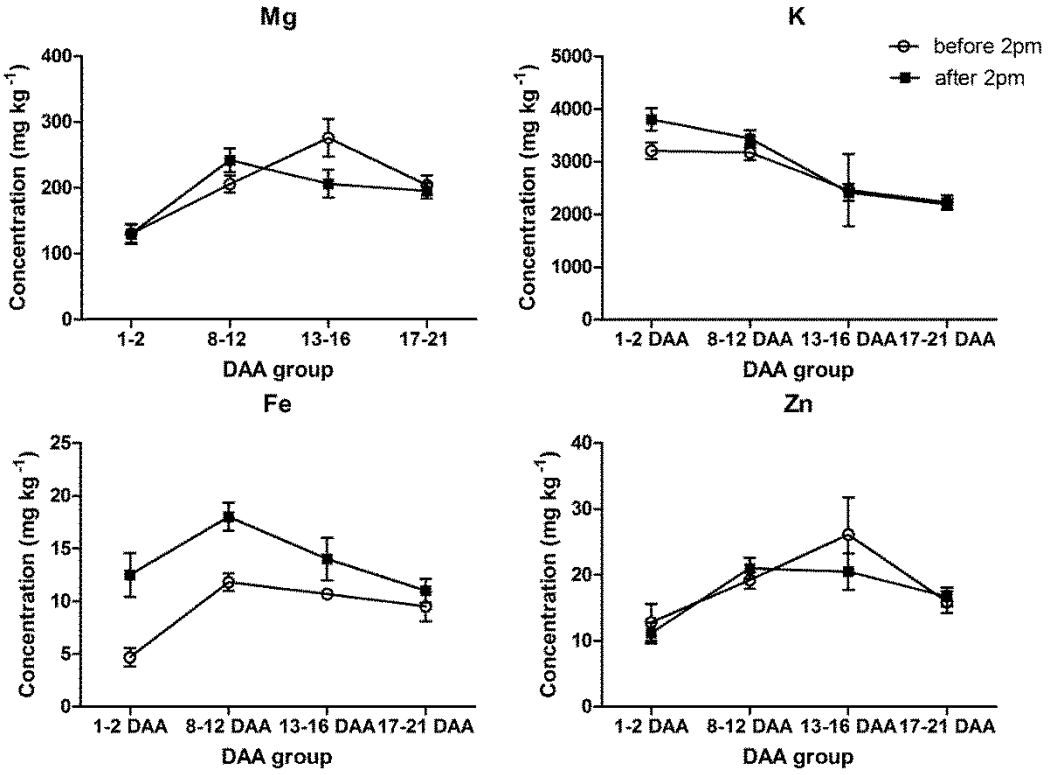

Figure 5.1 : The concentration of Mg, K, Fe and Zn in the phloem sampled before and after 2pm for different maturities.
(DAA = days after anthesis, values represent mean and standard error, sample sizes are listed in table 5.1.)

There was also a significant difference in K concentration for time of collection but only at 1-2 DAA, with 591.6 ± 257.10 mg kg^{-1} more K in the phloem after 2pm than before 2pm.

There were no significant differences for Mg and Zn concentrations in the phloem for direct comparisons between the two diurnal groupings sampled. There were however differences in the maturity related changes in the concentration of Zn for samples collected before and after 2pm which can be seen in Table 5.5 as there was a significant increase in Zn concentration in the phloem of on average 9.7 ± 2.39 mg kg^{-1} from the start of anthesis (1-2 DAA) to the beginning of peak grain loading (8-12 DAA) for samples collected after 2pm. However for samples collected before 2pm the average increase in Zn concentration in the phloem of 6.4 ± 2.66 mg kg^{-1} was not found to be significant ($p = 0.104$).

There were also differences in the maturity related changes for K and Fe. For K there was a decrease in phloem concentration as the plant matured for both collection start times (Table 5.4). For collections made before 2pm there was a significant decrease in K concentration, from 1-2 DAA to 17-21 DAA and 8-12 DAA to 17-21 DAA, of on average 984.7 ± 233.88 mg kg^{-1} and 944.2 ± 190.58 mg kg^{-1} respectively. For collections made after 2pm the main difference to those made before 2pm was that the decrease from 8-12 DAA to 13-16 DAA was statistically significant ($p < 0.001$) with an average decrease in K concentration in the phloem of 1022.2 ± 231.28 mg kg^{-1}. In the case of Fe, there were also significant changes in phloem concentration due to maturation, though these changes were different for sampling start times (Table 5.5). For samples taken before 2pm, there were significant differences in Fe phloem concentration between 1-2 DAA and both 8-12 and 17-21 DAA, with

increases of 7.1 ± 1.55 mg kg^{-1} and 4.8 ± 1.67 mg kg^{-1} respectively. For samples taken after 2pm there was a significant decrease in Fe phloem concentration of 7.0 ± 1.85 mg kg^{-1} from 8-12 DAA to 17-21 DAA.

For Mg there were no diurnal differences for the maturity related changes. For both before and after 2pm sampling times the concentration of Mg in the phloem significantly increased between 1-2 DAA and 8-12 DAA and then plateaued with all remaining maturities having no further significant changes and staying significantly higher than the Mg concentration in the phloem at 1-2 DAA (Table 5.4).

Table 5.3 : Results from independent t-tests for diurnal differences at different maturity groupings.

Element	DAA grouping	n < 2pm (I)	n >2pm (J)	Mean Difference (J - I)	Std. Error	Sig.
Mg	1-2 DAA [b]	16	25	-0.44	21.71	0.984
	8-12 DAA [a]	33	52	36.0	22.28	0.110
	13-16 DAA [b]	3	15	-69.6	49.43	0.178
	17-21 DAA [b]	29	54	-8.4	19.58	0.668
K	1-2 DAA [a]	16	24	591.6*	257.10	0.027
	8-12 DAA [b]	33	50	267.6	232.29	0.253
	13-16 DAA [b]	3	15	-44.6	457.04	0.924
	17-21 DAA [b]	30	56	-33.0	166.94	0.668
Fe	1-2 DAA [a]	15	21	7.8*	2.25	0.002
	8-12 DAA [a]	29	47	6.2*	1.58	<0.001
	13-16 DAA [a]	2	15	3.3	2.05	0.126
	17-21 DAA [b]	20	36	1.5	1.82	0.844
Zn	1-2 DAA [b]	16	24	-1.6	2.97	0.593
	8-12 DAA [b]	31	45	1.7	2.13	0.419
	13-16 DAA [b]	3	14	-5.6	6.51	0.407
	17-21 DAA [b]	27	42	0.82	2.20	0.711

Mean difference and standard error of the difference are in mg kg^{-1}. a = inhomogeneous variances, b = homogenous variances as determined from Leverne's test of equal variances,* indicates the mean difference is significant at the 0.05 level.

Table 5.4 : Post hoc statistical tests for comparisons of Mg and K phloem concentrations between maturity groupings for collections made before and after 2pm along with the mean and standard error of the difference.

element	Diurnal grouping	maturity grouping		Mean Difference	Std. Error	Sig.
		I	J	J-I		
Mg	before 2pm[a]	1-2 DAA	8-12 DAA	75.5*	22.00	0.006
			13-16 DAA	145.4*	45.43	0.012
			17-21 DAA	73.5*	22.49	0.010
		8-12 DAA	13-16 DAA	70.0	43.54	0.502
			17-21 DAA	-1.9	18.38	1.000
		13-16 DAA	17-21 DAA	-71.9	43.79	0.477
	after 2pm[b]	1-2 DAA	8-12 DAA	111.9*	23.45	0.000
			13-16 DAA	76.3*	25.79	0.030
			17-21 DAA	65.6*	19.16	0.006
		8-12 DAA	13-16 DAA	-35.6	27.74	0.578
			17-21 DAA	-46.4	21.72	0.150
		13-16 DAA	17-21 DAA	-10.7	24.23	0.970
K	before 2pm[a]	1-2 DAA	8-12 DAA	-40.5	230.15	1.000
			13-16 DAA	-750.5	475.32	0.523
			17-21 DAA	-984.7*	233.88	0.000
		8-12 DAA	13-16 DAA	-710.0	455.58	0.538
			17-21 DAA	-944.2*	190.58	0.000
		13-16 DAA	17-21 DAA	-234.2	457.47	0.996
	after 2pm[b]	1-2 DAA	8-12 DAA	-364.5	262.87	0.513
			13-16 DAA	-1386.7*	262.23	0.000
			17-21 DAA	-1609.4*	228.35	0.000
		8-12 DAA	13-16 DAA	-1022.2*	231.28	0.000
			17-21 DAA	-1244.9*	192.02	0.000
		13-16 DAA	17-21 DAA	-222.7	191.15	0.654

a = homogenous variances, Hochberg post hoc test, b = inhomogeneous variances, Games-Howell post hoc test, *indicates the mean difference is significant at the 0.05 level.

Table 5.5 : Post hoc statistical tests for comparisons of Fe and Zn phloem concentrations between maturity groupings for collections made before and after 2pm along with the mean and standard error of the difference.

element	Diurnal grouping	maturity grouping		Mean Difference	Std. Error	Sig.
		I	J	J-I		
Fe	before 2pm[a]	1-2 DAA	8-12 DAA	7.1*	1.55	0.000
			13-16 DAA	6.0	3.68	0.486
			17-21 DAA	4.8*	1.67	0.033
		8-12 DAA	13-16 DAA	-1.1	3.57	1.000
			17-21 DAA	-2.3	1.42	0.492
		13-16 DAA	17-21 DAA	-1.2	3.62	1.000
	after 2pm[a]	1-2 DAA	8-12 DAA	5.6	2.20	0.074
			13-16 DAA	1.5	2.83	0.995
			17-21 DAA	-1.5	2.30	0.988
		8-12 DAA	13-16 DAA	-4.0	2.48	0.495
			17-21 DAA	-7.0*	1.85	0.001
		13-16 DAA	17-21 DAA	-3.0	2.57	0.807
Zn	before 2pm[a]	1-2 DAA	8-12 DAA	6.4	2.66	0.107
			13-16 DAA	13.2	5.44	0.100
			17-21 DAA	3.1	2.73	0.836
		8-12 DAA	13-16 DAA	6.8	5.23	0.721
			17-21 DAA	-3.3	2.28	0.608
		13-16 DAA	17-21 DAA	-10.2	5.26	0.294
	after 2pm[a]	1-2 DAA	8-12 DAA	9.7*	2.39	0.001
			13-16 DAA	9.3*	3.18	0.025
			17-21 DAA	5.5	2.42	0.141
		8-12 DAA	13-16 DAA	-0.46	2.89	1.000
			17-21 DAA	-4.2	2.03	0.208
		13-16 DAA	17-21 DAA	-3.8	2.92	0.726

a = homogenous variances, Hochberg post hoc test, b = inhomogeneous variances, Games-Howell post hoc test, *indicates the mean difference is significant at the 0.05 level.

5.4.2 Diurnal Variability: Metabolite profile

In Tables 5.6, 5.7 and 5.8 are listed the 39 metabolites that were found to show significant diurnal changes within the phloem when sampled before and after 2pm at two different maturity ranges (8-12 DAA and 17-21 DAA). The four metabolites listed in Table 5.6 showed significant diurnal variability at both maturities sampled. Glutamine and Histidine showed a consistent diurnal change for both maturity sampling times, with an increase of between 2.6 and 5.9 fold for samples made before 2pm to those made after 2pm. Over this same period, 3-hydroxybenzoic acid had a significant decrease of between 4.4 and 15.7 fold in the phloem from earlier to later in the day for both maturities sampled. The unidentified metabolite "UN16" had a 1.6 fold decrease in the phloem at 8-12 DAA but a 2.2 fold increase at 17-21 DAA from earlier to later in the day. For the metabolites that showed significant diurnal changes in the phloem when sampled at 8-12 DAA (Table 5.7), there were 7 metabolites with a significant diurnal increase from early to late ranging from 1.5 fold for Homoserine to 3.7 fold for Asparagine. At the same maturity range there were 15 metabolites with a significant diurnal decrease between samples taken before, to those after, 2pm. The decreases ranged from 1.3 fold for Fructose to a 10.1 fold decrease for Itaconic acid. There were 13 metabolites that only showed significant diurnal changes in the phloem when sampled at 17-21 DAA (Table 5.8). These 13 metabolites all showed an increase from before 2pm to after 2pm with the increase ranging from a 1.7 fold increase for Putrescine to a 3.9 fold increase for 4-hydroxybenzoic acid.

Table 5.6 : Metabolites in the phloem metabolite profile with significant diurnal variability in metabolite relative response ratios (after 2pm minus before 2pm) for both maturities (8-12 DAA and 17-21 DAA).

Metabolite	transformation	DAA group	Sig. (2-tailed)	Fold change
3-hydroxybenzoic acid 2TMS	CBRT	8-12 DAA	.000 [un]	-15.7
		17-21 DAA	.000	-4.4
Glutamine 3TMS	CBRT	8-12 DAA	.007	3.3
		17-21 DAA	.034	5.9
Histidine 3TMS	Ln	8-12 DAA	.009	2.6
		17-21 DAA	.019	5.0
UN16_25.71_339	None	8-12 DAA	.035	-1.6
		17-21 DAA	.037	2.2

un = inhomogeneous sample variances as determined from Leverne's test of equal variances, CBRT = cube root, Ln = natural logarithm.
*x*TMS = Trimethylsilyl derivative where *x* = the number of TMS groups

Table 5.7 : Metabolites in the phloem metabolite profile with significant diurnal variability in metabolite relative response ratios (after 2pm minus before 2pm) for samples sampled 8-12 DAA.

Metabolite	transformation	Sig. (2-tailed)	Fold change
Asparagine_3TMS	Ln	0.022	3.7
Ornithine 3TMS	None	0.012[un]	3.6
3-amino-piperidin-2-one 2TMS	SQRT	0.015	2.4
UN08_17.96_360	CBRT	0.036	2.4
Glyceric-3-phosphate 4TMS	SQRT	0.049	1.9
Glycine 2TMS	None	0.040	1.8
Homoserine 3TMS	None	0.025	1.5
Fructose_MX1	None	0.045	-1.3
UN10_19.08_217	None	0.027	-1.3
Glucose MX1	None	0.027	-1.4
Octadecanoate 1TMS	SQRT	0.025	-1.6
Fumarate 2TMS	None	0.040 [un]	-1.6
Quinic acid 5TMS	SQRT	0.042	-1.7
Shikimic acid 4TMS	SQRT	0.036	-1.7
Succinate 2TMS	None	0.025 [un]	-1.8
UN04_15.56_185	None	0.005	-1.9
Hexadecanoate 1TMS	SQRT	0.001	-1.9
UN26_14.48_229	Ln	0.006	-2.3
UN03_14.36_320	Ln	0.000	-3.0
UN02_14.04_350	SQRT	0.003 [un]	-3.1
UN06_17.16_259	None	0.000 [un]	-5.1
Itaconic acid 2TMS	None	0.001 [un]	-10.1

un = inhomogeneous sample variances as determined from Leverne's test of equal variances, CBRT = cube root, Ln = natural logarithm, SQRT = square root. *x*TMS = Trimethylsilyl derivative where *x* = the number of TMS groups; MX1 = methoxyamine derivatised product

Table 5.8 : Metabolites in the phloem metabolite profile with significant diurnal variability in metabolite relative response ratios (after 2pm minus before 2pm) for samples sampled 17-21 DAA.

Metabolite	transformation	Sig. (2-tailed)	fold change
4-hydroxybenzoic acid 2TMS	None	0.000[un]	3.9
Tyrosine 3TMS	None	0.018	2.6
UN14_25.08_503	None	0.041	2.5
UN20_32.34_503	InvCBRT	0.004	2.4
UN22_33.13_513	SQRT	0.038	2.3
UN24_33.79_423	None	0.003	2.2
Lysine 4TMS	None	0.032	2.2
Phenylalanine 2TMS	None	0.030	2.2
Isoleucine 2TMS	None	0.044	2.1
UN21_32.89_387	None	0.001	2.0
Valine 2TMS	None	0.044	1.9
UN23_33.43_517	None	0.005	1.7
Putrescine 4TMS	None	0.044	1.7

un = inhomogeneous sample variances as determined from Leverne's test of equal variances, InvCBRT = inverse cube root, SQRT = square root. *x*TMS = Trimethylsilyl derivative where *x* = the number of TMS groups

There were 10 metabolites that had significant maturity related variability for samples collected both before and after 2pm (Table 5.9). All 10 metabolites had significant decreases in the phloem as the plant matured with the decreases ranging from 1.4 fold for Pyroglutamate after 2 pm to an 8.3 fold decrease for Trehalose before 2pm. Only four metabolites showed significant maturity related differences for samples collected before 2pm and these metabolites all showed a decrease of around 2-fold (2.1 to 2.2) in the phloem with increasing maturity (Table 5.10). For samples collected after 2pm there were 10 metabolites that showed a significant decrease in the phloem as the plants aged (Table 5.11), these decreases ranged from a 2.1 fold decrease for UN11_19.48_299 to a 5.3 fold decrease for Ornithine. There were 19 metabolites that had a significant increase in the phloem as the plants aged when sampled after 2 pm, the increases ranged from a 1.5 fold increase for fumarate to a 2.4 fold increase for shikimic acid.

Table 5.9 : Metabolites in the phloem metabolite profile with significant maturity variability in metabolite relative response ratios (17-21DAA minus 8-12 DAA) when collected before and after 2pm.

Metabolite	transformation	Collection time	Sig. (2-tailed)	fold change
3-amino-piperidin-2-one 2TMS	SQRT	Before 2pm	0.027	-5.1
		After 2pm	0.001	-3.3
Alanine 2TMS	SQRT	Before 2pm	0.042	-4.0
		After 2pm	0.011[un]	-2.0
Arginine 3TMS	Ln	Before 2pm	0.006	-5.7
		After 2pm	0.000	-3.4
Histidine 3TMS	Ln	Before 2pm	0.011	-5.6
		After 2pm	0.009	-2.9
Homoserine 3TMS	None	Before 2pm	0.026	-2.7
		After 2pm	0.000	-2.2
Lysine 4TMS	None	Before 2pm	0.001	-3.4
		After 2pm	0.010	-1.5
Pyroglutamate 2TMS	None	Before 2pm	0.006	-2.0
		After 2pm	0.024	-1.4
Serine 3TMS	None	Before 2pm	0.012	-2.8
		After 2pm	0.001	-1.7
Trehalose 8TMS	Ln	Before 2pm	0.008[un]	-8.3
		After 2pm	0.001	-3.7
UN26_14.48_229	Ln	Before 2pm	0.035[un]	-4.5
		After 2pm	0.024	-1.9

un = inhomogeneous sample variances as determined from Leverne's test of equal variances, Ln = natural logarithm, SQRT = square root. *x*TMS = Trimethylsilyl derivative where *x* = the number of TMS groups

Table 5.10 : Metabolites in the phloem metabolite profile with significant maturity variability in metabolite relative response ratios (17-21DAA minus 8-12 DAA) when collected before 2pm.

Metabolite	transformation	Sig. (2-tailed)	fold change
Isoleucine 2TMS	None	0.037	-2.1
Threonine 3TMS	None	0.034	-2.1
Valine 2TMS	None	0.031	-2.1
4-hydroxybenzoic acid 2TMS	None	0.022[un]	-2.2

un = inhomogeneous sample variances as determined from Leverne's test of equal variances. *x*TMS = Trimethylsilyl derivative where *x* = the number of TMS groups

Table 5.11 : Metabolites in the phloem metabolite profile with significant maturity variability in metabolite relative response ratios (17-21DAA minus 8-12 DAA) when collected after 2pm.

Metabolite	transformation	Sig. (2-tailed)	fold change
Shikimic acid 4TMS	SQRT	0.009 [un]	2.4
Quinic acid 5TMS	SQRT	0.037 [un]	2.2
Succinate 2TMS	None	0.024 [un]	2.1
Hexadecanoate 1TMS	SQRT	0.005 [un]	2.0
Glycine 3TMS	None	0.002 [un]	1.9
Octadecanoate 1TMS	SQRT	0.007 [un]	1.9
3-hydroxybenzoic acid 2TMS	CBRT	0.023	1.9
UN16_25.71_339	None	0.004 [un]	1.9
Sucrose 8TMS	SQRT	0.040 [un]	1.8
UN20_32.34_503	InvCBRT	0.031 [un]	1.8
Putrescine 4TMS	None	0.001	1.8

Continued on next page

Table 5.11 continued

Metabolite	transformation	Sig. (2-tailed)	fold change
UN04_15.56_185	None	0.013 [un]	1.8
Tyrosine 3TMS	None	0.010 [un]	1.7
Fructose_MX1	None	0.007 [un]	1.7
Citric acid 4TMS	None	0.014	1.6
UN17_27.24_375	None	0.009	1.6
Gluconic acid-1,5-lactone 4TMS	None	0.023	1.6
Glucose MX1	None	0.026	1.5
Fumarate 2TMS	None	0.027	1.5
UN11_19.48_299	CBRT	0.010	-2.1
UN09_18.15_275	CBRT	0.001	-2.3
UN07_17.62_275	Ln	0.001	-2.3
Pipecolic acid 2TMS	Ln	0.042	-2.3
Glutamate 3TMS	None	0.004	-2.5
UN01_10.61_158	CBRT	0.000	-2.8
Glutamine 3TMS	CBRT	0.004	-3.0
Asparagine_3TMS	Ln	0.015	-3.5
UN08_17.96_360	CBRT	0.000	-4.0
Ornithine 3TMS	None	0.005	-5.3

un = inhomogeneous sample variances as determined from Leverne's test of equal variances,
Ln = natural logarithm, InvCBRT = inverse cube root, SQRT = square root. *x*TMS = Trimethylsilyl derivative where *x* = the number of TMS groups; MX1 = methoxyamine derivatised product

5.5 Discussion

Very little is known about the direct effect of time of day on the composition of the phloem and this is mainly due to difficulties in the methods used for collecting phloem samples and the small amounts collected (Dinant and Kehr, 2013). Recent advances in analytical equipment have enabled the measurement of metabolites, elements and amino acids in volumes small enough to enable the examination of diurnal changes directly within the phloem (Gattolin et al., 2008; Palmer et al., 2014a; Palmer et al., 2014b). In work examining the change in amino acid concentration within the phloem from mid-day to late afternoon, the concentrations of 14 individual amino acids were reported in phloem (Gattolin et al., 2008). The concentrations for amino acids that couldn't be separated were also reported; these were histidine and valine (His/Val) and leucine and isoleucine (Leu/Ile) (Gattolin et al., 2008). Of the amino acids measured, 6 individual amino acids and both combined amino acids were found to increase in concentration as the day progressed (Gattolin et al., 2008). In the work presented here, of the amino acids identified in Gattolin et al., (2008) only leucine was not detected and aspartic acid was at the limit of detection for the analytical equipment used (data not shown). Of the remaining 16 amino acids, only proline was found to have no variability within the phloem for either diurnal or maturity change. Proline was also one of the amino acids reported to show diurnal variability in the phloem (Gattolin et al., 2008). Of the other amino acids shown previously to have diurnal variability, only arginine was found not to have diurnal variability at all under these conditions; it was however found to show a significant maturity difference with between 3- and 5-fold decrease in the phloem as the plants matured for both sampling points in the day (Table 5.9). A possible explanation for the lack of diurnal variability is that arginine and proline had the

smallest reported regression coefficients (Gattolin et al., 2008). This indicates that even though change was significant, the diurnal change observed was small. Unfortunately the actual change was not reported. The work reported in Gattolin et al., (2008) was also reported on a different genotype (Paragon) and on plants that were 3 weeks old and these may have also led to the differences in diurnal fluctuations within the phloem. This may also help to explain the significant diurnal variability observed for glutamine, glycine and ornithine (Tables 5.6 and 5.7) which were quantified but not found to have diurnal variability (Gattolin et al., 2008). Of most importance, this work confirms there is diurnal variability in amino acid composition within the phloem, based on an increase in the amount of the amino acids present as the day progresses.

Links have been made between diurnal and circadian rhythms and the activity of Fe transport (Tissot et al., 2014). These include the production of compounds that enhance Fe uptake into the roots (Reichman and Parker, 2007; Zhang et al., 1991) and storage within the leaf (Duc et al., 2009). In the work presented here we provide evidence of the effect of diurnal change on Fe transport within the phloem. We observed on average a significant increase in Fe concentration in the phloem of 5.0 mg kg^{-1} ± 1.06 ($p < 0.001$) from before 2pm to after 2pm across the grain loading period (Table 3). The largest difference observed for Fe concentration in the phloem occurred at 1-2 DAA with a significant increase of 7.8 mg kg^{-1} ± 2.25 ($p = 0.002$) from early to late in the day. At this same maturity, a significant increase in K concentration was also observed with an increase of 591.6 mg kg^{-1} ± 257.10 ($p = 0.027$) from before 2pm to after 2pm.

The main role of K in the phloem is in maintaining turgor through its osmotic potential (Marschner, 1995; Thompson and Zwieniecki, 2011). K has also been found to be involved in the process of loading both sucrose and amino acids into the phloem (Philippar et al., 2003) and (Servaites et al., 1979) and the uptake of sucrose along the transportation stream (Gajdanowicz et al., 2011). The role that K plays in assimilate transport is through its interaction with the proton symporter involved in assimilate loading (Gajdanowicz et al., 2011). Flow of K out of the phloem through potassium channels produces a negative potential within the phloem which enables the activation of the proton symporter, leading to loading of sucrose into the phloem (Gajdanowicz et al., 2011). This is likely to be of most importance for the scavenging of sucrose that has diffused from the phloem along the transportation stream where the ATP required for activation of the proton pump may be in short supply (Gajdanowicz et al., 2011). The balancing of the osmotic potential is likely the main reason for a decrease in K concentration with maturity during early stages of grain loading but the diurnal changes observed in the phloem K concentration are likely due to another reason. Unfortunately we do not have metabolite results for the beginning of anthesis but it would be expected that assimilate concentration would increase over the course of the day and this can be observed with amino acids showing increases across the day (Tables 5-7) for the two maturities measured and as reported previously (Gattolin et al., 2008). It is possible that the diurnal difference is due to the loss of K from the phloem in an effort to scavenge sucrose lost due to diffusion. This may also explain why there is no diurnal difference observed at later maturities as the main role of K becomes one of sucrose recovery. Diurnal variation in phloem K concentration may also be partially due to the role of the xylem in K transport from the roots and it's supply to the shoots (Thompson and Zwieniecki,

2011). Reduced xylem flow due to lower transpiration at the leaf early in the day may also reduce availability of K for phloem loading (Thompson and Zwieniecki, 2011).

It is thought that Fe and Zn follow a similar route into cereals with both being complexed by phytosiderophores released into the soil prior to being imported into the roots (Welch, 1995). For long distance transport, the route for Fe and Zn transport is not as clear. In a computer model based on reported phloem composition, it was estimated that NA would complex 99.0 % of Fe^{2+} but only 19.3 % of Fe^{3+}, whilst under the same conditions 54.4 % of Zn^{2+} would be complexed (Harris et al., 2012). For the remaining Fe ions, glutamate was the main ligand responsible for binding Fe (0.5 % of $Fe^{2+}$and 69.9 % of Fe^{3+}) (Harris et al., 2012). Citrate was also found to play a role in the complexing of Fe^{3+}, with the model showing 9.2 % of Fe being complexed by citrate and this amount was also shown to vary by up to 55.1 % under different Ca and Mg conditions (Harris et al., 2012). In the case of Zn, the S containing amino acid cysteine accounted for the remaining Zn complexing ligand (41.2 %), though a small amount of Zn (2.8 %) was modelled to be in a joint complex of cysteine and histidine. This model does not include DMA and since the publishing of this model work examining Fe and Zn, complexes in rice have been published (Nishiyama et al., 2012) which demonstrates that in the phloem of rice, Zn was present as a complex with NA whilst Fe was complexed with DMA in the Fe^{3+} form. The GC-MS method used here was unable to measure cysteine or phytsiderophores but we have reported glutamate. There was no significant diurnal variability for glutamate, but there was however a significant 2.5 fold decrease in glutamate in the phloem towards the end of grain loading for samples collected after 2pm (Table 5.11). This may help in partially explaining the significant decrease in

phloem Fe concentration from 8-12 DAA to 17-21 DAA that was also observed in samples collected after 2pm (Table 5.5). It has been reported in rice and barley that there is diurnal regulation of phytosiderophore synthesis and secretion from root tissues (Nozoye et al., 2004; Nozoye et al., 2014; Takagi et al., 1984). Though there is a relationship between deficiency of both Fe and Zn and the production of phytosiderophores, the import of Zn into the roots under sufficient conditions may not be an active process (Reid et al., 1996) and may only hinge on the activity of metal transport proteins such as the ZIP family of metal transporters, for loading into the long distance transport stream (Grotz and Guerinot, 2006). This difference in root loading may help explain the significant diurnal change observed for Fe concentration in the phloem and a lack of diurnal variability for Zn. It would be useful to explore further this relationship under deficient Fe and Zn conditions to determine the role of phytosiderphores in root uptake and the impact of diurnal rhythms on the uptake and long distance transport of these micronutrients.

Of the 79 metabolites detected by GC-MS, there were 26 that were unable to be identified (Palmer et al., 2014a). Of these 26 “unknown” metabolites, 14 had significant diurnal variability (Tables 5.6 to 5.88) and 10 showed significant maturity variability (Tables 5.9 to 5.11) within the phloem. One of these unknown metabolites may be of interest. For UN8_17.96_360, or Unknown 8 with a retention time of 17.96 minutes and a unique ion at 360 m/z, there was a significant 2.4 fold increase from morning to afternoon at 8-12 DAA and a 4.0 fold decrease from 8-12 DAA to 17-21 DAA for samples collected after 2pm, within the phloem metabolite profile. This follows a similar diurnal and maturity behaviour to what we observed for Fe. Further examination of the mass spectra enabled a tentative identification of a glutathione precursor Cys-Gly (data not shown). Further exploration of this

metabolite and the other unknowns may give further insight into the metabolic pathways in diurnal regulation of phloem transport.

The work presented here demonstrates the complex nature of the composition of phloem, with changes occurring in composition of both the metabolite and nutrient phloem profile at different times of day and maturities. This adds to our understanding of the long distance transport and the loading of essential micronutrients into the grain. Developments in methodology are in progress to add further metabolites such as sulphur containing amino acids and phytosiderphores which were not possible with the GC-MS method used here. This will enable further exploration of the metabolites that are proposed to complex Fe and Zn for long distance transport.

5.6 Acknowledgments

The authors wish to thank Daniel Dias and Ute Rossner at Melbourne University for their assistance with metabolite profiling. We would also like to thank both Jason Young at Flinders Analytical and Lyndon Palmer at the Waite Analytical Service for their assistance with the ICP-MS analysis.

5.7 Conflicts of Interest

The authors indicate that there are no known conflicts of interest pertaining to this work.

5.8 Author contributions:

LJP helped in conceiving study, collected phloem samples, did ICP-MS analysis, statistical analysis and drafted the manuscript. RG helped in the design of the study and drafting of manuscript. JS participated in conception and design of the study and assisted with drafting of manuscript. All authors read and approved the final manuscript.

Chapter 6. Enhanced levels of Fe and Zn in the Zn-dense wheat genotype SAMNYT 16 is associated with elevated levels of Fe, Zn and glutamate in the phloem during the early stages of grain loading.

Lachlan J. Palmer[1*], Robin D. Graham[1] and James C. R. Stangoulis[1]

[1] School of Biological Sciences, Flinders University, Bedford Park, South Australia 5042, Australia

*Corresponding Author: Lachlan James Palmer

Email: Lachlan.palmer@flinders.edu.au

6.1 Introduction

Biofortification of staple crops has been identified as a useful strategy for combating micronutrient deficiency in at-risk human populations (Mayer et al., 2008) and attempts to increase the levels of micronutrients and vitamins in the harvested and edible plant parts using genetic or agronomic techniques is currently underway (Murgia et al., 2012). An important part of the mineral biofortification process is the efficient transport of target micronutrients (i.e. Fe and Zn) from source to the sink (i.e. from soil, through to the roots, stems and leaves, and then to the seed) and therefore, the long-distance vascular pathways play significant roles in delivering nutrients to seeds (Borg et al., 2012). Genotypic differences in Zn turnover rates into the grain during grain loading have been demonstrated previously in two wheat varieties, SAMNYT 16 (S16) and Carnamah (Carn) (Stomph et al., 2011). S16 had a significantly higher Zn turnover rate into the grain during peak grain loading under high Zn supply (Stomph et al., 2011). In the work presented here we aim to explore further the supply of Zn, via the long distance transport pathway, to the grain in these two genotypes.

Within a plant, the long distance transport pathways of the xylem and phloem are the major routes for nutrient movement to developing seeds (Atwell et al., 1999). An example of the importance of nutrient transport has been demonstrated with work done overexpressing ferritin in the endosperm of rice where grain Fe was increased at the expense of leaf tissues (Brinch-Pedersen et al., 2007). In the case of wheat, the phloem is very important as there is a xylem discontinuity at the base of the grain (Zee and O'Brien, 1970) which results in all macro- and micro-nutrients having to transport to the phloem before unloading into the grain. During the transport of Fe and Zn in the phloem these minerals must be complexed owing to their reactive nature (Blindauer and Schmid, 2010). Several metabolites have been theorised to

complex Fe, Zn and other essential minerals within the phloem (Harris et al., 2012). In rice, nicotianamine (NA)has been demonstrated to complex Zn in the phloem whereas another phytosiderphore, 2'-deoxymugineic acid (DMA), was found to complex with Fe within the phloem (Nishiyama et al., 2012). In a model based on reported composition and conditions found within the phloem, Harris et al. (2012) demonstrated that there may be other agents involved in complexing mineral micro-nutrients for long distance transport, such as the amino acids glutamate and cysteine. In the past, access to appropriate analytical techniques for analysing small volumes of phloem has limited the analysis of phloem collected from cereals. Recent advances in analytical equipment and sampling methods have enabled the quantification of elements (Palmer et al., 2014b) and metabolites (Gattolin et al., 2008; Palmer et al., 2014a) in phloem volumes from 2 to 40 nl. The ability to analyse these small volumes, potentially collected across shorter periods of time, has enabled the exploration of diurnal variability within the phloem and variability in both the metabolite and elemental profile have been described (Gattolin et al., 2008, Chapter 5), thereby demonstrating the strength of these techniques.

The work presented here explores genotypic based variability of the elemental and metabolite profile of wheat phloem. Changes in genotypic variability during the grain loading phase of wheat will also be explored.

6.2 Materials and Methods

6.2.1 Solutions

Water-saturated paraffin oil (WSPO, LABCHEM™, Ajax Finechem) was produced by mixing two parts oil with one part Milli-Q water and shaking for 2 h on a rotary shaker. The solution was centrifuged briefly at 5000 rpm and excess water was removed. All HNO_3 solutions used in this research were prepared using Instrument Quality acid (Seastar) diluted v/v in high purity water (>18.2 MΩ cm^{-1} resistivity) using acid washed volumetric glassware. All inductively coupled plasma-mass spectrometry (ICP-MS) standards used in this research were prepared using a Gilson dual syringe auto-dilutor from certified single element stock solutions (1000 µg ml^{-1} High-Purity Standards). All final calibration and diluting solutions contain 2 µg L^{-1} indium (In) as an internal standard. Zinc sulphate was used to prepare 75 mg L^{-1} Zn solution needed for adding additional Zn to soil.

6.2.2 Plant Material

Wheat (*T. aestivum* L. cv. 'SAMNYT 16' and 'Carnamah') seedlings were grown in 70x100 mm pots filled with Debco™ Green Wizard potting mix within a growth room. Growth room conditions were 13/11 h light/dark at 20°C/10°C with a minimum of 400 µmol m^{-2} s^{-1} photosynthetic photon flux density at the leaf surface. When heads were fully emerged, additional Zn was applied to the soil at a rate of 750 µg Zn per pot which was equivalent to approximately 5 mg Zn kg^{-1} of soil.

6.2.3 Aphid Stylectomy

Aphid stylectomy procedures were adapted from Downing and Unwin (1977). Aphids were taken from an anholocyclic *Sitobion miscanthi* (Indian grain aphid) culture maintained at Flinders University on wheat plants kept under greenhouse conditions. Only apterous aphids were used in the experiments.

Aphids were secured to wheat plants (immediately below the head on the peduncle), a minimum of 12 h prior to stylectomy, using specially prepared cages. Plants were watered to saturation at the time of aphid caging. Stylectomy was performed using high-frequency micro-cauterisation under a Leica microscope (M165 C or MZ16) using an electrolytically-sharpened tungsten needle in combination with a micromanipulator. Exudate samples were collected using glass micro-capillaries (30-0017, Harvard Apparatus) pulled using a capillary puller (Narishige). Exudate sample collections were all started after 2pm with an average start time of 15:52:43 ± 0:09:58 (SE).

Collections were grouped on the basis of plant maturity and collection start time. Tables 6.1 and 6.2 show the mean maturity in days after anthesis (DAA) for both genotypes, Table 6.1 shows values for samples measured for micronutrients and Table 6.2 show values for metabolite profile samples.

Table 6.1 : Average maturity and standard error at time of sampling for each maturity grouping used for phloem elemental analysis.

Genotype	DAA grouping	n	Mean sample maturity	Std. Error of Mean
Carnamah	1-2 DAA	7	1.0	0.00
	8-12 DAA	9	9.7	0.24
	13-16 DAA	8	13.8	0.31
	17-21 DAA	6	18.5	0.34
SAMNYT 16	1-2 DAA	7	1.0	0.00
	8-12 DAA	30	9.3	0.14
	13-16 DAA	10	14.6	0.22
	17-21 DAA	27	18.6	0.18

DAA = Days after anthesis

Table 6.2 : Average maturity and standard error at time of sampling for each maturity grouping used for analysis of metabolite profile.

Genotype	DAA group	n	Mean sample maturity	Std. Error of Mean
SAMNYT 16	8-12 DAA	16	9.9	0.22
	17-21 DAA	20	18.5	0.17
Carnamah	8-12 DAA	6	9.8	0.31
	17-21 DAA	6	18.2	0.17

DAA = Days after anthesis

6.2.4 Tissue sampling and analysis

After phloem sampling was completed, the tiller that the sample was taken from was sampled 1cm above soil level. The tiller was separated into 4 parts, Flag leaf; second youngest leaf; head; and remaining tissues (stalk), and dried at 85 $^{\circ}$C for 24 hours. After drying, the seeds (if present) were separated from the head with both the seed and residual head tissues kept. The stalk and residual head tissues were ground using a Fritsch ball mill (Mini-Mill PULVERISETTE 23) with a ZrO_2 chamber and ball. All samples were sent to the Waite Analytical Service for analysis using the method outlined in Wheal et al. (2011)(Wheal et al., 2011). In this chapter, only the results for seed concentrations will be presented, refer to appendix 3 for full table of results for all tissues.

6.2.5 Microscope volume measurement of phloem exudate

Measurement of exudate volumes was modified from previously reported methods (Fisher and Cash-Clark, 2000; Gattolin et al., 2008) as recently reported (Palmer et al., 2013). Both methods were used for measuring phloem collection volumes. Samples analyzed by ICP-MS volumes were measured under WSPO, with each droplet immediately photographed within the WSPO using a Leica microscope (M165C or MZ16) with an attached camera (DFC295 or DFC280). The radius (µm) of the droplet was measured using the Leica Application Suite (LAS 3.6.0) with the additional Interactive Measurements Module and using the radius, the volume of the droplet estimated.

After samples were photographed, a 1.5 ml centrifuge tube was placed over the cap (containing the oil and the nanolitre droplet) and centrifuged briefly at 13,000 rpm to ensure the droplet was removed from the cap. 1 ml of diluting solution (2 % HNO_3, 2 µg L^{-1} In) was added and the tubes were vortexed briefly, and centrifuged at 13,000

rpm for approximately 30 s. The final aqueous solution was transferred, by pipette, to a new tube to reduce the amount of WSPO present during analysis.

For samples analysed by GC-MS, sample volumes were measured by using an estimated flow rate derived from photo sequences taken during sample collection (start, every 15 min and prior to collection, end) of the exuding stylet using a Leica microscope (M165C or MZ16) with an attached camera (DFC295 or DFC280) and the multi-time module from the Leica Application Suite software (v3.6.0). The average of the estimated flow rate from all sequences in each collection was multiplied by how long the sample was collected for, to give an estimate of the collection volume. A correction factor was applied to correct for evaporation (Palmer et al., 2013) and samples were deposited into 200 µl glass vial inserts (Agilent) containing 10 µl of Millipore, Milli-Q™ water (>18.2 MΩ cm^{-1}), centrifuged for 20 s at 14,000 rpm in a 1.5 ml microcentrifuge tube and then the insert was transferred to 2 ml auto sampler vials (Agilent) and stored at -80°C. After all samples had been collected, samples were lyophilized in a freeze dryer prior to shipment for metabolomics profiling and quantitation at Metabolomics Australia, School of Botany, The University of Melbourne.

6.2.6 ICP-MS analysis of phloem exudate

Samples were analysed by ICP-MS (Agilent 7500cx) (Palmer et al., 2014b). In brief samples were manually drawn directly from the 1.5 ml centrifuge tubes using a 500 mm length of 0.25 mm internal diameter (ID) sample tubing connected to 0.89 mm ID peristaltic tubing (0.89-ORG, Glass Expansion) with the attached peristaltic pump set at an uptake speed of 6 revolutions per minute. A 0.1 ml min^{-1} MicroMist nebulizer (Glass Expansion) was used for sample introduction. The reaction cell was run in He mode with a gas flow rate of 4.5 ml min^{-1} and the equipment was tuned

using the autotune function. Mass spectrum data acquisition was repeated three times per sample with a total acquisition time of 59.1 s per sample.

6.2.7 GC-MS analysis of phloem exudate

GC-MS analysis of phloem exudate samples was carried out using a method modified from Temmerman et al., (2012) as detailed previously (Palmer et al., 2014a). The lyophilized phloem samples were redissolved in 5 µl of 30 mg mL^{-1} methoxyamine hydrochloride in pyridine and derivatised at 37°C for 120 min with mixing at 500 rpm. The samples were then treated for 30 min with 10 µl *N,O-bis*-(trimethylsilyl)trifluoroacetamide (BSTFA) and 2.0 µl retention time standard mixture [0.029 % (*v*/*v*) *n* dodecane, *n*-pentadecane, *n*-nonadecane, *n*-docosane, *n*-octacosane, *n*-dotriacontane, *n*-hexatriacontane dissolved in pyridine] with mixing at 500 rpm. Each derivatised sample was allowed to rest for 60 min prior to injection.

Samples (1 µl) were injected into a GC-MS system comprised of a Gerstel 2.5.2 autosampler, a 7890A Agilent gas chromatograph and a 5975C Agilent quadrupole MS (Agilent, Santa Clara, USA). The MS was adjusted to 171 according to the manufacturer's recommendations using *tris*-(perfluorobutyl)-amine (CF43). The GC was performed on a 30 m VF-5MS column with 0.2 µm film thickness and a 10 m Integra guard column (Agilent J&W GC Column). The injection temperature was set at 250 °C, the MS transfer line at 280 °C, the ion source adjusted to 250 °C and the quadrupole at 150 °C. Helium was used as the carrier gas at a flow rate of 1.0 ml min^{-1}. For the polar metabolite analysis, the following temperature program was used; start at injection 70°C, a hold for 1 min, followed by a 7 °C min^{-1} oven temperature, ramp to 325 °C and a final 6 min heating at 325 °C. Both chromatograms and mass spectra were evaluated using the Chemstation Data Analysis program (Agilent, Santa Clara, USA). Mass spectra of eluting compounds

were identified and validated using the public domain mass spectra library of Max-Planck-Institute for Plant Physiology, Golm, Germany (http://csbdb.mpimp-golm.mpg.de/csbdb/dbma/msri.html) and the *in-house* Metabolomics Australia mass spectral library. All matching mass spectra were additionally verified by determination of the retention time by analysis of authentic standard substances. Resulting relative response ratios, that is, selected ion area of each metabolite was normalized to phloem volume for each identified metabolite. For metabolites which had multiple TMS derivatives, normalized ion areas are presented.

6.3 Results

6.3.1 Genotypic Variability: Elemental

6.3.1.1. Phloem

For both S16 and Carn there were significant changes in the elemental profile of the phloem during the course of grain loading which can be seen in Figure 6.1. There were also significant genotypic differences within the phloem elemental profile which can also be seen in Figure 6.1.

For the concentration of Mg in the phloem, there were no significant differences between the genotypes (Table 6.3). For the maturity related changes there was a significant increase in phloem Mg concentration from 1-2 DAA to 8-12 DAA for both genotypes (Table 6.4). The concentration of Mg in the phloem at 13-16 DAA was also significantly higher than that at 1-2 DAA for both genotypes. For S16 there was a significant decrease in phloem Mg concentration from 8-12 DAA to 17-21 DAA: this change was not observed in Carn (Table 6.4).

For K, at 8-12 DAA, there was a significant genotypic difference in phloem concentration between S16 and Carn, of 1164.0 ± 432.25 mg L^{-1}, $p = 0.011$ (Table 6.3). During grain loading both genotypes showed a decrease in K phloem concentration but only S16 had a significant decrease of 1353.6 ± 273.47 mg L^{-1}, $p < 0.001$ from 8-12 DAA to 17-21 DAA (Table 6.4).

There was 8.8 ± 3.48 mg L^{-1} ($p = 0.016$) more Fe in the phloem of S16 than in Carn at 8-12 DAA (Table 6.3). S16 also had a significant increase in Fe phloem concentration from 1-2 DAA to 8-12 DAA, with the phloem Fe concentration at 13-16 DAA also being significantly higher than at 1-2 DAA in S16. There was also a significant decrease in the Fe phloem concentration of S16 from 8-12 DAA to 17-21

DAA (Table 6.4). There were no significant maturity-related changes observed within the phloem of Carn (Table 6.4).

For Zn, there were no significant genotypic differences observed between S16 and Carn (Table 6.3); the largest difference in mean Zn phloem concentration was at 8-12 DAA with S16 Zn phloem concentration being 7.3 ± 4.27 mg L^{-1} ($p = 0.099$) greater than Carn (Table 6.3). Over the course of grain loading in S16 there was a significant increase in the Zn phloem concentration from 1-2 DAA to 8-12 DAA and a significant decrease from 8-12 DAA to 17-21 DAA (Table 6.4). There were no significant changes observed for the concentration of Zn in the phloem of Carn (Table 6.4). The largest increase in the phloem Zn concentration for Carn occurred from 1-2 DAA to 13-16 DAA, with an increase of 13.3 ± 5.18 mg L^{-1}, $p = 0.093$ (Table 6.4). For Carn, the largest decrease in Zn phloem concentration of 9.0 ± 5.46 mg L^{-1}, $p = 0.494$ was from 13-16 DAA to 17-21 DAA (Table 6.4).

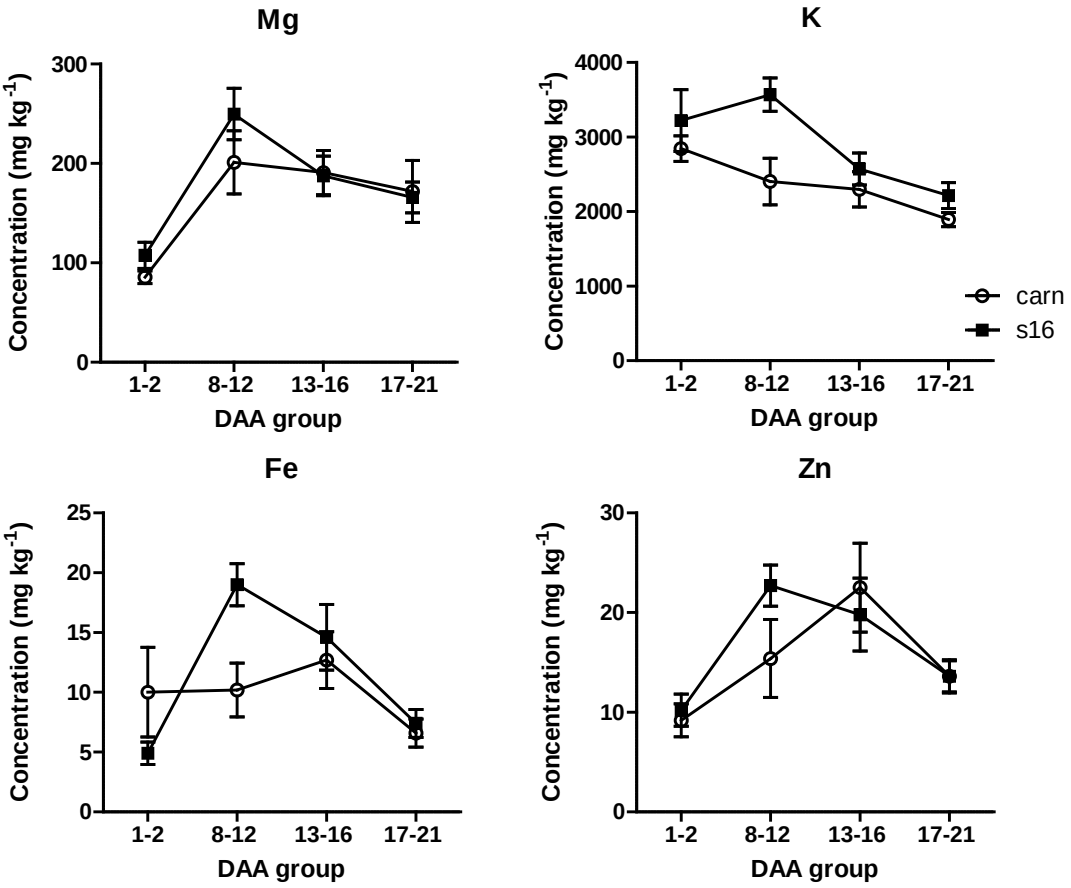

Figure 6.1 : The concentration of Mg, K, Fe and Zn in the phloem sampled from SAMNYT 16 (■, S16) and Carnamah (○, Carn) for different maturities (DAA = days after anthesis, values represent mean and standard error, sample sizes are listed in Table 6.3)

Table 6.3 : Results from independent t-tests for differences between the genotypes Carnamah (Carn) and SAMNYT 16 (S16) at different maturity groupings.

Element	Maturity grouping	Sample size (n) Carn	Sample size (n) S16	Mean Difference (Carn – S16)	Std. Error Difference	Sig. (2-tailed)
Mg	1-2 DAA	7	7	-22.0	14.63	0.158
	8-12 DAA	9	29	-48.8	49.94	0.335
	13-16 DAA	8	10	3.5	29.80	0.909
	17-21 DAA	6	27	6.0	35.99	0.868
K	1-2 DAA	7	7	-374.9	447.06	0.418
	8-12 DAA	9	28	-1164.0*	432.25	0.011
	13-16 DAA	8	10	-274.4	319.10	0.403
	17-21 DAA	6	27	-319.9	374.22	0.399
Fe	1-2 DAA[a]	7	7	5.1	3.86	0.227
	8-12 DAA	8	27	-8.8*	3.48	0.016
	13-16 DAA	8	10	-1.9	3.73	0.624
	17-21 DAA	5	12	-0.78	1.98	0.699
Zn	1-2 DAA	6	7	-0.94	2.32	0.691
	8-12 DAA	8	25	-7.3	4.27	0.099
	13-16 DAA	8	9	2.7	5.73	0.641
	17-21 DAA	5	19	-0.0047	3.21	0.999

DAA = days after anthesis.
Mean difference and standard error of the difference are in mg kg^{-1}.
a = inhomogeneous variances determined from Leverne's test of equal variances, *= the mean difference is significant at the 0.05 level.

Table 6.4 : Post hoc statistical tests for comparisons between collections obtained from SAMNYT 16 (S16) and Carnamah (Carn) at different maturities

Element	Genotype	DAA group (I)	DAA group (J)	Mean Difference (J-I)	Std. Error	Sig.
Mg	Carn[a]	1-2 DAA	8-12 DAA	115.5*	35.83	0.020
			13-16 DAA	105.4*	36.79	0.046
			17-21 DAA	86.4	39.55	0.198
		8-12 DAA	13-16 DAA	-10.0	34.54	1.000
			17-21 DAA	-29.1	37.47	0.965
		13-16 DAA	17-21 DAA	-19.0	38.39	0.996
	S16[b]	1-2 DAA	8-12 DAA	142.2*	29.03	0.000
			13-16 DAA	79.9*	23.76	0.021
			17-21 DAA	58.3*	20.29	0.039
		8-12 DAA	13-16 DAA	-62.3	32.59	0.243
			17-21 DAA	-83.8*	30.15	0.038
		13-16 DAA	17-21 DAA	-21.6	25.12	0.825
K	Carn[a]	1-2 DAA	8-12 DAA	-442.5	336.35	0.714
			13-16 DAA	-547.8	345.42	0.528
			17-21 DAA	-952.0	371.32	0.091
		8-12 DAA	13-16 DAA	-105.3	324.31	1.000
			17-21 DAA	-509.5	351.76	0.623
		13-16 DAA	17-21 DAA	-404.2	360.45	0.833
	S16[a]	1-2 DAA	8-12 DAA	346.6	428.45	0.960
			13-16 DAA	-648.4	499.66	0.726
			17-21 DAA	-1007.0	430.04	0.124
		8-12 DAA	13-16 DAA	-995.0	373.52	0.056
			17-21 DAA	-1353.6*	273.47	0.000
		13-16 DAA	17-21 DAA	-358.6	375.33	0.915
Fe	Carn[a]	1-2 DAA	8-12 DAA	0.17	3.68	1.000
			13-16 DAA	2.7	3.68	0.974
			17-21 DAA	-3.4	4.17	0.954
		8-12 DAA	13-16 DAA	2.5	3.56	0.977
			17-21 DAA	-3.6	4.06	0.936
		13-16 DAA	17-21 DAA	-6.1	4.06	0.584
	S16[b]	1-2 DAA	8-12 DAA	14.1*	1.99	0.000
			13-16 DAA	9.7*	2.89	0.028
			17-21 DAA	2.5	1.50	0.370
		8-12 DAA	13-16 DAA	-4.5	3.26	0.534
			17-21 DAA	-11.7*	2.11	0.000
		13-16 DAA	17-21 DAA	-7.2	2.98	0.126
Zn	Carn[a]	1-2 DAA	8-12 DAA	6.2	5.18	0.790
			13-16 DAA	13.3	5.18	0.093
			17-21 DAA	4.4	5.80	0.969
		8-12 DAA	13-16 DAA	7.1	4.79	0.598
			17-21 DAA	-1.8	5.46	1.000
		13-16 DAA	17-21 DAA	-9.0	5.46	0.494
	S16[a]	1-2 DAA	8-12 DAA	12.5*	3.83	0.011
			13-16 DAA	9.6	4.51	0.198
			17-21 DAA	3.4	3.96	0.945
		8-12 DAA	13-16 DAA	-2.9	3.48	0.955
			17-21 DAA	-9.1*	2.72	0.009
		13-16 DAA	17-21 DAA	-6.2	3.62	0.427

DAA = days after anthesis. Mean difference and standard error of the difference are in mg kg^{-1}. [a] = homogeneous variances, Hochberg post hoc test, [b] = inhomogeneous variances, Games-Howell post hoc test, *= the mean difference is significant at the 0.05 level.

6.3.1.2. Developing grain

For both S16 and Carn there were significant increases in elemental seed content during grain loading for all elements which can be seen in Figure 6.2 and Table 6.6. There were also significant genotypic differences within the phloem elemental profile which can also be seen in Figure 6.2.

For seed sampled at 8-12 DAA there was significantly more Fe, K and Mg per seed in Carn than S16 (0.16 ± 0.05, 22.66 ± 6.80 and 5.70 ± 2.12 µg grain^{-1} respectively, Table 6.5). For seed sampled at 13-16 DAA there was 0.24 ± 0.07 µg grain^{-1} ($p = 0.006$) more Zn per seed in S16 than Carn. Finally for seed taken at 17-21 DAA there was significantly more Fe and Mg per seed in Carn than S16 (0.16 ± 0.08, 4.41 ± 1.63 µg grain^{-1} respectively, Table 6.5).

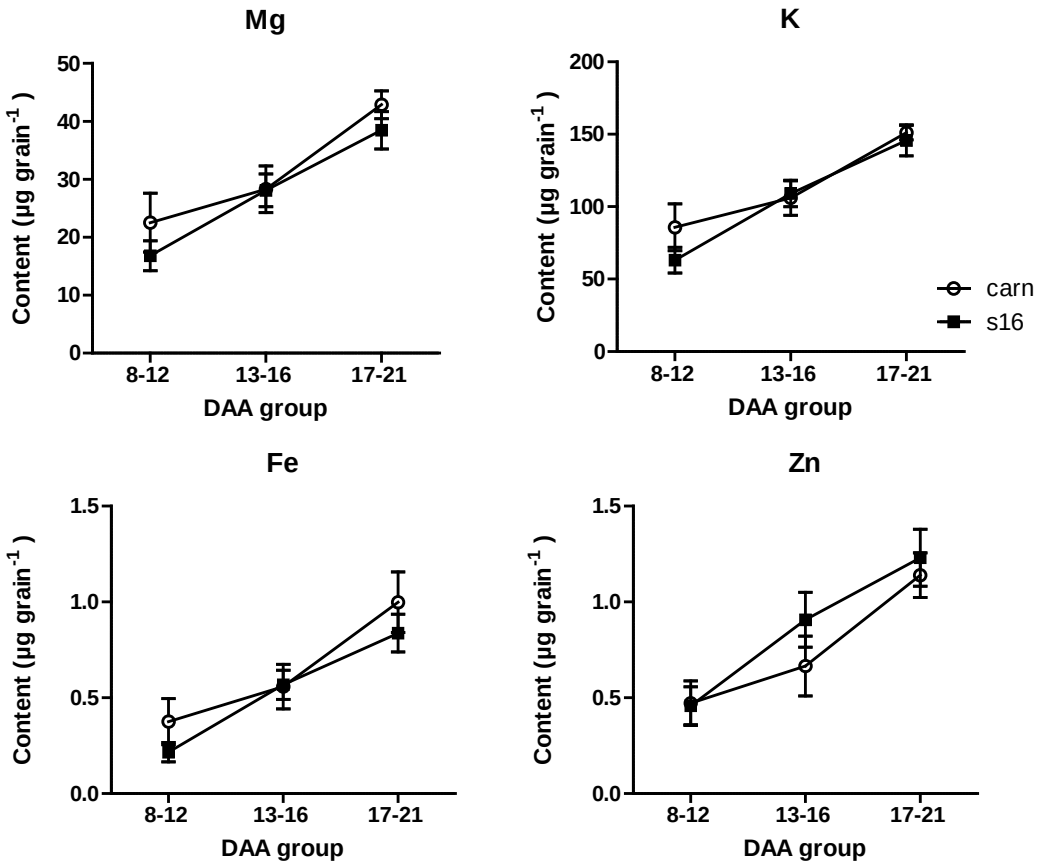

Figure 6.2 : The content (µg grain^{-1}) of Mg, K, Fe and Zn in developing seed sampled from SAMNYT 16 (■, S16) and Carnamah (○, Carn) for different maturities

(DAA = days after anthesis, values represent mean and standard error, sample sizes are listed in Table 6.5)

Table 6.5 : Results from independent t-tests for differences in seed content (µg grain^{-1}) between the genotypes Carnamah (Carn) and SAMNYT 16 (S16) at different maturity groupings.

Element	Maturity grouping	Sample size (n) Carn	Sample size (n) S16	Mean Difference (Carn – S16)	Std. Error Difference	Sig. (2-tailed)
Fe	8-12 DAA	9	7	0.16*	0.05	0.006
	13-16 DAA	8	8	-0.01	0.05	0.849
	17-21 DAA	6	6	0.16	0.08	0.060
Zn	8-12 DAA	9	7	0.01	0.06	0.800
	13-16 DAA	8	8	-0.24*	0.07	0.006
	17-21 DAA	6	6	-0.09	0.08	0.267
K	8-12 DAA	9	7	22.66*	6.80	0.005
	13-16 DAA	8	8	-3.10	5.31	0.569
	17-21 DAA	6	6	5.29	4.82	0.298
Mg	8-12 DAA	9	7	5.70*	2.12	0.017
	13-16 DAA	8	8	0.20	1.74	0.908
	17-21 DAA	6	6	4.41*	1.63	0.022

DAA = days after anthesis.
*= the mean difference is significant at the 0.05 level.

Table 6.6 : Post hoc statistical tests for comparisons of changes in elemental seed content (μg grain^{-1}) for SAMNYT 16 (S16) and Carnamah (Carn) at different maturities

Element	Genotype	DAA group (I)	DAA group (J)	Mean Difference (J-I)	Std. Error	Sig.
Fe	Carn	8-12 DAA	13-16 DAA	0.18*	0.06	0.026
			17-21 DAA	0.62*	0.07	0.000
		13-16 DAA	17-21 DAA	0.44*	0.07	0.000
	S16	8-12 DAA	13-16 DAA	0.35*	0.04	0.000
			17-21 DAA	0.62*	0.04	0.000
		13-16 DAA	17-21 DAA	0.27*	0.04	0.000
Zn	Carn	8-12 DAA	13-16 DAA	0.19*	0.06	0.020
			17-21 DAA	0.67*	0.07	0.000
		13-16 DAA	17-21 DAA	0.47*	0.07	0.000
	S16	8-12 DAA	13-16 DAA	0.45*	0.07	0.000
			17-21 DAA	0.77*	0.07	0.000
		13-16 DAA	17-21 DAA	0.32*	0.07	0.001
Mg	Carn	8-12 DAA	13-16 DAA	5.81*	2.03	0.028
			17-21 DAA	20.38*	2.20	0.000
		13-16 DAA	17-21 DAA	14.57*	2.25	0.000
	S16	8-12 DAA	13-16 DAA	11.30*	1.48	0.000
			17-21 DAA	21.66*	1.59	0.000
		13-16 DAA	17-21 DAA	10.36*	1.55	0.000
K	Carn	8-12 DAA	13-16 DAA	20.26*	6.15	0.011
			17-21 DAA	65.34*	6.67	0.000
		13-16 DAA	17-21 DAA	45.09*	6.84	0.000
	S16	8-12 DAA	13-16 DAA	46.01*	4.91	0.000
			17-21 DAA	82.71*	5.28	0.000
		13-16 DAA	17-21 DAA	36.70*	5.12	0.000

DAA = days after anthesis. *= the mean difference is significant at the 0.05 level.

6.3.2 Genotypic Variability: Metabolite profile

Nineteen metabolites were found to show significant differences within the phloem of S16 and Carn at two different maturity ranges (8-12 DAA and 17-21 DAA) (Tables 6.5 and 6.6). There was only one metabolite to have a significant difference between genotypes at both maturities. There was over 8 fold more 4-aminobutyric acid in the phloem of S16 than Carn at both 8-12 DAA and 17-21 DAA (Tables 6.5 and 6.6).

For the metabolites that showed significant genotypic differences in the phloem when sampled at 8-12 DAA (Table 6.5), apart from 4-aminobutyric acid there were 6 additional metabolites that comprised a significantly higher composition of the S16 phloem metabolite profile, with differences ranging from 1.7 fold more Serine to 9.9 fold more Proline. At the same maturity range there were 3 metabolites significantly higher in the Carn phloem metabolite profile with 1.4 fold more Fumarate, 1.9 fold more sucrose and 2.5 fold more Shikimic acid present in the profile of Carn phloem. There were 9 metabolites that only showed significant genotypic differences in the metabolite profiles between S16 and Carn when sampled at 17-21 DAA (Table 6.6). For the metabolites that showed significant genotypic differences in the phloem when sampled at 17-21 DAA, apart from 4-aminobutyric acid there were 6 additional metabolites that comprised a higher composition of the S16 phloem metabolite profile, with between 1.4-fold more UN23_33.43_517 and 5.5 fold more Glyceric acid-3-phosphate in the metabolite profile of S16. At the same maturity range there were 3 metabolites significantly higher in the Carn phloem metabolite profile with between 2.3 fold more Urea and 326.6 fold more Orotic acid present in the profile.

There were 7 metabolites that had significant maturity related variability for samples collected from both S16 and Carn (Table 6.7); the changes in metabolite profile had consistent changes for both genotypes. Of these metabolites, three had a significant increase within the metabolite profile from 8-12 DAA to 17-21 DAA with the increases ranging from 1.5 fold for UN16 in Carn to a 2.7 fold for Glycine in Carn (Table 6.7). The remaining four metabolites had a significant decrease in the metabolite profile from 8-12 DAA to 17-21 with decreases ranging from 2.0 fold for Alanine in S16 to a 3.4 fold decrease in Arginine for S16 (Table 6.7). There were 34 metabolites that had significant maturity related changes within the metabolite

profile of either S16 or Carn (Tables 6.8 and 6.9). For Carn there were 3 metabolites that showed a significant decrease within the phloem metabolite profile from 8-12 DAA to 17-21 DAA, the decreases ranged from 1.8 fold for UN21 to 4 fold for Glyceric acid-3-phosphate (Table 6.8). There were 15 metabolites that had a significant increase and 16 that decreased within the phloem metabolite profile of S16 between 8-12 DAA and 17-21 DAA (Table 6.9). The changes in the metabolite profile of S16 ranged from increase 1.5 fold for fumarate to 2.4 fold shikimic acid whilst the decreases ranged from 1.4 fold for pyroglutamte to 5.3 fold for ornithine (Table6.9).

Table 6.7 : Metabolites in the phloem with significant ($p < 0.05$) differences in metabolite relative response ratios between Carnamah (Carn, n=6) and SAMNYT 16 (S16, n=16) at 8-12 days after anthesis.

Metabolite	Transformation	Sig. (2-tailed)	fold difference
Proline 2TMS	Ln	0.032	9.9
4-aminobutyric acid 3TMS	SQRT	0.001[un]	8.2
Ornithine 3TMS	none	0.010[un]	3.9
Glutamine 4TMS	InvCBRT	0.025	3.3
3-amino-piperidin-2-one 2TMS	SQRT	0.048	2.7
Arginine 3TMS	Ln	0.029	2.1
Serine 3TMS	none	0.017	1.7
Fumarate 2TMS	none	0.014	-1.4
Sucrose 8TMS	SQRT	0.044	-1.9
Shikimic acid 4TMS	SQRT	0.009	-2.5

un = inhomogeneous sample variances as determined from Leverne's test of equal variances,
Ln = natural logarithm, InvCBRT = inverse cube root, SQRT = square root. *x*TMS = Trimethylsilyl derivative where *x* = the number of TMS groups;

Table 6.8 : Metabolites in the phloem with significant ($p < 0.05$) differences in metabolite relative response ratios between Carnamah (Carn, n=6) and SAMNYT 16 (S16, n=20)) at 17-21 days after anthesis.

Metabolite	Transformation	Sig. (2-tailed)	fold difference
4-aminobutyric acid 3TMS	SQRT	0.016[un]	8.1
Glyceric acid-3-phosphate 4TMS	SQRT	0.000	5.5
UN14_25.08_503	none	0.003 [un]	2.1
UN17_27.24_375	none	0.004 [un]	1.9
UN21_32.89_387	none	0.002	1.7
UN24_33.79_423	none	0.027	1.5
UN23_33.43_517	none	0.017	1.4
Urea 2TMS	CBRT	0.006	-2.3
Trehalose 8TMS	Ln	0.031	-3.3
Orotic acid 3TMS	InvCBRT	0.001 [un]	-326.6

un = inhomogeneous sample variances as determined from Leverne's test of equal variances,
Ln = natural logarithm, InvCBRT = inverse cube root, SQRT = square root, CBRT = cube root. *x*TMS = Trimethylsilyl derivative where *x* = the number of TMS groups

Table 6.9 : Metabolites in the phloem with significant ($p < 0.05$) differences between maturities in metabolite relative response ratios (17-21 DAA minus 8-12 DAA) for both genotypes.

Metabolite	Transformation	Genotype	Sig. (2-tailed)	fold change
Glycine 3TMS	none	Carn	0.000	2.7
		S16	0.002 [un]	1.9
Putrescine 4TMS	none	Carn	0.016 [un]	2.1
		S16	0.001	1.8
UN16_25.71_339	none	Carn	0.030	1.5
		S16	0.004 [un]	1.9
Alanine 2TMS	SQRT	Carn	0.013	-2.4
		S16	0.011 [un]	-2.0
Arginine 3TMS	Ln	Carn	0.045	-2.1
		S16	0.000	-3.4
Lysine 3TMS	none	Carn	0.031	-2.8
		S16	0.000	-2.7
UN01_10.61_158	CBRT	Carn	0.011	-2.5
		S16	0.000	-2.8

Carnamah = Carn, SAMNYT 16 = S16, un = inhomogeneous sample variances as determined from Leverne's test of equal variances, Ln = natural logarithm, SQRT = square root, CBRT = cube root. Carn at 8-12 DAA and 17-21 DAA, n = 6. S16 at 8-12 DAA, n=16 and for 17-21 DAA, n=20, *x*TMS = Trimethylsilyl derivative where *x* = the number of TMS groups

Table 6.10 : Metabolites in the phloem of Carnamah with a significant change in metabolite relative response ratios ($p < 0.05$) from 8-12 DAA (n=6) to 17-21 DAA (n = 6).

Metabolite	Transformation	Sig. (2-tailed)	fold change
UN21_32.89_387	none	0.029	-1.8
UN14_25.08_503	none	0.000	-3.1
Glyceric-3-phosphate 4TMS	SQRT	0.005	-4.0

un = inhomogeneous sample variances as determined from Leverne's test of equal variances, SQRT = square root. *x*TMS = Trimethylsilyl derivative where *x* = the number of TMS groups

Table 6.11 : Metabolites in the phloem of SAMNYT 16 with a significant change in metabolite relative response ratios ($p < 0.05$) from 8-12 DAA (n=16) to 17-21 DAA (n = 20).

Metabolite	Transformation	Sig. (2-tailed)	fold change
Shikimic acid 4TMS	SQRT	0.009 [un]	2.4
Quinic acid 5TMS	SQRT	0.037 [un]	2.2
Succinate 2TMS	None	0.024 [un]	2.1
Hexadecanoate 1TMS	SQRT	0.005 [un]	2.0
Octadecanoate 1TMS	SQRT	0.007 [un]	1.9
3-hydroxybenzoic acid 2TMS	CBRT	0.023	1.9
Sucrose 8TMS	SQRT	0.040 [un]	1.8
UN20_32.34_503	InvCBRT	0.031 [un]	1.8
UN04_15.56_185	None	0.013 [un]	1.8
Tyrosine 3TMS	None	0.010 [un]	1.7
Fructose_MX1	None	0.007 [un]	1.7
Citric acid 4TMS	None	0.014	1.6
UN17_27.24_375	None	0.009 [un]	1.6
Gluconic acid-1,5-lactone 4TMS	None	0.023 [un]	1.6
Glucose MX1	None	0.026 [un]	1.5
Fumarate 2TMS	None	0.027 [un]	1.5
Pyroglutamate 2TMS	None	0.024	-1.4
Serine 3TMS	None	0.001	-1.7
UN26_14.48_229	Ln	0.024	-1.9
UN11_19.48_299	CBRT	0.010	-2.1
Homoserine 3TMS	None	0.000	-2.2
UN09_18.15_275	CBRT	0.001	-2.3

Continued on next page.

Table 6.9 continued.

Metabolite	Transformation	Sig. (2-tailed)	fold change
UN07_17.62_275	Ln	0.001	-2.3
Pipecolic acid 2TMS	Ln	0.042	-2.3
Glutamate 3TMS	None	0.004 [un]	-2.5
Histidine 3TMS	Ln	0.009	-2.9
Glutamine 3TMS	CBRT	0.004	-3.0
3-amino-piperidin-2-one 2TMS	SQRT	0.001	-3.3
Asparagine_3TMS	Ln	0.015	-3.5
Trehalose 8TMS	Ln	0.001	-3.7
UN08_17.96_360	CBRT	0.000	-4.0
Ornithine 3TMS	None	0.005 [un]	-5.3

un = inhomogeneous sample variances as determined from Leverne's test of equal variances, SQRT = square root. *x*TMS = Trimethylsilyl derivative where *x* = the number of TMS groups; MX1 = methoxyamine derivatised product

6.4 Discussion

Previous research on genotypic variability in the phloem has been limited. To the author's knowledge there is only one report on genotypic differences in the element profile; significant differences in the concentration of Cd have been reported in the phloem of four rice genotypes (Kato et al., 2010). There have been more reports of genotypic differences in metabolites within the phloem, though for the most part these reports have covered differences in amino acids and sugars (Lohaus et al., 1998; Lohaus et al., 1994; Lohaus and Moellers, 2000; Sandström and Pettersson, 1994; Winzer et al., 1996). The genotypic differences for amino acids and sugars have been demonstrated in five genotypes of sugar beet (Lohaus et al., 1994; Winzer et al., 1996), two genotypes of maize (Lohaus et al., 1998) and two genotypes of rapeseed (*Brassica napus*) (Lohaus and Moellers, 2000). Genotypic differences have been reported for amino acids only in the phloem of five genotypes of pea (*Pisum sativum*) (Sandström and Pettersson, 1994). In more recent work, genotypic differences in the concentrations of glutathione and phytochelatin were reported in four genotypes of rice (Kato et al., 2010).

In all the cases listed above, significant genotypic variability was observed for phloem composition showing that there is the potential for exploring the role of long distance transport in genotypes that differ in a particular trait (i.e. differences in grain micronutrient content). In the past, the main limitation for exploring the phloem has been the volumes of phloem collected using the methods available (Dinant and Kehr, 2013). Recent advances have enabled smaller volumes to be collected and measured more accurately (Gattolin et al., 2008; Palmer et al., 2013). These methods have enabled the collection of samples over shorter time periods and also allowed increased numbers of samples to be collected within a day. These sampling

improvements have been combined with advances in the sensitivity of analytical hardware to explore diurnal variability (Gattolin et al., 2008; Chapter 5) and changes in the micronutrient and metabolite profile during grain loading (Palmer et al., 2014a; Palmer et al., 2014b). In the work presented here we have made use of these advances in sample collection and analysis to explore the genotypic variability in the elemental and metabolite profile of wheat phloem.

Genotypic differences were observed for all elements analysed as can be seen in Figure 6.1 and Table 6.3. The only statistically significant difference measured was at 8-12 DAA for both K and Fe, with S16 having more of both elements within the phloem at this maturity period than Carn. The main role of K in the phloem is in maintaining turgor through its osmotic potential (Marschner, 1995; Thompson and Zwieniecki, 2011). K has also been found to be involved in the process of loading both sucrose and amino acids into the phloem (Philippar et al., 2003; Servaites et al., 1979) and the uptake of sucrose along the transportation stream (Gajdanowicz et al., 2011). The role that K plays in assimilate transport is through its interaction with the proton symporter involved in assimilate loading (Gajdanowicz et al., 2011). Flow of K out of the phloem through potassium channels produces a negative potential within the phloem which enables the activation of the proton symporter, leading to loading of sucrose into the phloem (Gajdanowicz et al., 2011). This is likely to be of most importance for the scavenging of sucrose that has diffused from the phloem along the transportation stream where the ATP required for activation of the proton pump may be in short supply (Gajdanowicz et al., 2011). The balancing of the osmotic potential is likely the main reason for a decrease in K concentration with maturity but the genotypic differences observed in the phloem K concentration may be due to the second role of K as an energy source (that is for scavenging lost assimilates) and this

may increase the transport efficiency of amino acids and other complexing agents within the phloem involved in elemental transport. The secondary role of K as an energy source may be a partial reason for the higher levels of Zn, Mg and Fe observed at this same maturity. Though not statistically significant, the largest concentration differences between the genotypes for Mg and Zn occurs at 8-12 DAA. Unfortunately in the list of metabolites identified that showed significant variability between genotypes within the phloem at 8-12 DAA, none is as yet known to be involved in complexing Fe or Zn for transport in the phloem (Table 6.5). In a model of the speciation of trace metal ions in the phloem, based on a review of the chemistry and composition of phloem across a broad range of plant species, found the main metabolites responsible for binding Fe and Zn were the phytosiderophore NA and the amino acids glutamate and cysteine (Harris et al., 2012). Further work exploring the transport of Fe and Zn in the phloem of rice found that phytosiderophores were the only compounds involved in the complexing of these elements within the phloem (Nishiyama et al., 2012). For Zn in the phloem of rice, NA is responsible for chelation whilst Fe was bound to DMA (Nishiyama et al., 2012). The GC-MS metabolite profiling method used for the analysis presented here is unable to detect phytosiderophores but other methods are available and under further development for the analysis of these critical metabolites (Palmer et al., 2014a). It is also important that one of the larger significant differences between the genotypes within the metabolite profile was the 8.2 fold higher amount of 4-aminobutyric acid found in the metabolite profile of S16 in comparison to that of Carn (Table 6.5). The metabolite 4-aminobutyric acid is also known as *gamma*-aminobutyric acid or GABA (Bouché and Fromm, 2004). GABA has been found to be a significant signalling metabolite in the nervous system of vertebrates (Bouché

and Fromm, 2004). In plants, along with a role in signalling, GABA may also play role in defence against insects, protecting against oxidative stress and playing a role in osmoregulation (Bouché and Fromm, 2004). Of interest to the work presented here is research on duckweed (*Lemna minor* L.) where it was found that in cultures grown with and without GABA added to the culture solution, there were increases in tissue mineral composition for most macro and micronutrients when grown in additional GABA, indicating a role for GABA in modulating ion transport in plants (Kinnersley and Lin, 2000). As GABA is higher within the phloem of S16 than Carn at 8-12 DAA and this is also the stage of maturity where the greatest difference is observed for all elements measured in the phloem (Fig 6.1 and Table 6.3), this may provide further evidence for a role of GABA in both ion regulation and in long distance transport of these elements within the phloem.

This work was conducted on the genotypes Samnyt 16 and Carnamagh due to previous work that found that there was a significant difference in Zn concentration in the final grain of S16 when compared to Carn when additional Zn fertiliser was added (Stomph et al., 2011). The seed content results presented in this work are similar to that found previously with the average Zn content at 24 DAA for S16 being 1.58 ± SE 0.16 µg grain^{-1} whilst the average Zn conent in Carn was 1.53 ± SE 0.11 µg grain^{-1} (Stomph et al., 2011). We found that Zn content at 17-21 DAA was on average 1.14 ± SE 0.12 µg grain^{-1} for Carn and 1.23 ± SE 0.15 µg grain^{-1} in S16. We also found that there was a significant difference in Zn content at 13-16 DAA (Table 6.5). In the work presented by Stomph et al (2011) it was found that of the measurements taken, 14 DAA had the highest Zn turnover rate into the grain. In this work, the largest difference in Zn concentration in the phloem between the two genotypes occurs at 8-12 DAA with S16 having 7.3 ± 4.27 mg L^{-1} and though not

significant ($p = 0.099$) may provide some evidence of the role of phloem providing Zn to the head for the critical loading period at around 14 DAA. In the results presented in appendix 3 for the other tissue analysis there is some evidence that the head tissues of S16 (palea, lemma and rachis) are holding greater amounts of Zn. There is potential for further exploration of the role of tissues located near the developing seeds as stores for crucial nutrients.

Apart from the direct genotypic differences for elemental and metabolite profiles between the two genotypes as shown in Tables 6.3, 6.5 and 6.6, there were also differences in maturity related differences between the genotypes.

At 8-12 DAA there was a significant increase in sucrose within the Carn phloem, with there being 1.9 fold more sucrose in the metabolite profile of Carn when compared to that of S16 at 8-12 DAA (Table 6.5). This higher level of sucrose points towards the main role of K in maintaining osmotic potential (Marschner, 1995; Thompson and Zwieniecki, 2011), with less K when there is more sucrose present (Table 6.4). Also GABA acts on K transport as previously mentioned (Kinnersley and Lin, 2000).

For both Fe and Zn, the maximum concentration was at 8-12 DAA in S16 and 13-16 DAA in Carn (Table 6.4), most clearly seen with the significant difference in Fe concentration between the genotypes at 8-12 DAA (Table 6.3). The amino acid, glutamate was found to decline significantly within the phloem of S16 with a 2.5 fold decrease from 8-12 DAA to 17-21 DAA (Table 6.9) but no significant change for glutamate was seen across the same period in Carn (data not shown). Glutamate has been modelled to bind with up to 69.9 % of ferric Fe in the phloem. In the model, ferric Fe is the main form of Fe complexed and it is estimated that 96 % of Fe is in

this form (Harris et al., 2012). The significant decrease in glutamate within the phloem of S16 along with the significant decrease in Fe concentration across the same phase of maturity and genotype may provide further support for the model of trace metal speciation in respect to the role of glutamate in Fe complexation and also provides a possible reason for the genotypic difference between the two genotypes. A question is whether this finding extrapolates to a similar result within a larger wheat population? If it does, then this could eventually translate to the development of a marker (biochemical and molecular) for enhancing the Fe content of the grain.

It is also worth noting that there were 26 metabolites that were unable to be identified at the time of analysis. Of these unknowns, five were significantly higher in the phloem metabolite profile of S16 at 17-21 DAA when compared to that of Carn. Two unknowns had significant maturity related changes for both genotypes with one increasing and the other decreasing in the metabolite profile from 8-12 to 17-21 DAA. Finally there were ten unknown metabolites that had maturity related changes for only one genotype. These unknowns require further exploration to determine their identity and the role they might play in the long distance transport pathway of the phloem.

The work presented here gives further insight into the genotypic variability present within the phloem. This sets the ground work for further exploration of enhancing or changing the long distance transport pathway for the enhancement of loading essential micronutrients into the grain. Developments in methodology are in progress to add further metabolites such as sulphur containing amino acids and phytosiderphores which were not possible with the GC-MS method used here. This

will enable further exploration of the metabolites that are proposed to complex Fe and Zn for long distance transport.

Chapter 7. General Discussion

7.1 General Conclusions

The following general conclusions can be made regarding the exploration of phloem composition within wheat.

1. Optical based measurement of phloem sample collections under oil is affected by the shape of the oil surface.

2. Due to effects of oil surface on volume measurements it is critical to ensure that the oil surface is flat by determining the optimum oil volume when measuring phloem samples.

3. It is possible to apply a correction factor for the effect of evaporation on phloem collected and measured in air.

4. The elements K, Mg, Fe and Zn can be quantified using ICP-MS in phloem volumes as small as 15.5 nl.

5. Using GC-MS it is possible to semi-quantitatively measure 79 metabolites in the phloem of wheat, of which 53 are known (including, amino acids, organic acids, sugars and other metabolites) and 26 were designated as currently unknown, in volumes as small as 19.5nl.

6. Using LC-MS it was possible to measure the concentration of 26 amine containing compounds in volumes of wheat phloem as small as 43.4 nl. Using this method a further three metabolites were also able to be detected semi-quantitatively.

7. There are statistically significant changes in both the metabolite and micronutrient profile of the phloem during grain loading.

8. There are statistically significant changes in both the metabolite and micronutrient phloem profiles when sampled at different times of day.

9. There are statistically significant differences in the phloem metabolite and micronutrient phloem profiles between the high Zn loading wheat variety SAMNYT 16 and the low Zn loading variety Carnamah.

7.2 Experimental Variability

7.2.1 Volume measurement

Due to the nature of the method used for collecting phloem from wheat, sample volumes are very small, in the order of hundreds of nanolitres or less (Fisher and Frame, 1984). Previous methods used for sampling of the phloem using aphid stylectomy have detailed how evaporation is minimised but detail on measurement accuracy is secondary and or not mentioned at all (Downing, 1978; Pritchard, 1996). The work presented in this thesis has demonstrated a significant limitation in the use of oil during sample measurment. The oil surface can impact on optical based measurements introducing significant levels of error with small changes in the oil surface. It has also been mentioned that for some analytical methods, the use of oil is a serious contaminant (Gattolin et al., 2008). In appendix 1, evidence is presented that paraffin oil is a major issue with GC-MS analysis and so needs to be excluded if possible. A second method for volume measurement has been presented that is refined from a previous method (Gattolin et al., 2008) and demonstrates that a correction factor based on a linear model can be applied to samples collected in air to adjust for evaporation.

Even though the measurement accuracy of droplets under oil has been quantified for the method developed in this thesis, it may be possible to further improve accuracy.

In the work detailed in this thesis, no oil was used at the stylet-capillary interface so there may have been some loss of volume due to evaporation. The use of a well or oil droplet at the plant surface could be used during sample collection and then measured in oil using the method detailed in this thesis. There is also a need to compare the sample collection methods outlined in this work to the method of using microcaps for collection (Fukumorita and Chino, 1982; Kennedy and Mittler, 1953). This will help further explore the accuracy of sampling methods used for phloem collection.

7.2.2 Analytical methods

Analysis of phloem components has been limited due to the poor sensitivity of analytical equipment and the low volumes of sample collected (Fukumorita et al., 1983; Lohaus et al., 2000). Improvements in analytical sensitivity have enabled the measurement of phloem components in volumes less than 50 nl as demonstrated in Chapters 3 and 4. The methods described in these chapters further explored the capability of a variety of mass spectrometric analytical techniques. In Chapter 3 a novel method that enables the quantification of K, Mg, Fe and Zn within the phloem using ICP-MS is described. In addition to this being the first report of Fe and Zn concentration in wheat phloem, some of the limits of the method have been quantified including the method limit of detection. In Chapter 4 an analytical method for determining the metabolite profile of phloem samples as small as 19.5 nl using GC-MS was demonstrated along with a LC-MS method that enabled the quantification of a selection of amine containing compounds in volumes as small 43.4 nl. The methods used in Chapter 4 produced the first report of the quantification of nicotianamine and also the first report of a metabolite profile from the phloem of wheat.

Further work is required to improve and expand the analytical methods. Metabolites critical to the transport of micronutrients such as 2' deoxymugineic acid and S containing amino acids were either not detected, had poor sensitivity or not identified. The LC-MS amine method was not fully explored and further optimisation may help improve analysis for these metabolites. The GC-MS method found 26 metabolites that were unkown at the time of analysis and further exploration of these may provide even greater insight into wheat phloem dynamics. The method outlined in Chapter 4 aimed to attempt to capture information about as many metabolites as possible, which meant that only semi-quantitative analysis was possible due to the complexity of the analysis and the broad range of metabolites analysed. For important metabolites identified as playing a crucial role, there is potential for developing a method for quantification using GC-MS and this may be worth pursing further. For micronutrient analysis of phloem, the method presented in Chapter 3 was not the first method development attempted. An additional method which requires further development has the potential to add Cu, Mn and B to the analysis of phloem. This method needs less dilutant for sample preparation so has a greater potential sensitivity for elements at lower concentrations or with issues due to background interferences. With micronutrient analysis contamination known to be a major issue (Wheal et al., 2011) and in the method detailed in chapter 3, some of the results were excluded, owing to their having extremely high concentrations which was most likely due to contamination. Further exploration of the sources of contamination from sample collection to the final analysis may help reduce the prevalence of contamination as well as possibly reducing sources of variability that may obscure biological variability of interest.

7.3 Botanical Variability

7.3.3 Maturity variability

For maturity based variability in the phloem of cereals there are only two previous reports of changes in phloem composition with the reports detailing change in K and sucrose concentration along with total amino acid content (Fisher, 1987) or individual amino acid concentrations (Hayashi and Chino, 1990). The information presented in Chapters 3 to 6 further expand on these reports with the addition of information on the changes in an expanded metabolite profile and additional elements that compose the phloem during grain development and loading. For the concentrations of K, Mg, Fe and Zn it was possible to determine statistically significant concentration changes in the phloem of wheat in the period after anthesis and during grain loading. There were increases in Mg, Fe and Zn concentrations from the start of anthesis to the beginning of peak grain loading (9-12 DAA) and a decrease in K concentration from anthesis to the end of peak grain loading (13-16 DAA). Within the metabolite profile of wheat phloem, 39 metabolites had significant changes with a change in reproductive maturity. Of these, 21 were shown to increase and 18 decreased as the plant matured. Of particular interest were significant decreases in Glutamate and UN8 along with an increase in citrate during grain loading. Un8 has been tentatively identified as a glutathione precursor and this metabolite along with glutamate and citrate may play pivotal roles in micronutrient complex formation and transport within the phloem (Harris et al., 2012).

There were some indicators that there may be a small decrease in Fe and Zn concentration from peak grain loading to the end of grain loading (17-21 DAA) and though not always statistically significant, it may point to a potential limitation of supply during late grain loading. Further work examining and exploring this dynamic

may provide useful insight into issues with loading of micronutrients into grain. Due to costs related to metabolite profiling, only two maturity times were examined for the metabolite profile, and expansion to explore additional maturities especially vegetative or immediately after anthesis may enable the identification of more metabolites crucial to the transport of essential micronutrients within the phloem.

7.3.4 Diurnal variability

Previous research into diurnal variability within the phloem is limited to one report exploring changes in amino acid concentrations in wheat phloem sampled at different times of day (Gattolin et al., 2008). This report makes use of advances in analytical sensitivity along with a novel volume measurement method to enable sampling in a shorter period of time and analysis of samples as small as 2 nl (Gattolin et al., 2008). The method development done as part of this project has enabled the addition of elemental analysis and an expanded metabolite profile to the examination of diurnal variability within the phloem which has been detailed in Chapter 5. Significant diurnal variability was observed for Fe and K concentrations within the phloem with both Fe and K having higher concentrations later in day during the early stages of grain loading. Within the phloem metabolite profile, 39 metabolites were found to show significant diurnal variability. Of these the metabolite unknown 8 (UN08_17.96_360), which has been tentatively identified as a glutathione precursor (Cys-Gly), showed significant diurnal variability with more present in the metabolite profile later in the day. Glutathione has been found to be involved in tolerance to Fe deficiency (Kabir et al., 2013) as well as playing a role in reducing oxidative damage due to stress (Noctor and Foyer, 1998). The glutathione pathway may be worth further exploration in relation to long distance micronutrient transport. It was of interest to note that Fe and Zn appear to follow different pathways with diurnal

changes observed in Fe concentration but not for Zn. This is further supported by the literature where under sufficient conditions, Zn can move within the apoplasm without needing to be complexed (Reid et al., 1996) so uptake from the soil is only an issue under deficiency and this is when the phytosiderophore pathway may lead to an effect on Zn transport. It would be of interest to explore diurnal phloem variability under Fe and Zn deficiency conditions to further elucidate what mechanisms and relationships impact on micronutrient transport.

7.3.5 Genotypic Variability

Limited research has been published exploring genotypic based variability in phloem composition. For variability in the composition of cereal phloem there has been a single report exploring the genotypic variability in both elemental (Cd) concentration and metabolites (glutathione and phytochelatin 2) (Kato et al., 2010). There is another report demonstrating genotypic based differences in maize metabolites (sugars and/or amino acids) within the phloem (Lohaus et al., 1998). Both of these reports demonstrated genotypic based variability occurs within the phloem. The work presented in Chapter 6 has added further evidence that various genotypes show significant phloem composition variability for both elemental and metabolite composition. Significantly more Fe and K was measured in the phloem of S16 at the beginning of the peak grain loading period (8-12 DAA), also though not statistically significant there was more Mg and Zn in the phloem of S16 also at this time. Nineteen metabolites were found to show significant genotypic variability within the phloem metabolite profile at two different maturities. Only one of these metabolites, 4-aminobutyric acid (GABA) was found to be significantly different at both maturities sampled. GABA was more than 8 fold higher in the phloem metabolite profile of S16 than that of Carn. The action of GABA in plants is mostly associated

with stress responses or its role in maintaining the C:N balance (Bouché and Fromm, 2004) but links have also been made to relationships with ion transport (Kinnersley and Lin, 2000). S16 and Carn were selected as they have been found to have differences in final grain Zn (Stomph et al., 2011), the differences observed within the phloem at peak grain loading may help provide some evidence of the process for this difference observed in mature grain between these genotypes. Further exploration of other genotypes that differ in other traits of interest may provide further differences of interest in phloem metabolite composition.

7.4 Conclusions

The methods outlined in Chapters 2, 3 and 4 will assist in opening up the field of phloem physiology. The results presented demonstrate the importance of rigorous sample collection and the potential of advances in analytical techniques and existing methodology that will help revolutionise the exploration of phloem composition, physiology and chemistry. Using the foundation of the methods outlined in this thesis the need for careful planning of phloem physiology experiments was demonstrated in Chapters 3, 4 and 5. Careful consideration of sampling maturity and the time of day of sampling needs to be incorporated into any phloem based analysis due to the variability that has been demonstrated in this thesis. With these sources of biological variability taken into account, in Chapter 6 it was possible in demonstrate significant genotypic variability in the phloem that otherwise may have been missed. Further exploration of the basis of genotypic variability may provide useful insights into the long distance transport of key nutrients and provide targets for breeding or genetic modification. There is also potential to explore the relationships between deficiency and changes in phloem composition as a means for determining the role of phloem in tolerance pathways. This project has only presented analysis and exploration of the

phloem composition sampled from a single location. An expansion to include, tissues, xylem and other sampling points would further enhance our understanding of the dynamics involved in long distance transport and signaling.

The hope is that the work presented in this thesis will be the first step in further unlocking the role of the phloem as the plants information highway. Being able to explore the information contained within the metabolite and the nutrient profile of the phloem when used with other molecular and physiological techniques may open many facets of knowledge to phloem physiology. There is also the potential to add further methods for exploring the phloem. Within our group there has been some success in exploring the proteome of the phloem and micro RNA fragments have also been successfully detected. The exploration of the phloem has only just started and this thesis demonstrates the potential of what can be achieved with the advances being developed in the fields of analytical and molecular biology.

References

World Health Organisation. (2002) The world health report 2002 - reducing risks, promoting healthy life Geneva, Switzerland.

Aizat, W.M., Dias, D.A., Stangoulis, J.C.R., Able, J.A., Roessner, U., Able, A.J. (2014) Metabolomics of capsicum ripening reveals modification of the ethylene related-pathway and carbon metabolism. Postharvest Biology and Technology, **89**(0), 19-31.

Aki, T., Shigyo, M., Nakano, R., Yoneyama, T., Yanagisawa, S. (2008) Nano scale proteomics revealed the presence of regulatory proteins including three FT-Like proteins in phloem and xylem saps from rice. Plant and Cell Physiology, **49**(5), 767-790.

Amiard, V., Morvan-Bertrand, A., Cliquet, J.-B., Jean-Pierre, B., Huault, C., Sandström, J.P., Prud'homme, M.-P. (2004) Carbohydrate and amino acid composition in phloem sap of *Lolium perenne* L. before and after defoliation. Canadian Journal of Botany, **82**(11), 1594-1601.

Amiard, V., Mueh, K.E., Demmig-Adams, B., Ebbert, V., Turgeon, R., Adams, W.W. (2005) Anatomical and photosynthetic acclimation to the light environment in species with differing mechanisms of phloem loading. Proceedings of the National Academy of Sciences of the United States of America, **102**(36), 12968-12973.

Ando, Y., Nagata, S., Yanagisawa, S., Yoneyama, T. (2013) Copper in xylem and phloem saps from rice (Oryza sativa): the effect of moderate copper concentrations in the growth medium on the accumulation of five essential metals and a speciation analysis of copper-containing compounds. Functional Plant Biology, **40**(1), 89-100.

Andrés-Colás, N., Perea-García, A., Puig, S., Peñarrubia, L. (2010) Deregulated copper transport affects *Arabidopsis* development especially in the absence of environmental cycles. Plant Physiology, **153**(1), 170-184.

Atwell, B.B.J., Kriedmann, P.E., Turnbull, C.G.N. (1999) *Plants in Action: Adaptation in Nature, Performance in Cultivation* MacMillan Education Australia, South Yarra, Australia.

Barlow, C.A. and McCully, M.E. (1972) The ruby laser as an instrument for cutting the stylets of feeding aphids. Canadian Journal of Zoology, **50**(11), 1497-1498.

Blindauer, C.A. and Schmid, R. (2010) Cytosolic metal handling in plants: determinants for zinc specificity in metal transporters and metallothioneins. Metallomics, **2**(8), 510-529.

Borg, S., Brinch-Pedersen, H., Tauris, B., Madsen, L.H., Darbani, B., Noeparvar, S., Holm, P.B. (2012) Wheat ferritins: Improving the iron content of the wheat grain. Journal of Cereal Science, **56**(2), 204-213.

Bouché, N. and Fromm, H. (2004) GABA in plants: just a metabolite? Trends in Plant Science, **9**(3), 110-115.

Boughton, B.A., Callahan, D.L., Silva, C., Bowne, J., Nahid, A., Rupasinghe, T., Tull, D.L., McConville, M.J., Bacic, A., Roessner, U. (2011) Comprehensive Profiling and Quantitation of Amine Group Containing Metabolites. Analytical Chemistry, **83**(19), 7523-7530.

Bowden, P., Edwards, J., Ferguson, N., McNee, T., Manning, B., Roberts, K., Schipp, A., Schulze, K., Wilkins, J. (2008) *Wheat growth & development* NSW Dept. of Primary Industries, Orange, N.S.W.

Brinch-Pedersen, H., Borg, S., Tauris, B., Holm, P.B. (2007) Molecular genetic approaches to increasing mineral availability and vitamin content of cereals. Journal of Cereal Science, **46**(3), 308-326.

Dinant, S., Bonnemain, J.-L., Girousse, C., Kehr, J. (2010) Phloem sap intricacy and interplay with aphid feeding. Comptes Rendus Biologies, **333**(6-7), 504-515.

Dinant, S. and Kehr, J. (2013) Sampling and analysis of phloem sap. In Plant Mineral Nutrients (F.J.M. Maathuis, ed, Humana Press, New York: pp 185-194.

Ding, Z., Millar, A.J., Davis, A.M., Davis, S.J. (2007) TIME FOR COFFEE encodes a nuclear regulator in the *Arabidopsis thaliana* circadian clock. The Plant Cell Online, **19**(5), 1522-1536.

Downing, N. (1978) Short communications: Measurements of the osmotic concentrations of stylet sap, haemolymph and honeydew from an aphid under osmotic stress. Journal of Experimental Biology, **77**(1), 247-250.

Downing, N. and Unwin, D.M. (1977) A new method for cutting the mouth-parts of feeding aphids, and for collecting plant sap. Physiological Entomology, **2**(4), 275-277.

Duc, C., Cellier, F., Lobréaux, S., Briat, J.-F., Gaymard, F. (2009) Regulation of iron homeostasis in *Arabidopsis thaliana* by the clock regulator Time for Coffee. Journal of Biological Chemistry, **284**(52), 36271-36281.

Field, A. (2007) *Discovering Statistics Using SPSS* SAGE Publications, London, UK.

Fisher, D. (1987) Changes in the concentration and composition of peduncle sieve tube sap during grain filling in normal and phosphate-deficient wheat plants. Functional Plant Biology, **14**(2), 147-156.

Fisher, D.B. and Cash-Clark, C.E. (2000) Gradients in water potential and turgor pressure along the translocation pathway during grain filling in normally watered and water-stressed wheat plants. Plant Physiology, **123**(1), 139-148.

Fisher, D.B. and Frame, J.M. (1984) A guide to the use of the exuding-stylet technique in phloem physiology. Planta, **161**(5), 385-393.

Fisher, D.B. and Gifford, R.M. (1986) Accumulation and conversion of sugars by developing wheat grains : VI. gradients along the transport pathway from the peduncle to the endosperm cavity during grain filling. Plant Physiology, **82**(4), 1024-1030.

Fukumorita, T. and Chino, M. (1982) Sugar, amino acid and inorganic contents in rice phloem sap. Plant and Cell Physiology, **23**(2), 273-283.

Fukumorita, T., Noziri, Y., Haraguchi, H., Chino, M. (1983) Inorganic content in rice phloem sap. Soil Science and Plant Nutrition, **29**(2), 185-192.

Gajdanowicz, P., Michard, E., Sandmann, M., Rocha, M., Corrêa, L.G.G., Ramírez-Aguilar, S.J., Gomez-Porras, J.L., González, W., Thibaud, J.-B., van Dongen, J.T., Dreyer, I. (2011) Potassium (K+) gradients serve as a mobile energy source in plant vascular tissues. Proceedings of the National Academy of Sciences, **108**(2), 864-869.

Gattolin, S., Newbury, H.J., Bale, J.S., Tseng, H.-M., Barrett, D.A., Pritchard, J. (2008) A diurnal component to the variation in sieve tube amino acid content in wheat. Plant Physiology, **147**(2), 912-921.

Gaupels, F., Buhtz, A., Knauer, T., Deshmukh, S., Waller, F., van Bel, A.J.E., Kogel, K.-H., Kehr, J. (2008) Adaptation of aphid stylectomy for analyses of proteins and mRNAs in barley phloem sap. Journal of Experimental Botany, **59**(12), 3297-3306.

Girousse, C., Bonnemain, J.-L., Delrot, S., Bournoville, R. (1991) Sugar and amino acid composition of phloem sap of Medicago sativa: a comparative study of two collecting methods. Plant physiology and biochemistry, **29**(1), 41-48.

Grotz, N. and Guerinot, M.L. (2006) Molecular aspects of Cu, Fe and Zn homeostasis in plants. Biochimica et Biophysica Acta (BBA) - Molecular Cell Research, **1763**(7), 595-608.

Hall, A., Bastow, R.M., Davis, S.J., Hanano, S., McWatters, H.G., Hibberd, V., Doyle, M.R., Sung, S., Halliday, K.J., Amasino, R.M., Millar, A.J. (2003) The TIME FOR COFFEE gene maintains the amplitude and timing of *Arabidopsis* circadian clocks. The Plant Cell Online, **15**(11), 2719-2729.

Hall, S.M. and Baker, D.A. (1972) The chemical composition of *Ricinus* phloem exudate. Planta, **106**(2), 131-140.

Harris, W.R., Sammons, R.D., Grabiak, R.C. (2012) A speciation model of essential trace metal ions in phloem. Journal of Inorganic Biochemistry, **116**(0), 140-150.

Hayashi, H. and Chino, M. (1986) Collection of pure phloem sap from wheat and its chemical composition. Plant and Cell Physiology, **27**(7), 1387-1393.

Hayashi, H. and Chino, M. (1990) Chemical composition of phloem sap from the uppermost internode of the rice plant. Plant and Cell Physiology, **31**(2), 247-251.

Haydon, M.J., Bell, L.J., Webb, A.A.R. (2011) Interactions between plant circadian clocks and solute transport. Journal of Experimental Botany.

Hecht, E. (2002) *Optics* Addison Wesley, San Francisco, CA.

Hocking, P.J. (1980) The composition of phloem exudate and xylem sap from tree tobacco (*Nicotiana glauca* Grah.). Annals of Botany, **45**(6), 633-643.

Hocking, P.J. (1983) The dynamics of growth and nutrient accumulation by fruits of *Grevillea leucopteris* meissn., a proteaceous shrub, with special reference to the composition of xylem and phloem sap. New Phytologist, **93**(4), 511-529.

Kabir, A.H., Paltridge, N.G., Roessner, U., Stangoulis, J.C.R. (2013) Mechanisms associated with Fe-deficiency tolerance and signaling in shoots of Pisum sativum. Physiologia Plantarum, **147**(3), 381-395.

Kato, M., Ishikawa, S., Inagaki, K., Chiba, K., Hayashi, H., Yanagisawa, S., Yoneyama, T. (2010) Possible chemical forms of cadmium and varietal differences in cadmium concentrations in the phloem sap of rice plants (Oryza sativa L.). Soil Science and Plant Nutrition, **56**(6), 839-847.

Kawabe, S., Fukumorita, T., Chino, M. (1980) Collection of rice phloem sap from stylets of homopterous insects severed by YAG laser. Plant and Cell Physiology, **21**(8), 1319-1327.

Kennedy, J.S. and Mittler, T.E. (1953) A method of obtaining phloem sap via the mouth-parts of aphids. Nature, **171**(4351), 528-528.

Kinnersley, A. and Lin, F. (2000) Receptor modifiers indicate that 4-aminobutyric acid (GABA) is a potential modulator of ion transport in plants. Plant Growth Regulation, **32**(1), 65-76.

Kopka, J., Schauer, N., Krueger, S., Birkemeyer, C., Usadel, B., Bergmüller, E., Dörmann, P., Weckwerth, W., Gibon, Y., Stitt, M., Willmitzer, L., Fernie, A.R., Steinhauser, D. (2005) GMD@CSB.DB: the Golm Metabolome Database. Bioinformatics, **21**(8), 1635-1638.

Liu, D.D., Chao, W.M., Turgeon, R. (2012) Transport of sucrose, not hexose, in the phloem. Journal of Experimental Botany, **63**(11), 4315-4320.

Lohaus, G., Büker, M., Hußmann, M., Soave, C., Heldt, H.W. (1998) Transport of amino acids with special emphasis on the synthesis and transport of asparagine in the Illinois Low Protein and Illinois High Protein strains of maize. Planta, **205**(2), 181-188.

Lohaus, G., Burba, M., Heldt, H.W. (1994) Comparison of the contents of sucrose and amino acids in the leaves, phloem sap and taproots of high and low sugar-producing hybrids of sugar beet (Beta vulgaris L.). Journal of Experimental Botany, **45**(8), 1097-1101.

Lohaus, G., Hussmann, M., Pennewiss, K., Schneider, H., Zhu, J.J., Sattelmacher, B. (2000) Solute balance of a maize (*Zea mays* L.) source leaf as affected by salt treatment with special emphasis on phloem retranslocation and ion leaching. Journal of Experimental Botany, **51**(351), 1721-1732.

Lohaus, G. and Moellers, C. (2000) Phloem transport of amino acids in two Brassica napus L. genotypes and one B. carinata genotype in relation to their seed protein content. Planta, **211**(6), 833-840.

Maas, F.M., van de Wetering, D.A.M., van Beusichem, M.L., Bienfait, H.F. (1988) Characterization of phloem iron and Its possible role in the regulation of Fe-efficiency reactions. Plant Physiology, **87**(1), 167-171.

Marschner, H. (1995) *Mineral Nutrition of Higher Plants* Acad. Press.

Mayer, J.E., Pfeiffer, W.H., Beyer, P. (2008) Biofortified crops to alleviate micronutrient malnutrition. Current Opinion in Plant Biology, **11**, 1-5.

McLean, E., Cogswell, M., Egli, I., Wojdyla, D., de Benoist, B. (2009) Worldwide prevalence of anaemia, WHO vitamin and mineral nutrition information system, 1993–2005. Public Health Nutrition, **12**(4), 444-454.

Mendoza-Cózatl, D.G., Butko, E., Springer, F., Torpey, J.W., Komives, E.A., Kehr, J., Schroeder, J.I. (2008) Identification of high levels of phytochelatins, glutathione and cadmium in the phloem sap of *Brassica napus*. A role for thiol-peptides in the long-distance transport of cadmium and the effect of cadmium on iron translocation. The Plant Journal, **54**(2), 249-259.

Michael, T.P., Mockler, T.C., Breton, G., McEntee, C., Byer, A., Trout, J.D., Hazen, S.P., Shen, R., Priest, H.D., Sullivan, C.M., Givan, S.A., Yanovsky, M., Hong, F., Kay, S.A., Chory, J. (2008) Network discovery pipeline elucidates conserved time-of-day–specific cis-regulatory modules. PLoS Genet, **4**(2), e14.

Mittler, T.E. (1958) Studies on the feeding and nutrition of *Tuberolachnus salignus* (Gmelin) (Homoptera, Aphididae) : II. The nitrogen and sugar composition of ingested phloem sap and excreted honeydew. Journal of Experimental Biology, **35**(1), 74-84.

Murgia, I., Arosio, P., Tarantino, D., Soave, C. (2012) Biofortification for combating 'hidden hunger' for iron. Trends in Plant Science, **17**(1), 47-55.

Negishi, T., Nakanishi, H., Yazaki, J., Kishimoto, N., Fujii, F., Shimbo, K., Yamamoto, K., Sakata, K., Sasaki, T., Kikuchi, S., Mori, S., Nishizawa, N.K. (2002) cDNA microarray analysis of gene expression during Fe-deficiency stress in barley suggests that polar transport of vesicles is implicated in phytosiderophore secretion in Fe-deficient barley roots. The Plant Journal, **30**(1), 83-94.

Nishiyama, R., Kato, M., Nagata, S., Yanagisawa, S., Yoneyama, T. (2012) Identification of Zn–nicotianamine and Fe–2′-deoxymugineic acid in the phloem sap from rice plants (*Oryza sativa* L.). Plant and Cell Physiology, **53**(2), 381-390.

Noctor, G. and Foyer, C.H. (1998) ASCORBATE AND GLUTATHIONE: Keeping Active Oxygen Under Control. Annual Review of Plant Physiology and Plant Molecular Biology, **49**(1), 249-279.

Nozoye, T., Itai, R.N., Nagasaka, S., Takahashi, M., Nakanishi, H., Mori, S., Nishizawa, N.K. (2004) Diurnal changes in the expression of genes that participate in phytosiderophore synthesis in rice. Soil Science and Plant Nutrition, **50**(7), 1125-1131.

Nozoye, T., Nagasaka, S., Bashir, K., Takahashi, M., Kobayashi, T., Nakanishi, H., Nishizawa, N.K. (2014) Nicotianamine synthase 2 localizes to the vesicles of iron-deficient rice roots, and its mutation in the YXXφ or LL motif causes the disruption of vesicle formation or movement in rice. The Plant Journal, **77**(2), 246-260.

O'Dell, B.L. and Sunde, R.A. (1997) *Handbook of nutritionally essential mineral elements* Marcel Dekker, New York.

Palmer, L., Dias, D., Boughton, B., Roessner, U., Graham, R., Stangoulis, J. (2014a) Metabolite profiling of wheat (*Triticum aestivum* L.) phloem exudate. Plant Methods, **10**(1), 27.

Palmer, L.J., Palmer, L.T., Pritchard, J., Graham, R.D., Stangoulis, J.C.R. (2013) Improved techniques for measurement of nanolitre volumes of phloem exudate from aphid stylectomy. Plant Methods, **9**, 18.

Palmer, L.J., Palmer, L.T., Rutzke, M.A., Graham, R.D., Stangoulis, J.C.R. (2014b) Nutrient variability in phloem: examining changes in K, Mg, Zn and Fe concentration during grain loading in common wheat (*Triticum aestivum* L.). Physiologia Plantarum, **152**, 729-737.

Peel, A.J. (1975) Investigations with aphid stylets into the physiology of the sieve tube. In Transport in Plants 1 Phloem Transport (M.H. Zimmerman & J.A. Milburn, eds), Springer, Berlin Heidelberg New York: pp 171-195.

Peuke, A.D. (2010) Correlations in concentrations, xylem and phloem flows, and partitioning of elements and ions in intact plants. A summary and statistical re-evaluation of modelling experiments in *Ricinus communis*. Journal of Experimental Botany, **61**(3), 635-655.

Philippar, K., Büchsenschütz, K., Abshagen, M., Fuchs, I., Geiger, D., Lacombe, B., Hedrich, R. (2003) The K+ channel KZM1 mediates potassium uptake into the phloem and guard cells of the C4 grass *Zea mays*. Journal of Biological Chemistry, **278**(19), 16973-16981.

Ponder, K.L., Pritchard, J., Harrington, R., Bale, J.S. (2000) Difficulties in location and acceptance of phloem sap combined with reduced concentration of phloem amino acids explain lowered performance of the aphid Rhopalosiphum padi on nitrogen deficient barley (Hordeum vulgare) seedlings. Entomologia Experimentalis et Applicata, **97**(2), 203-210.

Pritchard, J. (1996) Aphid stylectomy reveals an osmotic step between sieve tube and cortical cells in barley roots. Journal of Experimental Botany, **47**(10), 1519-1524.

Ravet, K., Touraine, B., Boucherez, J., Briat, J.-F., Gaymard, F., Cellier, F. (2009) Ferritins control interaction between iron homeostasis and oxidative stress in *Arabidopsis*. The Plant Journal, **57**(3), 400-412.

Reichman, S.M. and Parker, D.R. (2007) Probing the effects of light and temperature on diurnal rhythms of phytosiderophore release in wheat. New Phytologist, **174**(1), 101-108.

Reid, R., Brookes, J., Tester, M., Smith, F.A. (1996) The mechanism of zinc uptake in plants. Planta, **198**(1), 39-45.

Rengel, Z. and Römheld, V. (2000) Root exudation and Fe uptake and transport in wheat genotypes differing in tolerance to Zn deficiency. Plant and Soil, **222**(1), 25-34.

Richardson, P.T., Baker, D.A., Ho, L.C. (1982) The chemical composition of cucurbit vascular exudates. Journal of Experimental Botany, **33**(6), 1239-1247.

Riens, B., Lohaus, G., Heineke, D., Heldt, H.W. (1991) Amino acid and sucrose content determined in the cytosolic, chloroplastic, and vacuolar compartments and in the phloem sap of spinach leaves. Plant Physiology, **97**(1), 227-233.

Sandström, J. and Pettersson, J. (1994) Amino acid composition of phloem sap and the relation to intraspecific variation in pea aphid (*Acyrthosiphon pisum*) performance. Journal of Insect Physiology, **40**(11), 947-955.

Sandström, J., Telang, A., Moran, N.A. (2000) Nutritional enhancement of host plants by aphids — a comparison of three aphid species on grasses. Journal of Insect Physiology, **46**(1), 33-40.

Schmidke, I., Krüger, C., Frömmichen, R., Scholz, G., Stephan, U.W. (1999) Phloem loading and transport characteristics of iron in interaction with plant-endogenous ligands in castor bean seedlings. Physiologia Plantarum, **106**(1), 82-89.

Schmidke, I. and Stephan, U.W. (1995) Transport of metal micronutrients in the phloem of castor bean (*Ricinus communis*) seedlings. Physiologia Plantarum, **95**(1), 147-153.

Serra Bonvehi, J. and Orantes Bermejo, F.J. (2012) Detection of adulterated commercial Spanish beeswax. Food Chemistry, **132**(1), 642-648.

Servaites, J.C., Schrader, L.E., Jung, D.M. (1979) Energy-dependent loading of amino acids and sucrose into the phloem of soybean. Plant Physiology, **64**(4), 546-550.

Shelp, B.J. (1987) The composition of phloem exudate and xylem sap from broccoli (*Brassica oleracea* var. italica) supplied with NH_4^+, NO_3^- or NH_4NO_3. Journal of Experimental Botany, **38**(10), 1619-1636.

Stangoulis, J., Tate, M., Graham, R., Bucknall, M., Palmer, L., Boughton, B., Reid, R. (2010) The mechanism of boron mobility in wheat and canola phloem. Plant Physiology, **153**(2), 876-881.

Stangoulis, J.C.R., Brown, P.H., Bellaloui, N., Reid, R.J., Graham, R.D. (2001) The efficiency of boron utilisation in canola. Functional Plant Biology, **28**(11), 1109-1114.

Stein, R.J., Ricachenevsky, F.K., Fett, J.P. (2009) Differential regulation of the two rice ferritin genes (OsFER1 and OsFER2). Plant Science, **177**(6), 563-569.

Stephan, U., Schmidke, I., Pich, A. (1994) Phloem translocation of Fe, Cu, Mn, and Zn in Ricinus seedlings in relation to the concentrations of nicotianamine, an endogenous chelator of divalent metal ions, in different seedling parts. Plant and Soil, **165**(2), 181-188.

Stephan, U.W. and Scholz, G. (1993) Nicotianamine: mediator of transport of iron and heavy metals in the phloem? Physiologia Plantarum, **88**(3), 522-529.

Stomph, T.J., Choi, E.Y., Stangoulis, J.C.R. (2011) Temporal dynamics in wheat grain zinc distribution: is sink limitation the key? Annals of Botany, **107**(6), 927-937.

Taiz, L. and Zeiger, E. (2002) *Plant Physiology* Sinauer Associates, Sunderland, Massachusetts U.S.A.

Takagi, S.i., Nomoto, K., Takemoto, T. (1984) Physiological aspect of mugineic acid, a possible phytosiderophore of graminaceous plants. Journal of Plant Nutrition, **7**(1-5), 469-477.

Temmerman, L., Livera, A.M.D., Bowne, J.B., Sheedy, J.R., Callahan, D.L., Nahid, A., Souza, D.P.D., Schoofs, L., Tull, D.L., McConville, M.J., Roessner, U., Wentworth, J.M. (2012) Cross-platform urine metabolomics of experimental hyperglycemia in type 2 diabetes. Journal of Diabetes & Metabolism, **S6**, 002.

Thompson, G.A. and van Bel, A.J.E. (2012) Phloem: Molecular cell biology, systemic communication, biotic interactions, Wiley-Blackwell, Oxford, UK.

Thompson, M.V. (2006) Phloem: the long and the short of it. Trends in Plant Science, **11**(1), 26-32.

Thompson, M.V. and Zwieniecki, M.A. (2011) The role of potassium in long distance transport. In Vascular Transport in Plants (N.M. Holbrook & M.A. Zwieniecki, eds), Elsevier Science, Burlington, MA, USA: pp 221-240.

Tissot, N., Przybyla-Toscano, J., Reyt, G., Castel, B., Duc, C., Boucherez, J., Gaymard, F., Briat, J.-F., Dubos, C. (2014) Iron around the clock. Plant Science, **224**(0), 112-119.

Turgeon, R. (1996) Phloem loading and plasmodesmata. Trends in Plant Science, **1**(12), 418-423.

Turgeon, R. and Wolf, S. (2009) Phloem transport: Cellular pathways and molecular trafficking. Annual Review of Plant Biology, **60**(1), 207-221.

Van Bel, A.J.E. (1993) Strategies of Phloem Loading. Annual Review of Plant Physiology and Plant Molecular Biology, **44**(1), 253-281.

Van Bel, A.J.E. (2003) The phloem, a miracle of ingenuity. Plant, Cell & Environment, **26**, 125-149.

Welch, R.M. (1995) Micronutrient nutrition of plants. Critical Reviews in Plant Sciences, **14**(1), 49 - 82.

Wheal, M.S., Fowles, T.O., Palmer, L.T. (2011) A cost-effective acid digestion method using closed polypropylene tubes for inductively coupled plasma optical emission spectrometry (ICP-OES) analysis of plant essential elements. Analytical Methods, **3**(12), 2854-2863.

Wijnen, H. and Young, M.W. (2006) Interplay of circadian clocks and metabolic rhythms. Annual Review of Genetics, **40**(1), 409-448.

Winter, H., Lohaus, G., Heldt, H.W. (1992) Phloem Transport of Amino Acids in Relation to their Cytosolic Levels in Barley Leaves. Plant Physiology, **99**(3), 996-1004.

Winzer, T., Lohaus, G., Heldt, H.-W. (1996) Influence of phloem transport, N-fertilization and ion accumulation on sucrose storage in the taproots of fodder beet and sugar beet. Journal of Experimental Botany, **47**(7), 863-870.

Wolswinkel, P. (1999) Chapter 4: long distance nutrient transport in plants and movement into developing grains. In Mineral nutrition of crops: fundamental mechanisms and implications (Z. Rengel, ed, Food Products Press, New York: pp 91-115.

Yoneyama, T., Gosho, T., Kato, M., Goto, S., Hayashi, H. (2010) Xylem and phloem transport of Cd, Zn and Fe into the grains of rice plants (*Oryza sativa* L.) grown in continuously flooded Cd-contaminated soil. Soil Science and Plant Nutrition, **56**(3), 445-453.

Zadoks, J.C., Chang, T.T., Konzak, C.F. (1974) A decimal code for the growth stages of cereals. Weed Research, **14**(6), 415-421.

Zee, S.Y. and O'Brien, T.P. (1970) A special type of tracheary element associated with "xylem discontinuity" in the floral axis of wheat. Australian Journal of Biological Sciences, **23**, 783-791.

Zhang, C., Yu, X., Ayre, B.G., Turgeon, R. (2012) The origin and composition of cucurbit “phloem” exudate. Plant Physiology, **158**(4), 1873-1882.

Zhang, F.-S., Römheld, V., Marschner, H. (1991) Diurnal rhythm of release of phytosiderophores and uptake rate of zinc in iron-deficient wheat. Soil Science and Plant Nutrition, **37**(4), 671-678.

Zimmermann, M.R., Hafke, J.B., Van Bel, A.J.E., Furch, A.C.U. (2013) Interaction of xylem and phloem during exudation and wound occlusion in *Cucurbita maxima*. Plant, Cell & Environment, **36**(1), 237-247.

Appendix 1: Further information on GC-MS analysis.

This appendix includes an example of separation traces with and without oil contamination, a complete list of metabolites detected, replicated derivatives and un-normalisable metabolites.

Supplementary Table 1: Mean and standard error for metabolite relative response ratios identified using GC-MS that were normally distributed or could be transformed to a normal distribution. (CBRT = cube root, SQRT = square root, Ln = natural logarithm and InvCBRT = inverse cube root). (xTMS = Trimethylsilyl derivative where x = the number of TMS groups; yMX = methoxyamine derivatised product where y = 1 or 2)

Metabolite	Transformation	DAA group	N	Mean	Std. Error
3-amino-piperidin-2-one 2TMS	SQRT	8-12 DAA	15	0.76	0.060
3-amino-piperidin-2-one 2TMS	SQRT	17-21 DAA	16	0.41	0.044
3-hydroxybenzoic acid 2TMS	CBRT	8-12 DAA	13	0.21	0.013
3-hydroxybenzoic acid 2TMS	CBRT	17-21 DAA	14	0.25	0.017
4-aminobutyric acid 3TMS	SQRT	8-12 DAA	15	0.72	0.10
4-aminobutyric acid 3TMS	SQRT	17-21 DAA	16	1.1	0.21
4-hydroxybenzoic acid 2TMS	None	8-12 DAA	15	0.21	0.028
4-hydroxybenzoic acid 2TMS	None	17-21 DAA	16	0.27	0.031
Alanine 2TMS	SQRT	8-12 DAA	15	0.85	0.033
Alanine 2TMS	SQRT	17-21 DAA	16	0.62	0.074
Arginine 3TMS	Ln	8-12 DAA	15	-2.38	0.16
Arginine 3TMS	Ln	17-21 DAA	16	-3.23	0.13
Asparagine_3TMS	Ln	8-12 DAA	15	-1.45	0.33
Asparagine_3TMS	Ln	17-21 DAA	16	-2.33	0.33
Aspartate 3TMS	None	8-12 DAA	6	5.3	1.4
Aspartate 3TMS	None	17-21 DAA	3	3.6	1.0
Beta-alanine 3TMS	SQRT	8-12 DAA	12	0.12	0.013
Beta-alanine 3TMS	SQRT	17-21 DAA	15	0.16	0.023
Caffeic acid 3TMS	None	8-12 DAA	0		
Caffeic acid 3TMS	None	17-21 DAA	1	0.011	
Citric acid 4TMS	None	8-12 DAA	15	0.29	0.042

Citric acid 4TMS	None	17-21 DAA	16	0.53	0.032
Fructose_MX1	None	8-12 DAA	15	0.34	0.025
Fructose_MX1	None	17-21 DAA	16	0.61	0.054
Fructose-1-phosphate	None	8-12 DAA	6	0.012	0.0031
Fructose-1-phosphate	None	17-21 DAA	6	0.013	0.0029
Fructose-6-phosphate MX1	CBRT	8-12 DAA	15	0.49	0.017
Fructose-6-phosphate MX1	CBRT	17-21 DAA	16	0.49	0.018
Fumarate 2TMS	None	8-12 DAA	14	0.016	0.0010
Fumarate 2TMS	None	17-21 DAA	15	0.025	0.0027
Gluconic acid-1,5-lactone 4TMS	None	8-12 DAA	15	0.47	0.054
Gluconic acid-1,5-lactone 4TMS	None	17-21 DAA	16	0.82	0.082
Gluconic acid-6-phosphate 7TMS	None	8-12 DAA	14	0.029	0.0031
Gluconic acid-6-phosphate 7TMS	None	17-21 DAA	15	0.032	0.0037
Glucose MX1	None	8-12 DAA	15	0.95	0.077
Glucose MX1	None	17-21 DAA	16	1.6	0.16
Glucose-6-phosphate MX1	Ln	8-12 DAA	15	-2.27	0.17
Glucose-6-phosphate MX1	Ln	17-21 DAA	16	-2.16	0.17
Glutamate 3TMS	None	8-12 DAA	15	2.0	0.31
Glutamate 3TMS	None	17-21 DAA	16	0.89	0.18
Glutamine 3TMS	CBRT	8-12 DAA	15	1.3	0.051
Glutamine 3TMS	CBRT	17-21 DAA	16	0.92	0.075
Glyceric acid-3-phosphate 4TMS	SQRT	8-12 DAA	15	0.39	0.024
Glyceric acid-3-phosphate 4TMS	SQRT	17-21 DAA	16	0.38	0.022
Glycerol-3-phosphate 4TMS	Ln	8-12 DAA	13	-2.80	0.10
Glycerol-3-phosphate 4TMS	Ln	17-21 DAA	6	-3.88	0.57
Glycine 3TMS	None	8-12 DAA	14	0.14	0.015
Glycine 3TMS	None	17-21 DAA	16	0.31	0.030
Hexadecanoate 1TMS	SQRT	8-12 DAA	15	0.75	0.039
Hexadecanoate 1TMS	SQRT	17-21 DAA	16	1.0	0.10
Histidine 3TMS	Ln	8-12 DAA	15	-0.47	0.19
Histidine 3TMS	Ln	17-21 DAA	16	-1.09	0.20
Homoserine 3TMS	None	8-12 DAA	15	0.17	0.015
Homoserine 3TMS	None	17-21 DAA	16	0.088	0.011
Isoleucine 2TMS	None	8-12 DAA	15	4.4	0.33
Isoleucine 2TMS	None	17-21 DAA	16	4.6	0.48
Itaconic acid 2TMS	None	8-12 DAA	6	0.0014	0.00030
Itaconic acid 2TMS	None	17-21 DAA	3	0.0016	0.00064
Lysine 4TMS	None	8-12 DAA	15	2.0	0.16
Lysine 4TMS	None	17-21 DAA	16	1.4	0.12
Malic acid 3TMS	SQRT	8-12 DAA	15	0.46	0.047
Malic acid 3TMS	SQRT	17-21 DAA	16	0.57	0.074
Methionine 1TMS	None	8-12 DAA	15	0.019	0.0014

Methionine 1TMS	None	17-21 DAA	16	0.025	0.0018
Myoinositol 6TMS	None	8-12 DAA	15	0.27	0.055
Myoinositol 6TMS	None	17-21 DAA	16	0.25	0.052
Octadecanoate 1TMS	SQRT	8-12 DAA	15	0.62	0.039
Octadecanoate 1TMS	SQRT	17-21 DAA	16	0.83	0.076
Ornithine 3TMS	None	8-12 DAA	15	0.23	0.056
Ornithine 3TMS	None	17-21 DAA	16	0.051	0.010
Orotic acid 3TMS	InvCBRT	8-12 DAA	10	9.4	1.9
Orotic acid 3TMS	InvCBRT	17-21 DAA	14	7.2	1.5
Phenylalanine 2TMS	None	8-12 DAA	15	2.3	0.31
Phenylalanine 2TMS	None	17-21 DAA	16	3.4	0.29
Pipecolic acid 2TMS	Ln	8-12 DAA	15	-3.20	0.18
Pipecolic acid 2TMS	Ln	17-21 DAA	16	-3.85	0.31
Proline 2TMS	Ln	8-12 DAA	15	0.62	0.37
Proline 2TMS	Ln	17-21 DAA	16	-0.24	0.30
Putrescine 4TMS	None	8-12 DAA	15	0.90	0.10
Putrescine 4TMS	None	17-21 DAA	16	1.7	0.091
Pyroglutamate 2TMS	None	8-12 DAA	15	13.8	0.88
Pyroglutamate 2TMS	None	17-21 DAA	16	10.5	0.93
Quinic acid 5TMS	SQRT	8-12 DAA	15	0.55	0.051
Quinic acid 5TMS	SQRT	17-21 DAA	16	0.87	0.10
Serine 3TMS	None	8-12 DAA	15	12.8	0.62
Serine 3TMS	None	17-21 DAA	16	8.0	0.97
Shikimic acid 4TMS	SQRT	8-12 DAA	15	0.34	0.031
Shikimic acid 4TMS	SQRT	17-21 DAA	16	0.57	0.048
Succinate 2TMS	None	8-12 DAA	15	0.041	0.0052
Succinate 2TMS	None	17-21 DAA	16	0.094	0.017
Sucrose 8TMS	SQRT	8-12 DAA	15	0.85	0.069
Sucrose 8TMS	SQRT	17-21 DAA	16	1.1	0.12
Threonine 3TMS	None	8-12 DAA	15	2.2	0.12
Threonine 3TMS	None	17-21 DAA	16	2.1	0.18
Trehalose 8TMS	Ln	8-12 DAA	15	0.17	0.14
Trehalose 8TMS	Ln	17-21 DAA	16	-1.09	0.14
Tryptophan 2TMS	SQRT	8-12 DAA	15	0.42	0.037
Tryptophan 2TMS	SQRT	17-21 DAA	16	0.46	0.042
Tyrosine 3TMS	None	8-12 DAA	15	1.3	0.14
Tyrosine 3TMS	None	17-21 DAA	16	2.4	0.20
UN01_10.61_158	CBRT	8-12 DAA	15	0.29	0.0093
UN01_10.61_158	CBRT	17-21 DAA	16	0.22	0.012
UN02_14.04_350	SQRT	8-12 DAA	15	0.19	0.0073
UN02_14.04_350	SQRT	17-21 DAA	16	0.21	0.0065
UN03_14.36_320	Ln	8-12 DAA	15	-4.02	0.19
UN03_14.36_320	Ln	17-21 DAA	16	-3.66	0.13
UN04_15.56_185	None	8-12 DAA	15	0.13	0.018
UN04_15.56_185	None	17-21 DAA	16	0.24	0.038
UN06_17.16_259	None	8-12 DAA	15	0.0020	0.00020
UN06_17.16_259	None	17-21 DAA	11	0.0020	0.00027
UN07_17.62_275	Ln	8-12 DAA	15	-2.49	0.11
UN07_17.62_275	Ln	17-21 DAA	16	-3.17	0.17
UN08_17.96_360	CBRT	8-12 DAA	15	0.57	0.039
UN08_17.96_360	CBRT	17-21 DAA	16	0.38	0.034
UN09_18.15_275	CBRT	8-12 DAA	15	0.41	0.015
UN09_18.15_275	CBRT	17-21 DAA	16	0.32	0.020
UN10_19.08_217	None	8-12 DAA	15	1.1	0.077

UN10_19.08_217	None	17-21 DAA	16	1.6	0.13
UN11_19.48_299	CBRT	8-12 DAA	15	0.40	0.0089
UN11_19.48_299	CBRT	17-21 DAA	16	0.31	0.023
UN13_25.04_130	None	8-12 DAA	3	0.21	0.063
UN13_25.04_130	None	17-21 DAA	13	0.58	0.11
UN14_25.08_503	None	8-12 DAA	15	0.23	0.035
UN14_25.08_503	None	17-21 DAA	16	0.19	0.021
UN15_25.55_425	None	8-12 DAA	15	0.014	0.00090
UN15_25.55_425	None	17-21 DAA	16	0.016	0.0011
UN16_25.71_339	None	8-12 DAA	15	0.012	0.0011
UN16_25.71_339	None	17-21 DAA	16	0.020	0.0028
UN17_27.24_375	None	8-12 DAA	15	0.020	0.0017
UN17_27.24_375	None	17-21 DAA	16	0.036	0.0034
UN18_28.91_437	None	8-12 DAA	15	0.020	0.0015
UN18_28.91_437	None	17-21 DAA	16	0.034	0.0033
UN19_29.64_437	None	8-12 DAA	15	0.045	0.0086
UN19_29.64_437	None	17-21 DAA	16	0.067	0.0080
UN20_32.34_503	InvCBRT	8-12 DAA	15	3.6	0.26
UN20_32.34_503	InvCBRT	17-21 DAA	16	3.0	0.15
UN21_32.89_387	None	8-12 DAA	15	0.014	0.0018
UN21_32.89_387	None	17-21 DAA	16	0.013	0.00079
UN22_33.13_513	SQRT	8-12 DAA	15	0.14	0.010
UN22_33.13_513	SQRT	17-21 DAA	16	0.14	0.0041
UN23_33.43_517	None	8-12 DAA	15	0.019	0.0020
UN23_33.43_517	None	17-21 DAA	16	0.018	0.0010
UN24_33.79_423	None	8-12 DAA	15	0.060	0.0066
UN24_33.79_423	None	17-21 DAA	16	0.074	0.0044
UN25_33.99_373	SQRT	8-12 DAA	15	0.13	0.0087
UN25_33.99_373	SQRT	17-21 DAA	16	0.13	0.0039
UN26_14.48_229	Ln	8-12 DAA	15	-0.84	0.065
UN26_14.48_229	Ln	17-21 DAA	16	-1.46	0.14
Urea 2TMS	CBRT	8-12 DAA	15	0.53	0.017
Urea 2TMS	CBRT	17-21 DAA	16	0.58	0.027
Valine 2TMS	None	8-12 DAA	15	7.2	0.49
Valine 2TMS	None	17-21 DAA	16	7.0	0.59
Xylofuranose 4TMS	None	8-12 DAA	15	0.74	0.13
Xylofuranose 4TMS	None	17-21 DAA	16	1.1	0.15

Supplementary Table 2: summary statistics of replicated derivative metabolite relative response ratios also identified by GC-MS also used in calculation of response ratios.

Metabolite	Transformation	DAA group	N	Mean	Std. Error
Fructose_MX2	None	8-12 DAA	15	0.34	0.025
Fructose_MX2	None	17-21 DAA	16	0.61	0.054
Glucose MX2	None	8-12 DAA	15	0.20	0.013
Glucose MX2	None	17-21 DAA	16	0.31	0.026
Glutamine 4TMS	InvCBRT	8-12 DAA	15	2.9	0.24
Glutamine 4TMS	InvCBRT	17-21 DAA	15	3.6	0.20
Glycine 2TMS	None	8-12 DAA	15	0.025	0.0036
Glycine 2TMS	None	17-21 DAA	16	0.025	0.0021
INSD Docosane	None	8-12 DAA	15	1.1	0.13
INSD Docosane	None	17-21 DAA	16	1.8	0.24
Lysine 3TMSa	None	8-12 DAA	15	0.35	0.041
Lysine 3TMSa	None	17-21 DAA	16	0.14	0.025
Lysine 3TMSb	None	8-12 DAA	15	0.10	0.011
Lysine 3TMSb	None	17-21 DAA	16	0.087	0.0046
Methionine 2TMS	None	8-12 DAA	14	0.65	0.14
Methionine 2TMS	None	17-21 DAA	16	0.76	0.088
Serine 2TMS	None	8-12 DAA	15	0.028	0.0036
Serine 2TMS	None	17-21 DAA	16	0.024	0.0027
Threonine 2TMS	None	8-12 DAA	15	0.15	0.014
Threonine 2TMS	None	17-21 DAA	16	0.13	0.019
Tryptophan 3TMS	SQRT	8-12 DAA	15	0.44	0.047
Tryptophan 3TMS	SQRT	17-21 DAA	16	0.55	0.066

Supplementary Table 3: Summary of metabolite relative response ratios for metabolites that could not be transformed to produce a normal distribution.

metabolite	DAA group	n	Mean	SE
UN12_20.05_370	8-12 DAA	15	0.0039	0.00051
UN12_20.05_370	17-21 DAA	16	0.0071	0.00040
UN5_16.19_299	8-12 DAA	14	0.099	0.016
UN5_16.19_299	17-21 DAA	15	0.060	0.012

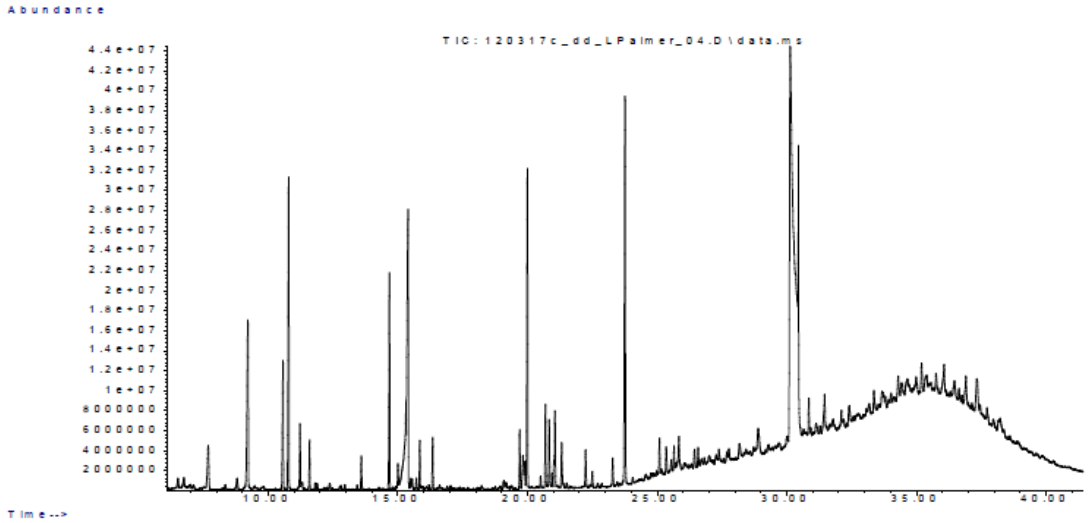

Supplementary Figure 1: Phloem sample measured in oil.
Note the baseline deviation starting at approximately 23 minutes.

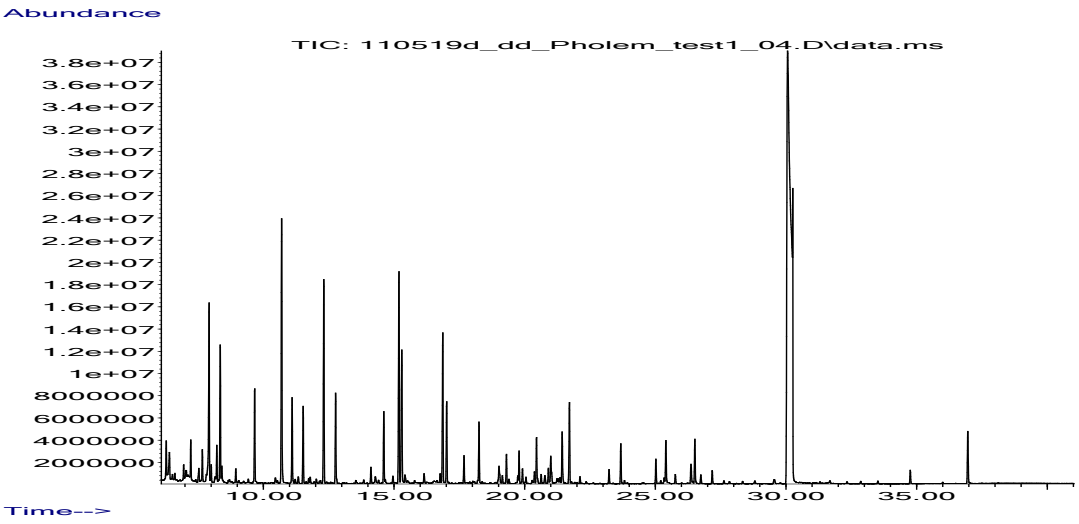

Supplementary Figure 2: phloem sample measured in air.
Note the comparatively flat baseline with no deviation in the second half of the run.

Appendix 2: Specifications and method for constructing aphid cages.

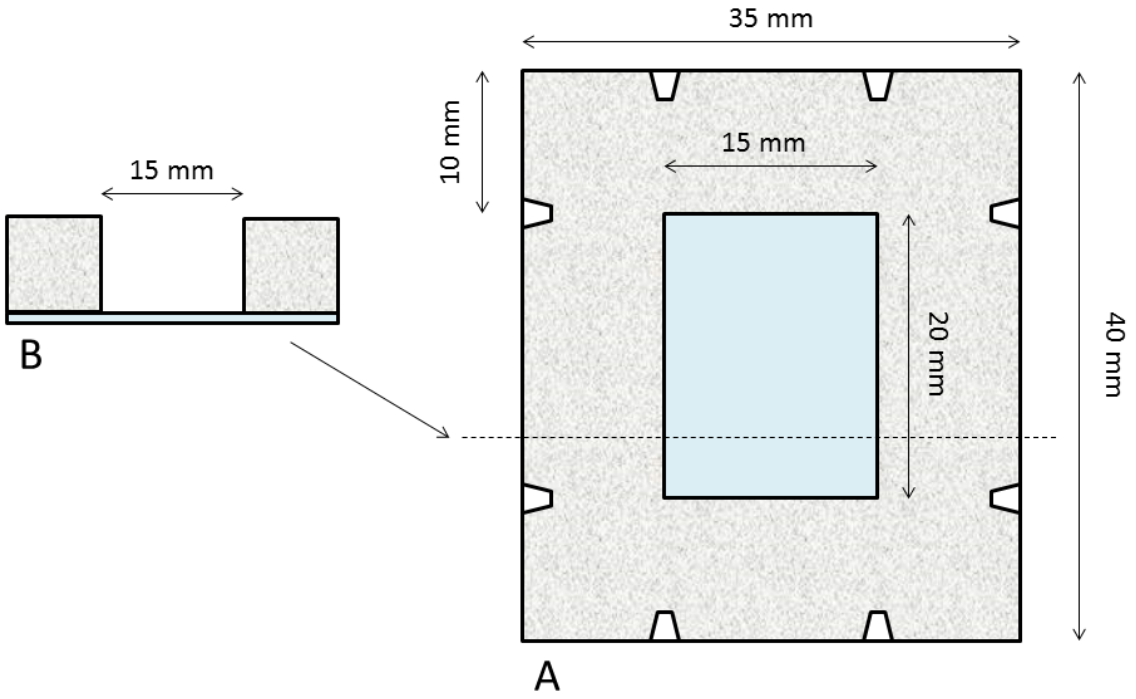

Figure 1: specifications for construction of aphid cages. (A) is top down view of one half of cage, (B) is view of cross section at dotted line on (A).

Materials:

- Polyethylene (PE) “peeled” foam, 12 mm thick (Clark Rubber, Australia)
- Stiff plastic sheet, Rigid PVC sheet 0.5 mm thick (Plastic Centre, Australia) or 0.8 mm thick polypropylene sheet (Eckersley’s art and craft, Australia) or PVC plastic from waste packaging (for example container of Agilent boxed vials (5182-0714)).
- Plastics glue (Selleys, Australia)

Cage Construction:

1. Cut plastic sheet to size as specified in Fig 1
2. Cut foam to same size as in 1. and cut hole in foam as specified in Fig 1 (blue shaded section of A).
3. Glue foam and plastic together (Plastic surface needs to be primed with primer pen, prior to glue application)
4. When dry, cut notches 10 mm in from each corner
5. Repeat steps 1 to 4 for other half of cage.

Appendix 3: Raw results from Tissue analysis discussed in Chapter 6.

Table of raw results from additional tissue analysis conducted in Chapter 6. ConcN = tissue concentration (mg kg^{-1}), ContT = tissue content ng per whole tissue type.

ID	Genotype	DAA grouping	Sample_type	Amount (g)	Fe	Zn	Mg	K
PG1-01	Samnyt 16	1	2nd leaf_ConcN	0.1139	46.348	12.743	1190	36000
PG1-02	Carnamagh	1	2nd leaf_ConcN	0.0923	137.739	45.774	4800	55000
PG1-03	Carnamagh	1	2nd leaf_ConcN	0.0968	165.390	56.199	4600	50000
PG1-04	Samnyt 16	1	2nd leaf_ConcN	0.0973	114.277	36.810	3000	45000
PG1-05	Samnyt 16	1	2nd leaf_ConcN	0.1392	57.030	11.792	970	32000
PG1-06	Carnamagh	1	2nd leaf_ConcN	0.1017	43.258	13.064	2400	44000
PG1-07	Carnamagh	1	2nd leaf_ConcN	0.0697	67.325	13.819	2200	49000
PG1-08	Samnyt 16	1	2nd leaf_ConcN	0.0987	57.429	15.056	1200	39000
PG1-09	Carnamagh	1	2nd leaf_ConcN	0.0669	49.719	15.000	2200	39000
PG1-10	Carnamagh	1	2nd leaf_ConcN	0.0803	54.618	13.501	2700	40000
PG1-11	Samnyt 16	1	2nd leaf_ConcN	0.0907	72.865	18.068	1380	45000
PG1-12	Samnyt 16	1	2nd leaf_ConcN	0.0801	56.927	14.338	1190	45000
PG2-01	Carnamagh	2	2nd leaf_ConcN	0.095	29.599	18.484	3800	42000
PG2-02	Samnyt 16	2	2nd leaf_ConcN	0.1363	27.727	10.982	1450	29000
PG2-03	Samnyt 16	2	2nd leaf_ConcN	0.0936	34.435	13.283	1880	22000
PG2-04	Carnamagh	2	2nd leaf_ConcN	0.101	25.161	12.169	3300	33000
PG2-05	Carnamagh	2	2nd leaf_ConcN	0.109	22.811	16.786	3700	33000
PG2-06	Samnyt 16	2	2nd leaf_ConcN	0.1085	98.493	37.542	2800	29000
PG2-07	Samnyt 16	2	2nd leaf_ConcN	0.1307	36.278	11.247	1240	27000
PG2-08	Carnamagh	2	2nd leaf_ConcN	0.0956	11.758	5.867	1940	28000
PG2-09	Carnamagh	2	2nd leaf_ConcN	0.1337	23.657	11.357	2400	33000
PG2-10	Samnyt 16	2	2nd leaf_ConcN	0.0986	57.684	18.307	1880	34000
PG2-11	Carnamagh	2	2nd leaf_ConcN	0.0738	22.056	7.705	2200	23000
PG2-12	Carnamagh	2	2nd leaf_ConcN	0.0939	14.637	6.579	2400	35000
PG2-13	Carnamagh	2	2nd leaf_ConcN	0.0785	28.805	10.315	2200	25000
PG2-14	Samnyt 16	2	2nd leaf_ConcN	0.1114	37.487	12.304	1660	29000
PG2-15	Carnamagh	2	2nd leaf_ConcN	0.0761	37.694	8.600	2900	12300
PG2-16	Samnyt 16	2	2nd leaf_ConcN	0.109	36.375	9.047	1270	36000
PG3-01	Carnamagh	3	2nd leaf_ConcN	0.1108	43.271	30.025	4000	37000
PG3-02	Samnyt 16	3	2nd leaf_ConcN	0.1343	24.712	12.184	1820	29000
PG3-03	Samnyt 16	3	2nd leaf_ConcN	0.0736	18.211	13.256	1420	25000
PG3-04	Carnamagh	3	2nd leaf_ConcN	0.0885	27.461	14.061	3400	31000
PG3-05	Carnamagh	3	2nd leaf_ConcN	0.0681	12.835	8.313	3200	32000
PG3-06	Samnyt 16	3	2nd leaf_ConcN	0.1219	33.265	13.478	1760	29000
PG3-07	Samnyt 16	3	2nd leaf_ConcN	0.1144	35.739	10.279	1440	27000
PG3-08	Samnyt 16	3	2nd leaf_ConcN	0.1175	22.260	8.521	1460	26000
PG3-09	Carnamagh	3	2nd leaf_ConcN	0.0815	7.181	7.189	4100	32000
PG3-10	Carnamagh	3	2nd leaf_ConcN	0.0764	20.633	8.937	3000	34000
PG3-11	Carnamagh	3	2nd leaf_ConcN	0.1039	15.351	8.812	2300	34000
PG3-12	Carnamagh	3	2nd leaf_ConcN	0.1048	13.254	6.898	2500	34000
PG3-13	Carnamagh	3	2nd leaf_ConcN	0.1052	18.014	10.768	2400	32000
PG3-14	Samnyt 16	3	2nd leaf_ConcN	0.075	29.145	10.595	3000	44000
PG3-15	Samnyt 16	3	2nd leaf_ConcN	0.0733	10.002	6.498	1010	35000
PG3-16	Samnyt 16	3	2nd leaf_ConcN	0.1114	28.328	11.287	1510	26000
PG4-01	Carnamagh	4	2nd leaf_ConcN	0.1057	41.969	30.792	5000	31000
PG4-02	Carnamagh	4	2nd leaf_ConcN	0.1071	49.023	24.962	4200	28000
PG4-03	Samnyt 16	4	2nd leaf_ConcN	0.0642	22.100	19.186	3600	56000

PG4-04	Samnyt 16	4	2nd leaf_ConcN	0.088	7.881	5.444	2300	34000
PG4-05	Carnamagh	4	2nd leaf_ConcN	0.0612	9.821	8.340	4800	43000
PG4-06	Samnyt 16	4	2nd leaf_ConcN	0.0864	13.555	4.989	870	32000
PG4-07	Carnamagh	4	2nd leaf_ConcN	0.0642	5.944	7.865	4900	32000
PG4-08	Samnyt 16	4	2nd leaf_ConcN	0.0629	8.366	9.936	2100	35000
PG4-09	Carnamagh	4	2nd leaf_ConcN	0.0868	13.056	9.017	3700	35000
PG4-10	Carnamagh	4	2nd leaf_ConcN	0.0726	6.793	6.731	4300	34000
PG4-11	Samnyt 16	4	2nd leaf_ConcN	0.0743	18.690	8.669	1170	39000
PG4-12	Samnyt 16	4	2nd leaf_ConcN	0.0937	61.409	16.742	1760	24000
PG1-01	Samnyt 16	1	2nd leaf_ContT	0.1139	5.279	1.451	135.5	4100.4
PG1-02	Carnamagh	1	2nd leaf_ContT	0.0923	12.713	4.225	443.0	5076.5
PG1-03	Carnamagh	1	2nd leaf_ContT	0.0968	16.010	5.440	445.3	4840.0
PG1-04	Samnyt 16	1	2nd leaf_ContT	0.0973	11.119	3.582	291.9	4378.5
PG1-05	Samnyt 16	1	2nd leaf_ContT	0.1392	7.939	1.641	135.0	4454.4
PG1-06	Carnamagh	1	2nd leaf_ContT	0.1017	4.399	1.329	244.1	4474.8
PG1-07	Carnamagh	1	2nd leaf_ContT	0.0697	4.693	0.963	153.3	3415.3
PG1-08	Samnyt 16	1	2nd leaf_ContT	0.0987	5.668	1.486	118.4	3849.3
PG1-09	Carnamagh	1	2nd leaf_ContT	0.0669	3.326	1.003	147.2	2609.1
PG1-10	Carnamagh	1	2nd leaf_ContT	0.0803	4.386	1.084	216.8	3212.0
PG1-11	Samnyt 16	1	2nd leaf_ContT	0.0907	6.609	1.639	125.2	4081.5
PG1-12	Samnyt 16	1	2nd leaf_ContT	0.0801	4.560	1.149	95.3	3604.5
PG2-01	Carnamagh	2	2nd leaf_ContT	0.095	2.812	1.756	361.0	3990.0
PG2-02	Samnyt 16	2	2nd leaf_ContT	0.1363	3.779	1.497	197.6	3952.7
PG2-03	Samnyt 16	2	2nd leaf_ContT	0.0936	3.223	1.243	176.0	2059.2
PG2-04	Carnamagh	2	2nd leaf_ContT	0.101	2.541	1.229	333.3	3333.0
PG2-05	Carnamagh	2	2nd leaf_ContT	0.109	2.486	1.830	403.3	3597.0
PG2-06	Samnyt 16	2	2nd leaf_ContT	0.1085	10.687	4.073	303.8	3146.5
PG2-07	Samnyt 16	2	2nd leaf_ContT	0.1307	4.742	1.470	162.1	3528.9
PG2-08	Carnamagh	2	2nd leaf_ContT	0.0956	1.124	0.561	185.5	2676.8
PG2-09	Carnamagh	2	2nd leaf_ContT	0.1337	3.163	1.518	320.9	4412.1
PG2-10	Samnyt 16	2	2nd leaf_ContT	0.0986	5.688	1.805	185.4	3352.4
PG2-11	Carnamagh	2	2nd leaf_ContT	0.0738	1.628	0.569	162.4	1697.4
PG2-12	Carnamagh	2	2nd leaf_ContT	0.0939	1.374	0.618	225.4	3286.5
PG2-13	Carnamagh	2	2nd leaf_ContT	0.0785	2.261	0.810	172.7	1962.5
PG2-14	Samnyt 16	2	2nd leaf_ContT	0.1114	4.176	1.371	184.9	3230.6
PG2-15	Carnamagh	2	2nd leaf_ContT	0.0761	2.869	0.654	220.7	936.0
PG2-16	Samnyt 16	2	2nd leaf_ContT	0.109	3.965	0.986	138.4	3924.0
PG3-01	Carnamagh	3	2nd leaf_ContT	0.1108	4.794	3.327	443.2	4099.6
PG3-02	Samnyt 16	3	2nd leaf_ContT	0.1343	3.319	1.636	244.4	3894.7
PG3-03	Samnyt 16	3	2nd leaf_ContT	0.0736	1.340	0.976	104.5	1840.0
PG3-04	Carnamagh	3	2nd leaf_ContT	0.0885	2.430	1.244	300.9	2743.5
PG3-05	Carnamagh	3	2nd leaf_ContT	0.0681	0.874	0.566	217.9	2179.2
PG3-06	Samnyt 16	3	2nd leaf_ContT	0.1219	4.055	1.643	214.5	3535.1
PG3-07	Samnyt 16	3	2nd leaf_ContT	0.1144	4.089	1.176	164.7	3088.8
PG3-08	Samnyt 16	3	2nd leaf_ContT	0.1175	2.616	1.001	171.6	3055.0
PG3-09	Carnamagh	3	2nd leaf_ContT	0.0815	0.585	0.586	334.2	2608.0
PG3-10	Carnamagh	3	2nd leaf_ContT	0.0764	1.576	0.683	229.2	2597.6
PG3-11	Carnamagh	3	2nd leaf_ContT	0.1039	1.595	0.916	239.0	3532.6
PG3-12	Carnamagh	3	2nd leaf_ContT	0.1048	1.389	0.723	262.0	3563.2
PG3-13	Carnamagh	3	2nd leaf_ContT	0.1052	1.895	1.133	252.5	3366.4
PG3-14	Samnyt 16	3	2nd leaf_ContT	0.075	2.186	0.795	225.0	3300.0
PG3-15	Samnyt 16	3	2nd leaf_ContT	0.0733	0.733	0.476	74.0	2565.5
PG3-16	Samnyt 16	3	2nd leaf_ContT	0.1114	3.156	1.257	168.2	2896.4
PG4-01	Carnamagh	4	2nd leaf_ContT	0.1057	4.436	3.255	528.5	3276.7
PG4-02	Carnamagh	4	2nd leaf_ContT	0.1071	5.250	2.673	449.8	2998.8
PG4-03	Samnyt 16	4	2nd leaf_ContT	0.0642	1.419	1.232	231.1	3595.2
PG4-04	Samnyt 16	4	2nd leaf_ContT	0.088	0.693	0.479	202.4	2992.0
PG4-05	Carnamagh	4	2nd leaf_ContT	0.0612	0.601	0.510	293.8	2631.6
PG4-06	Samnyt 16	4	2nd leaf_ContT	0.0864	1.171	0.431	75.2	2764.8
PG4-07	Carnamagh	4	2nd leaf_ContT	0.0642	0.382	0.505	314.6	2054.4

PG4-08	Samnyt 16	4	2nd leaf_ContT	0.0629	0.526	0.625	132.1	2201.5
PG4-09	Carnamagh	4	2nd leaf_ContT	0.0868	1.133	0.783	321.2	3038.0
PG4-10	Carnamagh	4	2nd leaf_ContT	0.0726	0.493	0.489	312.2	2468.4
PG4-11	Samnyt 16	4	2nd leaf_ContT	0.0743	1.389	0.644	86.9	2897.7
PG4-12	Samnyt 16	4	2nd leaf_ContT	0.0937	5.754	1.569	164.9	2248.8
PG1-01	Samnyt 16	1	flag leaf_ConcN	0.1064	58.239	13.458	1250	15700
PG1-02	Carnamagh	1	flag leaf_ConcN	0.0861	147.498	32.707	4400	35000
PG1-03	Carnamagh	1	flag leaf_ConcN	0.0925	183.112	36.310	4600	32000
PG1-04	Samnyt 16	1	flag leaf_ConcN	0.1002	109.789	26.707	3000	25000
PG1-05	Samnyt 16	1	flag leaf_ConcN	0.096	72.882	18.111	1590	18800
PG1-06	Carnamagh	1	flag leaf_ConcN	0.0957	49.394	13.043	2300	25000
PG1-07	Carnamagh	1	flag leaf_ConcN	0.056	71.918	15.330	2500	26000
PG1-08	Samnyt 16	1	flag leaf_ConcN	0.0766	64.054	17.519	1570	21000
PG1-09	Carnamagh	1	flag leaf_ConcN	0.0529	430.000	15.269	2200	18900
PG1-10	Carnamagh	1	flag leaf_ConcN	0.0464	62.509	16.821	2900	24000
PG1-11	Samnyt 16	1	flag leaf_ConcN	0.0954	76.427	18.522	1550	27000
PG1-12	Samnyt 16	1	flag leaf_ConcN	0.0788	57.729	17.537	1440	23000
PG2-01	Carnamagh	2	flag leaf_ConcN	0.1109	41.576	15.445	3800	15900
PG2-02	Samnyt 16	2	flag leaf_ConcN	0.1505	35.677	7.828	1470	15600
PG2-03	Samnyt 16	2	flag leaf_ConcN	0.0753	50.042	8.350	1700	8700
PG2-04	Carnamagh	2	flag leaf_ConcN	0.1045	31.296	11.178	3100	14100
PG2-05	Carnamagh	2	flag leaf_ConcN	0.1407	39.238	12.308	3600	20000
PG2-06	Samnyt 16	2	flag leaf_ConcN	0.0683	103.918	25.991	2800	19400
PG2-07	Samnyt 16	2	flag leaf_ConcN	0.0908	46.611	10.505	1690	16500
PG2-08	Carnamagh	2	flag leaf_ConcN	0.0933	17.271	5.918	1920	13900
PG2-09	Carnamagh	2	flag leaf_ConcN	0.1275	32.296	10.775	3000	15700
PG2-10	Samnyt 16	2	flag leaf_ConcN	0.0811	77.555	15.268	2200	16100
PG2-11	Carnamagh	2	flag leaf_ConcN	0.0369	37.669	8.337	2800	18000
PG2-12	Carnamagh	2	flag leaf_ConcN	0.1196	21.585	6.748	2400	15700
PG2-13	Carnamagh	2	flag leaf_ConcN	0.0675	35.852	10.263	2400	12800
PG2-14	Samnyt 16	2	flag leaf_ConcN	0.0833	52.944	8.994	1870	13000
PG2-15	Carnamagh	2	flag leaf_ConcN	0.1024	27.929	12.951	2400	26000
PG2-16	Samnyt 16	2	flag leaf_ConcN	0.1134	40.353	9.445	1510	17800
PG3-01	Carnamagh	3	flag leaf_ConcN	0.1067	59.348	17.325	4700	24000
PG3-02	Samnyt 16	3	flag leaf_ConcN	0.1319	29.808	6.068	1680	14000
PG3-03	Samnyt 16	3	flag leaf_ConcN	0.0646	18.237	12.146	1570	10700
PG3-04	Carnamagh	3	flag leaf_ConcN	0.1158	43.952	12.242	4100	27000
PG3-05	Carnamagh	3	flag leaf_ConcN	0.064	16.034	6.357	2700	17700
PG3-06	Samnyt 16	3	flag leaf_ConcN	0.0951	52.175	9.225	2300	13800
PG3-07	Samnyt 16	3	flag leaf_ConcN	0.0792	50.044	6.931	1740	18100
PG3-08	Samnyt 16	3	flag leaf_ConcN	0.0789	53.098	11.733	2800	15000
PG3-09	Carnamagh	3	flag leaf_ConcN	0.0891	12.349	6.579	4800	13300
PG3-10	Carnamagh	3	flag leaf_ConcN	0.0948	30.210	9.605	4000	19700
PG3-11	Carnamagh	3	flag leaf_ConcN	0.0967	23.540	7.575	2800	16600
PG3-12	Carnamagh	3	flag leaf_ConcN	0.1126	22.619	6.682	2700	18000
PG3-13	Carnamagh	3	flag leaf_ConcN	0.1011	29.306	8.758	2900	21000
PG3-14	Samnyt 16	3	flag leaf_ConcN	0.0752	48.725	8.005	3800	12500
PG3-15	Samnyt 16	3	flag leaf_ConcN	0.0615	14.090	4.367	1500	13900
PG3-16	Samnyt 16	3	flag leaf_ConcN	0.0922	29.453	6.298	2400	17500
PG4-01	Carnamagh	4	flag leaf_ConcN	0.1013	78.686	25.601	6900	25000
PG4-02	Carnamagh	4	flag leaf_ConcN	0.1042	91.425	21.526	5600	26000
PG4-03	Samnyt 16	4	flag leaf_ConcN	0.1334	23.043	10.646	3300	36000
PG4-04	Samnyt 16	4	flag leaf_ConcN	0.0944	17.581	4.693	2500	15200
PG4-05	Carnamagh	4	flag leaf_ConcN	0.0936	14.851	6.481	4900	21000
PG4-06	Samnyt 16	4	flag leaf_ConcN	0.0836	20.264	5.221	1930	18600
PG4-07	Carnamagh	4	flag leaf_ConcN	0.0704	7.715	5.358	5700	14800
PG4-08	Samnyt 16	4	flag leaf_ConcN	0.0719	6.419	8.150	3000	14900
PG4-09	Carnamagh	4	flag leaf_ConcN	0.1053	25.371	7.438	4800	23000
PG4-10	Carnamagh	4	flag leaf_ConcN	0.091	9.969	4.782	4300	19500
PG4-11	Samnyt 16	4	flag leaf_ConcN	0.072	14.857	4.172	1510	25000

PG4-12	Samnyt 16	4	flag leaf_ConcN	0.0578	72.619	4.896	2100	15100
PG1-01	Samnyt 16	1	flag leaf_ContT	0.1064	6.197	1.432	133.0	1670.5
PG1-02	Carnamagh	1	flag leaf_ContT	0.0861	12.700	2.816	378.8	3013.5
PG1-03	Carnamagh	1	flag leaf_ContT	0.0925	16.938	3.359	425.5	2960.0
PG1-04	Samnyt 16	1	flag leaf_ContT	0.1002	11.001	2.676	300.6	2505.0
PG1-05	Samnyt 16	1	flag leaf_ContT	0.096	6.997	1.739	152.6	1804.8
PG1-06	Carnamagh	1	flag leaf_ContT	0.0957	4.727	1.248	220.1	2392.5
PG1-07	Carnamagh	1	flag leaf_ContT	0.056	4.027	0.858	140.0	1456.0
PG1-08	Samnyt 16	1	flag leaf_ContT	0.0766	4.907	1.342	120.3	1608.6
PG1-09	Carnamagh	1	flag leaf_ContT	0.0529	22.747	0.808	116.4	999.8
PG1-10	Carnamagh	1	flag leaf_ContT	0.0464	2.900	0.780	134.6	1113.6
PG1-11	Samnyt 16	1	flag leaf_ContT	0.0954	7.291	1.767	147.9	2575.8
PG1-12	Samnyt 16	1	flag leaf_ContT	0.0788	4.549	1.382	113.5	1812.4
PG2-01	Carnamagh	2	flag leaf_ContT	0.1109	4.611	1.713	421.4	1763.3
PG2-02	Samnyt 16	2	flag leaf_ContT	0.1505	5.369	1.178	221.2	2347.8
PG2-03	Samnyt 16	2	flag leaf_ContT	0.0753	3.768	0.629	128.0	655.1
PG2-04	Carnamagh	2	flag leaf_ContT	0.1045	3.270	1.168	324.0	1473.5
PG2-05	Carnamagh	2	flag leaf_ContT	0.1407	5.521	1.732	506.5	2814.0
PG2-06	Samnyt 16	2	flag leaf_ContT	0.0683	7.098	1.775	191.2	1325.0
PG2-07	Samnyt 16	2	flag leaf_ContT	0.0908	4.232	0.954	153.5	1498.2
PG2-08	Carnamagh	2	flag leaf_ContT	0.0933	1.611	0.552	179.1	1296.9
PG2-09	Carnamagh	2	flag leaf_ContT	0.1275	4.118	1.374	382.5	2001.8
PG2-10	Samnyt 16	2	flag leaf_ContT	0.0811	6.290	1.238	178.4	1305.7
PG2-11	Carnamagh	2	flag leaf_ContT	0.0369	1.390	0.308	103.3	664.2
PG2-12	Carnamagh	2	flag leaf_ContT	0.1196	2.582	0.807	287.0	1877.7
PG2-13	Carnamagh	2	flag leaf_ContT	0.0675	2.420	0.693	162.0	864.0
PG2-14	Samnyt 16	2	flag leaf_ContT	0.0833	4.410	0.749	155.8	1082.9
PG2-15	Carnamagh	2	flag leaf_ContT	0.1024	2.860	1.326	245.8	2662.4
PG2-16	Samnyt 16	2	flag leaf_ContT	0.1134	4.576	1.071	171.2	2018.5
PG3-01	Carnamagh	3	flag leaf_ContT	0.1067	6.332	1.849	501.5	2560.8
PG3-02	Samnyt 16	3	flag leaf_ContT	0.1319	3.932	0.800	221.6	1846.6
PG3-03	Samnyt 16	3	flag leaf_ContT	0.0646	1.178	0.785	101.4	691.2
PG3-04	Carnamagh	3	flag leaf_ContT	0.1158	5.090	1.418	474.8	3126.6
PG3-05	Carnamagh	3	flag leaf_ContT	0.064	1.026	0.407	172.8	1132.8
PG3-06	Samnyt 16	3	flag leaf_ContT	0.0951	4.962	0.877	218.7	1312.4
PG3-07	Samnyt 16	3	flag leaf_ContT	0.0792	3.963	0.549	137.8	1433.5
PG3-08	Samnyt 16	3	flag leaf_ContT	0.0789	4.189	0.926	220.9	1183.5
PG3-09	Carnamagh	3	flag leaf_ContT	0.0891	1.100	0.586	427.7	1185.0
PG3-10	Carnamagh	3	flag leaf_ContT	0.0948	2.864	0.911	379.2	1867.6
PG3-11	Carnamagh	3	flag leaf_ContT	0.0967	2.276	0.732	270.8	1605.2
PG3-12	Carnamagh	3	flag leaf_ContT	0.1126	2.547	0.752	304.0	2026.8
PG3-13	Carnamagh	3	flag leaf_ContT	0.1011	2.963	0.885	293.2	2123.1
PG3-14	Samnyt 16	3	flag leaf_ContT	0.0752	3.664	0.602	285.8	940.0
PG3-15	Samnyt 16	3	flag leaf_ContT	0.0615	0.867	0.269	92.3	854.9
PG3-16	Samnyt 16	3	flag leaf_ContT	0.0922	2.716	0.581	221.3	1613.5
PG4-01	Carnamagh	4	flag leaf_ContT	0.1013	7.971	2.593	699.0	2532.5
PG4-02	Carnamagh	4	flag leaf_ContT	0.1042	9.526	2.243	583.5	2709.2
PG4-03	Samnyt 16	4	flag leaf_ContT	0.1334	3.074	1.420	440.2	4802.4
PG4-04	Samnyt 16	4	flag leaf_ContT	0.0944	1.660	0.443	236.0	1434.9
PG4-05	Carnamagh	4	flag leaf_ContT	0.0936	1.390	0.607	458.6	1965.6
PG4-06	Samnyt 16	4	flag leaf_ContT	0.0836	1.694	0.436	161.3	1555.0
PG4-07	Carnamagh	4	flag leaf_ContT	0.0704	0.543	0.377	401.3	1041.9
PG4-08	Samnyt 16	4	flag leaf_ContT	0.0719	0.462	0.586	215.7	1071.3
PG4-09	Carnamagh	4	flag leaf_ContT	0.1053	2.672	0.783	505.4	2421.9
PG4-10	Carnamagh	4	flag leaf_ContT	0.091	0.907	0.435	391.3	1774.5
PG4-11	Samnyt 16	4	flag leaf_ContT	0.072	1.070	0.300	108.7	1800.0
PG4-12	Samnyt 16	4	flag leaf_ContT	0.0578	4.197	0.283	121.4	872.8
PG1-01	Samnyt 16	1	head_ConcN	0.4904	28.517	23.804	870	9700
PG1-02	Carnamagh	1	head_ConcN	0.3761	36.046	23.505	1590	12600
PG1-03	Carnamagh	1	head_ConcN	0.477	42.425	26.996	1650	12200

PG1-04	Samnyt 16	1	head_ConcN	0.5115	27.816	24.857	1150	11200
PG1-05	Samnyt 16	1	head_ConcN	0.4098	27.908	26.731	1140	10900
PG1-06	Carnamagh	1	head_ConcN	0.4189	24.147	16.798	1030	10600
PG1-07	Carnamagh	1	head_ConcN	0.4183	22.821	15.289	1070	10700
PG1-08	Samnyt 16	1	head_ConcN	0.5097	22.885	23.233	910	10400
PG1-09	Carnamagh	1	head_ConcN	0.2992	25.855	18.446	950	10400
PG1-10	Carnamagh	1	head_ConcN	0.4465	23.682	18.888	1080	11200
PG1-11	Samnyt 16	1	head_ConcN	0.4781	29.564	29.041	990	10700
PG1-12	Samnyt 16	1	head_ConcN	0.4285	24.486	25.507	880	9900
PG2-01	Carnamagh	2	head_ConcN	0.5135	32.255	14.635	560	8000
PG2-02	Samnyt 16	2	head_ConcN	0.5644	29.953	19.795	570	7000
PG2-03	Samnyt 16	2	head_ConcN	0.4419	33.973	22.397	610	4900
PG2-04	Carnamagh	2	head_ConcN	0.4318	26.680	13.707	610	7500
PG2-05	Carnamagh	2	head_ConcN	0.4944	26.556	13.249	720	7800
PG2-06	Samnyt 16	2	head_ConcN	0.4137	36.926	29.091	1100	8400
PG2-07	Samnyt 16	2	head_ConcN	0.5894	28.893	21.550	530	7000
PG2-08	Carnamagh	2	head_ConcN	0.3897	23.278	11.647	600	6800
PG2-09	Carnamagh	2	head_ConcN	0.4637	26.062	13.227	810	8200
PG2-10	Samnyt 16	2	head_ConcN	0.5578	36.677	24.566	550	7000
PG2-11	Carnamagh	2	head_ConcN	0.3814	24.822	10.809	640	6600
PG2-12	Carnamagh	2	head_ConcN	0.4676	26.712	12.842	560	7100
PG2-13	Carnamagh	2	head_ConcN	0.4111	24.038	14.755	720	7100
PG2-14	Samnyt 16	2	head_ConcN	0.5947	38.828	23.644	600	6000
PG2-15	Carnamagh	2	head_ConcN	0.5317	33.465	17.898	960	7500
PG2-16	Samnyt 16	2	head_ConcN	0.5125	30.667	22.728	660	6700
PG3-01	Carnamagh	3	head_ConcN	0.2626	30.825	15.034	810	9700
PG3-02	Samnyt 16	3	head_ConcN	0.5163	38.540	26.428	760	8300
PG3-03	Samnyt 16	3	head_ConcN	0.4046	24.138	13.715	380	4900
PG3-04	Carnamagh	3	head_ConcN	0.4965	23.728	12.516	670	8400
PG3-05	Carnamagh	3	head_ConcN	0.3342	20.824	8.647	580	5900
PG3-06	Samnyt 16	3	head_ConcN	0.7229	40.232	19.357	450	5700
PG3-07	Samnyt 16	3	head_ConcN	0.6017	31.772	20.197	650	6900
PG3-08	Samnyt 16	3	head_ConcN	0.5888	35.506	23.550	720	4800
PG3-09	Carnamagh	3	head_ConcN	0.4803	24.026	13.003	590	6800
PG3-10	Carnamagh	3	head_ConcN	0.5963	21.923	11.960	600	7100
PG3-11	Carnamagh	3	head_ConcN	0.521	25.103	12.484	670	7100
PG3-12	Carnamagh	3	head_ConcN	0.5237	25.163	11.452	550	7500
PG3-13	Carnamagh	3	head_ConcN	0.5347	24.054	12.970	710	7700
PG3-14	Samnyt 16	3	head_ConcN	0.6755	47.214	22.295	900	5500
PG3-15	Samnyt 16	3	head_ConcN	0.5605	31.056	14.065	410	4800
PG3-16	Samnyt 16	3	head_ConcN	0.6204	41.453	24.597	700	7400
PG4-01	Carnamagh	4	head_ConcN	0.4522	31.405	15.667	1000	11000
PG4-02	Carnamagh	4	head_ConcN	0.4875	40.635	16.073	880	10200
PG4-03	Samnyt 16	4	head_ConcN	0.7028	18.882	13.822	470	8300
PG4-04	Samnyt 16	4	head_ConcN	0.5631	25.715	17.066	620	5900
PG4-05	Carnamagh	4	head_ConcN	0.5558	24.297	12.595	720	7500
PG4-06	Samnyt 16	4	head_ConcN	0.6376	24.474	15.668	480	6500
PG4-07	Carnamagh	4	head_ConcN	0.5163	19.809	11.612	460	6500
PG4-08	Samnyt 16	4	head_ConcN	0.4658	20.997	13.949	350	4900
PG4-09	Carnamagh	4	head_ConcN	0.5998	27.438	13.488	760	7800
PG4-10	Carnamagh	4	head_ConcN	0.5544	18.045	11.403	580	6800
PG4-11	Samnyt 16	4	head_ConcN	0.6316	29.952	16.134	420	6300
PG4-12	Samnyt 16	4	head_ConcN	0.6079	45.812	27.338	690	8500
PG1-01	Samnyt 16	1	head_ContT	0.4904	13.985	11.674	426.6	4756.9
PG1-02	Carnamagh	1	head_ContT	0.3761	13.557	8.840	598.0	4738.9
PG1-03	Carnamagh	1	head_ContT	0.477	20.237	12.877	787.1	5819.4
PG1-04	Samnyt 16	1	head_ContT	0.5115	14.228	12.714	588.2	5728.8
PG1-05	Samnyt 16	1	head_ContT	0.4098	11.437	10.954	467.2	4466.8
PG1-06	Carnamagh	1	head_ContT	0.4189	10.115	7.037	431.5	4440.3
PG1-07	Carnamagh	1	head_ContT	0.4183	9.546	6.395	447.6	4475.8

PG1-08	Samnyt 16	1	head_ContT	0.5097	11.664	11.842	463.8	5300.9
PG1-09	Carnamagh	1	head_ContT	0.2992	7.736	5.519	284.2	3111.7
PG1-10	Carnamagh	1	head_ContT	0.4465	10.574	8.434	482.2	5000.8
PG1-11	Samnyt 16	1	head_ContT	0.4781	14.134	13.885	473.3	5115.7
PG1-12	Samnyt 16	1	head_ContT	0.4285	10.492	10.930	377.1	4242.2
PG2-01	Carnamagh	2	head_ContT	0.5135	16.563	7.515	287.6	4108.0
PG2-02	Samnyt 16	2	head_ContT	0.5644	16.905	11.172	321.7	3950.8
PG2-03	Samnyt 16	2	head_ContT	0.4419	15.013	9.897	269.6	2165.3
PG2-04	Carnamagh	2	head_ContT	0.4318	11.520	5.919	263.4	3238.5
PG2-05	Carnamagh	2	head_ContT	0.4944	13.129	6.550	356.0	3856.3
PG2-06	Samnyt 16	2	head_ContT	0.4137	15.276	12.035	455.1	3475.1
PG2-07	Samnyt 16	2	head_ContT	0.5894	17.030	12.702	312.4	4125.8
PG2-08	Carnamagh	2	head_ContT	0.3897	9.071	4.539	233.8	2650.0
PG2-09	Carnamagh	2	head_ContT	0.4637	12.085	6.133	375.6	3802.3
PG2-10	Samnyt 16	2	head_ContT	0.5578	20.458	13.703	306.8	3904.6
PG2-11	Carnamagh	2	head_ContT	0.3814	9.467	4.122	244.1	2517.2
PG2-12	Carnamagh	2	head_ContT	0.4676	12.491	6.005	261.9	3320.0
PG2-13	Carnamagh	2	head_ContT	0.4111	9.882	6.066	296.0	2918.8
PG2-14	Samnyt 16	2	head_ContT	0.5947	23.091	14.061	356.8	3568.2
PG2-15	Carnamagh	2	head_ContT	0.5317	17.793	9.516	510.4	3987.8
PG2-16	Samnyt 16	2	head_ContT	0.5125	15.717	11.648	338.3	3433.8
PG3-01	Carnamagh	3	head_ContT	0.2626	8.095	3.948	212.7	2547.2
PG3-02	Samnyt 16	3	head_ContT	0.5163	19.898	13.645	392.4	4285.3
PG3-03	Samnyt 16	3	head_ContT	0.4046	9.766	5.549	153.7	1982.5
PG3-04	Carnamagh	3	head_ContT	0.4965	11.781	6.214	332.7	4170.6
PG3-05	Carnamagh	3	head_ContT	0.3342	6.959	2.890	193.8	1971.8
PG3-06	Samnyt 16	3	head_ContT	0.7229	29.083	13.993	325.3	4120.5
PG3-07	Samnyt 16	3	head_ContT	0.6017	19.117	12.152	391.1	4151.7
PG3-08	Samnyt 16	3	head_ContT	0.5888	20.906	13.866	423.9	2826.2
PG3-09	Carnamagh	3	head_ContT	0.4803	11.540	6.246	283.4	3266.0
PG3-10	Carnamagh	3	head_ContT	0.5963	13.073	7.132	357.8	4233.7
PG3-11	Carnamagh	3	head_ContT	0.521	13.078	6.504	349.1	3699.1
PG3-12	Carnamagh	3	head_ContT	0.5237	13.178	5.997	288.0	3927.8
PG3-13	Carnamagh	3	head_ContT	0.5347	12.862	6.935	379.6	4117.2
PG3-14	Samnyt 16	3	head_ContT	0.6755	31.893	15.061	608.0	3715.3
PG3-15	Samnyt 16	3	head_ContT	0.5605	17.407	7.884	229.8	2690.4
PG3-16	Samnyt 16	3	head_ContT	0.6204	25.717	15.260	434.3	4591.0
PG4-01	Carnamagh	4	head_ContT	0.4522	14.201	7.085	452.2	4974.2
PG4-02	Carnamagh	4	head_ContT	0.4875	19.810	7.836	429.0	4972.5
PG4-03	Samnyt 16	4	head_ContT	0.7028	13.270	9.714	330.3	5833.2
PG4-04	Samnyt 16	4	head_ContT	0.5631	14.480	9.610	349.1	3322.3
PG4-05	Carnamagh	4	head_ContT	0.5558	13.505	7.000	400.2	4168.5
PG4-06	Samnyt 16	4	head_ContT	0.6376	15.605	9.990	306.0	4144.4
PG4-07	Carnamagh	4	head_ContT	0.5163	10.227	5.995	237.5	3356.0
PG4-08	Samnyt 16	4	head_ContT	0.4658	9.780	6.498	163.0	2282.4
PG4-09	Carnamagh	4	head_ContT	0.5998	16.457	8.090	455.8	4678.4
PG4-10	Carnamagh	4	head_ContT	0.5544	10.004	6.322	321.6	3769.9
PG4-11	Samnyt 16	4	head_ContT	0.6316	18.918	10.190	265.3	3979.1
PG4-12	Samnyt 16	4	head_ContT	0.6079	27.849	16.619	419.5	5167.2